National Institute of
Environmental Health Sciences

NIEHS Report on the In Vivo Repeat Dose Biological Potency Study of 2,3-Benzofluorene (CASRN 243-17-4) in Sprague Dawley (Hsd:Sprague Dawley® SD®) Rats (Gavage Studies)

NIEHS 09

March 2023

NIEHS Report on the In Vivo Repeat Dose Biological Potency Study of 2,3-Benzofluorene (CASRN 243-17-4) in Sprague Dawley (Hsd:Sprague Dawley® SD®) Rats (Gavage Studies)

NIEHS Report 09

March 2023

National Institute of Environmental Health Sciences
Public Health Service
U.S. Department of Health and Human Services
ISSN: 2768-5632

Research Triangle Park, North Carolina, USA

Foreword

The National Institute of Environmental Health Sciences (NIEHS) is one of 27 institutes and centers of the National Institutes of Health, which is part of the U.S. Department of Health and Human Services. The NIEHS mission is to discover how the environment affects people in order to promote healthier lives. NIEHS works to accomplish its mission by conducting and funding research on human health effects of environmental exposures; developing the next generation of environmental health scientists; and providing critical research, knowledge, and information to citizens and policymakers who are working to prevent hazardous exposures and reduce the risk of disease and disorders connected to the environment. NIEHS is a foundational leader in environmental health sciences and committed to ensuring that its research is directed toward a healthier environment and healthier lives for all people.

The NIEHS Report series began in 2022. The environmental health sciences research described in this series is conducted primarily by the Division of Translational Toxicology (DTT) at NIEHS. NIEHS/DTT scientists conduct innovative toxicology research that aligns with real-world public health needs and translates scientific evidence into knowledge that can inform individual and public health decision-making.

NIEHS reports are available free of charge on the NIEHS/DTT website and cataloged in PubMed, a free resource developed and maintained by the National Library of Medicine (part of the National Institutes of Health).

Table of Contents

Tables

About This Report

Authors

Scott S. Auerbach[1], Kristin L. Aillon[2], Jeff D. Ballin[3], Bradley J. Collins[1], Michelle C. Cora[1], Nathan S. Duncan[2], Jennifer M. Fostel[1], Season P. Kerns[2], Ying F. Liu[4], Jeanne Luh[5], Nicholas J. Machesky[3], Sarah J. Pickett[2], Lisa M. Prince[5], Georgia K. Roberts[1], Kelly A. Shipkowski[1], Anthony J. Skowronek[3], Barney R. Sparrow[3], Heather Toy[6], Suramya Waidyanatha[1], AtLee T.D. Watson[1]

[1]Division of Translational Toxicology, National Institute of Environmental Health Sciences, Research Triangle Park, North Carolina, USA

[2]MRIGlobal, Kansas City, Missouri, USA

[3]Battelle, Columbus, Ohio, USA

[4]ASRC Federal, Research Triangle Park, North Carolina, USA

[5]ICF, Reston, Virginia, USA

[6]AmplifyBio, West Jefferson, Ohio, USA

Division of Translational Toxicology, National Institute of Environmental Health Sciences, Research Triangle Park, North Carolina, USA
Evaluated and interpreted the results and reported findings; developed reporting framework
Scott S. Auerbach, Ph.D., Study Scientist
Michelle C. Cora, D.V.M.
Georgia K. Roberts, Ph.D.
Kelly A. Shipkowski, Ph.D.
AtLee T.D. Watson, Ph.D.

Coordinated data integration
Jennifer M. Fostel, Ph.D.

Analyzed and interpreted analytical chemistry data
Bradley J. Collins, M.S.P.H.
Suramya Waidyanatha, Ph.D.

Battelle, Columbus, Ohio, USA
Provided contract oversight
Barney R. Sparrow, Ph.D.

Conducted in-life studies
Anthony J. Skowronek, D.V.M., Ph.D.

Performed RNA isolation
Nicholas J. Machesky, Ph.D.

Conducted thyroid biomarker analysis
Jeff D. Ballin, Ph.D.

AmplifyBio, West Jefferson, Ohio, USA
Compiled results
Heather Toy, B.S., Study Director

MRIGlobal, Kansas City, Missouri, USA
Conducted prestart chemistry activities, dose formulations, and biological sample chemistry analyses
Kristin L. Aillon, Ph.D., Principal Investigator
Nathan S. Duncan, Ph.D.
Season P. Kerns, M.S.
Sarah J. Pickett, B.S.

ICF, Reston, Virginia, USA
Contributed to technical writing and data integration and ensured report quality
Jeanne Luh, Ph.D.
Lisa M. Prince, Ph.D.

ASRC Federal, Research Triangle Park, North Carolina, USA
Developed data tables and supplemental materials
Ying F. Liu, Ph.D.

Contributors

Division of Translational Toxicology, National Institute of Environmental Health Sciences, Research Triangle Park, North Carolina, USA
Critically reviewed report and results
John R. Bucher, Ph.D.
Fred M. Parham, Ph.D.
Nigel J. Walker, Ph.D.

Contributed to development and review of reporting framework
Michael J. DeVito, Ph.D.
William M. Gwinn, Ph.D.
Alison H. Harrill, Ph.D.
Scott A. Masten, Ph.D.
Matthew D. Stout, Ph.D.
Greg S. Travlos, D.V.M.
Mary S. Wolfe, Ph.D.

Developed and updated BMDS software package
Andrew J. Shapiro, M.S.P.H.

RTI International, Research Triangle Park, North Carolina, USA
Conducted biological sample chemistry analyses of total thyroid hormone levels
Reshan A. Fernando, Ph.D., Principal Investigator
Melanie A.R. Silinski, Ph.D.

ASRC Federal, Research Triangle Park, North Carolina, USA
Developed data tables and supplemental materials

Julie Berke, B.S.
Shihan He, Ph.D.
Christina Myers, M.S.

CSS Corporation, Research Triangle Park, North Carolina, USA
Prepared quality assessment audits
Steven Brecher, Ph.D., Principal Investigator
Sudha Iyer, B.S.
Varghese S. Tharakan, D.V.M.

Sciome LLC, Research Triangle Park, North Carolina, USA
Provided bioinformatics analysis
Michele R. Balik-Meisner, Ph.D.
Dhiral P. Phadke, M.S.
Ruchir R. Shah, Ph.D.

ICF, Reston, Virginia, USA
Provided contract oversight
David F. Burch, M.E.M., Principal Investigator
Cary E. Haver, M.P.H.
Jessica A. Wignall, M.S.P.H.

Prepared and edited report
Lauren M. Browning, M.S.
Tara Hamilton, M.S.
Pamela A. Hartman, M.E.M.
Samantha J. Snow, Ph.D.
Jonathan R. Thompson, B.S.
Nkoli Ukpabi, M.S.

Peer Review

This report was modeled after the *NTP Research Report on In Vivo Repeat Dose Biological Potency Study of Triphenyl Phosphate (CAS No. 115-86-6) in Male Sprague Dawley (Hsd:Sprague Dawley® SD®) Rats (Gavage Studies)* (https://doi.org/10.22427/NTP-RR-8), which was reviewed internally at the National Institute of Environmental Health Sciences and peer reviewed by external experts. Importantly, these reports employ mathematical model-based approaches to identify and report potency of dose-responsive effects and do not attempt more subjective interpretation (i.e., make calls or reach conclusions on hazard). The peer reviewers of the initial 5-day research report determined that the study design, analysis methods, and results presentation were appropriate. The study design, analysis methods, and results presentation employed for this study are identical to those previously reviewed, approved, and reported; therefore, following internal review, the *NIEHS Report on the In Vivo Repeat Dose Biological Potency Study of 2,3-Benzofluorene (CASRN 243-17-4) in Sprague Dawley (Hsd:Sprague Dawley® SD®) Rats (Gavage Studies)* was not subjected to further external peer review.

Publication Details

Publisher: National Institute of Environmental Health Sciences

Publishing Location: Research Triangle Park, NC

ISSN: 2768-5632

DOI: https://doi.org/10.22427/NIEHS-09

Report Series: NIEHS Report Series

Report Series Number: 09

Official citation: Auerbach SS, Aillon KL, Ballin JD, Collins BJ, Cora MC, Duncan NS, Fostel JM, Kerns SP, Liu YF, Luh J, Machesky NJ, Pickett SJ, Prince LM, Roberts GK, Shipkowski KA, Skowronek AJ, Sparrow BR, Toy H, Waidyanatha S, Watson ATD. 2023. NIEHS report on the in vivo repeat dose biological potency study of 2,3-benzofluorene (CASRN 243-17-4) in Sprague Dawley (Hsd:Sprague Dawley® SD®) rats (gavage studies). Research Triangle Park, NC: National Institute of Environmental Health Sciences. NIEHS Report 09.

Acknowledgments

This work was supported by the Intramural Research Program (ES103316, ES103318, ES103319, and ES102505) at the National Institute of Environmental Health Sciences (NIEHS), National Institutes of Health and performed for NIEHS under contracts HHSN273201800006C, HHSN273201700005C, HHSN273201700001C, GS00Q14OADU417 (Order No. HHSN273201600015U), HHSN273201500006C, HHSN273201400020C, HHSN273201400022C, HHSN273201300004C, and HHSN316201200054W.

Abstract

Background: 2,3-Benzofluorene (2,3-BF) is a member of the polycyclic aromatic hydrocarbon class of compounds to which humans are widely exposed. Toxicological information on this class of chemicals is sparse. A short-term, in vivo transcriptomic study was used to assess the biological potency of 2,3-BF.

Methods: A short-term in vivo biological potency study on 2,3-BF in adult male and female Sprague Dawley (Hsd:Sprague Dawley® SD®) rats was conducted. 2,3-BF was formulated in corn oil and administered once daily for 5 consecutive days by gavage (study days 0–4). 2,3-BF was administered at 10 doses (0, 0.15, 0.5, 1.4, 4, 12, 37, 111, 333, and 1,000 mg/kg body weight [mg/kg]). Blood was collected from animals dedicated for internal dose assessment in the 4 and 37 mg/kg groups. On study day 5, the day after the final dose was administered, animals were euthanized, standard toxicological measures were assessed, and the liver and kidney were assayed in gene expression studies using the TempO-Seq assay. Modeling was conducted to identify the benchmark doses (BMDs) associated with apical toxicological endpoints and transcriptional changes in the liver and kidney. A benchmark response of one standard deviation was used to model all endpoints.

Results: Several clinical pathology and organ weight measurements showed dose-related changes from which BMD values were calculated. In male rats, the effects included significantly decreased reticulocyte count, increased thyroid stimulating hormone concentration, and decreased total thyroxine concentration. The BMDs and benchmark dose lower confidence limits (BMD_Ls) were 11.837 (6.978), 44.526 (19.298), and 61.426 (24.276) mg/kg, respectively. In female rats, the effects included significantly increased thyroid stimulating hormone concentration, increased absolute liver weight, and increased cholesterol concentration. The BMDs (BMD_Ls) were 1.078 (0.267), 24.928 (7.768), and 288.242 (226.543), respectively. Average 2,3-BF plasma concentrations at 2 hours postdose were lower in female rats than in male rats. At 24 hours postdose, the concentration decreased and fell below the limit of detection of the analytical method in female rats and close to it in male rats. Half-lives in males, estimated using the two time points, were 25.3 and 4.4 hours for the 4 and 37 mg/kg groups, respectively.

In the liver of male and female rats, no Gene Ontology biological process or individual genes had BMD median values below the lower limit of extrapolation (<0.050 mg/kg). The most sensitive gene sets in male rats for which a reliable estimate of the BMD could be made were regulation of ossification and kidney development with median BMDs of 5.660 and 5.765 mg/kg and median BMD_Ls of 2.158 and 1.618 mg/kg, respectively. The most sensitive gene sets in female rats for which a reliable estimate of the BMD could be made were DNA conformation change and chromosome organization, both with a median BMD of 1.874 mg/kg and a median BMD_L of 0.497 mg/kg. The most sensitive upregulated genes in male rats with reliable BMD estimates included *G0s2*, *Trib3*, *Akr7a3*, *Nqo1*, and *Ephx1* with BMDs (BMD_Ls) of 3.451 (1.074), 16.895 (6.465), 19.850 (12.797), 24.112 (16.415), and 24.878 (15.487) mg/kg, respectively. The most sensitive downregulated genes in male rats with reliable BMD estimates were *Zfp354a*, *Tsku*, *Egr1*, *C7*, and *Loc100911558*/*Spink1l* with BMDs (BMD_Ls) of 3.267 (1.720), 6.126 (1.466), 8.263 (1.517), 13.843 (5.329), and 26.630 (12.428) mg/kg, respectively. The most sensitive upregulated genes in female rats with reliable BMD estimates included *Kif22*, *Anln*, *Anlnl1*, *Asns*, and *Nr1d2* with BMDs (BMD_Ls) of 0.962 (0.282), 3.325 (1.105), 3.325 (1.105), 6.056 (2.744), and 9.460 (2.213) mg/kg, respectively. The most sensitive downregulated genes in female rats with reliable BMD estimates were *Car3*, *Aass*, *A2m*, *Loc100911545*/*A2m*,

and *Sez6* with BMDs (BMD_Ls) of 3.449 (2.131), 5.811 (2.605), 8.459 (1.870), 8.459 (1.870), and 10.639 (3.960) mg/kg, respectively.

In the kidney of male and female rats, no Gene Ontology biological process had BMD median values below the lower limit of extrapolation (<0.050 mg/kg). The most sensitive gene sets in male rats for which a reliable estimate of the BMD could be made were brain development and cellular process involved in reproduction in multicellular organism, with median BMDs of 6.167 and 12.334 mg/kg, and median BMD_Ls of 1.732 and 3.464 mg/kg, respectively. The most sensitive gene sets in female rats for which a reliable estimate of the BMD could be made were regulation of fibroblast proliferation and negative regulation of fibroblast proliferation with median BMDs of 14.574 and 14.763 mg/kg and median BMD_Ls of 7.161 and 9.430 mg/kg, respectively. In male rats, one individual kidney gene, *Nefh,* had a median BMD value <0.050 mg/kg and was downregulated. The next most sensitive downregulated genes with reliable BMD estimates included *Top2a*, *Ect2*, *Hmgcs2*, *Nfil3*, *Mt1,* and *Cyp2c11* with BMDs (BMD_Ls) of 12.334 (3.464), 31.232 (16.473), 106.351 (59.870), 121.321 (82.552), 168.588 (103.554), and 216.743 (139.563) mg/kg, respectively. The most sensitive upregulated genes with reliable BMD estimates included *Nqo1, Cyp1a1,* and *Rassf1* with BMDs (BMD_Ls) of 40.551 (21.583), 49.045 (39.236), and 903.848 (608.514) mg/kg, respectively. In female rats, no individual genes had median BMD values <0.050 mg/kg. The most sensitive upregulated genes in female rats with reliable BMD estimates included *Cyp1a1*, *Gstp1*, *Cyp26b1*, and *Nqo1* with BMDs (BMD_Ls) of 12.886 (9.131), 14.763 (9.430), 18.187 (10.018), and 25.681 (7.739) mg/kg, respectively. The most sensitive downregulated genes in female rats with reliable BMD estimates included *Vwf, Abcb1b*, *Npas2*, *Arntl*, *C4a,* and *Loc103689965*/*C4a* with BMDs (BMD_Ls) of 19.676 (4.116), 20.794 (8.254), 21.088 (11.331), 22.913 (11.412), 24.209 (8.100), and 24.209 (8.100) mg/kg, respectively.

Summary: Taken together, in male rats, the most sensitive gene set BMD (BMD_L) median, individual gene BMD (BMD_L), and apical endpoint BMD (BMD_L) values that could be reliably determined occurred at 5.660 (2.158), 3.267 (1.720), and 11.837 (6.978) mg/kg, respectively. The BMD (BMD_L) could not be determined for one individual gene and was estimated to be <0.050 mg/kg. In female rats, the most sensitive gene set BMD (BMD_L) median, individual gene BMD (BMD_L), and apical endpoint BMD (BMD_L) values that could be reliably determined occurred at 1.874 (0.497), 0.962 (0.282), and 1.078 (0.267) mg/kg, respectively.

Background

2,3-Benzofluorene (2,3-BF) (CASRN: 243-17-4, U.S. Environmental Protection Agency [EPA] Chemical Dashboard: DTXSID1022477,[1] PubChem CID: 9201,[2] European Committee Number: 205-952-2[3]) is a member of the polycyclic aromatic hydrocarbon class of compounds that are associated with numerous toxicological effects.[4] There is widespread human exposure to this class of compounds.[4] No exposure information was available for 2,3-BF. A review of the existing literature failed to identify any in vivo toxicological information on 2,3-BF, and according to the EPA Chemical Dashboard, no quantitative risk assessment values or quantitative hazard values exist for this test article.[5] Consistent with the absence of data on 2,3-BF, it is listed in Group 3 (not classifiable as to its carcinogenicity to humans) in the International Agency for Research on Cancer (IARC) Carcinogenicity Classification.[6] Publicly available information on 2,3-BF can be found in PubChem[2] and the EPA Chemical Dashboard.[1]

Recent studies have demonstrated that short-term in vivo gavage studies coupled with transcriptomics on select target organs can be used to estimate a biological potency that provides a reasonable approximation of toxicological potency in long-term guideline toxicological assessments.[7] To estimate biological potency and gain insight into the nature of biological changes elicited by 2,3-BF, the National Institute of Environmental Health Sciences performed a short-term in vivo biological potency study of male and female Sprague Dawley (Hsd:Sprague Dawley® SD®) rats. The results of this study are presented in this report.

Materials and Methods

Study Design

Male and female Sprague Dawley (Hsd:Sprague Dawley® SD®) rats were obtained from Envigo (Haslett, MI). On receipt, the rats were 6–7 weeks of age. Animals were quarantined for a minimum of 10 days and then randomly assigned to 1 of 10 dose groups. The rats in each dose group were then administered 2,3-benzofluorene (2,3-BF) in corn oil by gavage for 5 consecutive days (study days 0–4) at a dose level of 0, 0.15, 0.5, 1.4, 4, 12, 37, 111, 333, or 1,000 mg/kg body weight (mg/kg). There were 5 rats per sex in each dosed group and 10 per sex in the vehicle control group; an additional 3 rats per sex were added to the 4 and 37 mg/kg groups for internal dose assessment. Dosage volume was 5 mL/kg body weight and was based on each animal's most recent body weight. Euthanasia, blood/serum collection, and tissue sample collection were completed on study day 5, the day following the final administration of the test article. Blood was also collected from animals dedicated for internal dose assessment at 2 and 24 hours following the last dose administered on study day 4. Animal identification numbers and FASTQ data file names for each animal are presented in Appendix B.

Dose Selection Rationale

Dose selection was informed by a median lethal dose (LD_{50}) prediction from the OPEn structure-activity/property Relationship App (OPERA),[8; 9] which estimated 2,250 mg/kg/day with an uncertainty range of 1,127–4,490 mg/kg/day. Due to challenges with chemical formulation and a desire to have the top dose level within a range deemed generally acceptable, a top dose of 1,000 mg/kg was chosen, and approximately half-log dose spacing of nine lower dose levels, including a vehicle control, was selected to carry out the study.

Chemistry

2,3-BF was obtained from Finetech Industry Limited (London, United Kingdom; lot 20200113002). The identity of the chemical was confirmed by mass spectrometry, and purity (98.74%; three impurities) was determined by ultra-performance liquid chromatograph (UPLC) with ultraviolet (UV) detectors. Bulk chemical was stored at room temperature under inert headspace.

Dose formulations were prepared in corn oil at 0 (vehicle control), 0.03, 0.10, 0.28, 0.80, 2.4, 7.4, 22.2, 66.6, and 200 mg/mL. The preadministration concentration of test article in the vehicle was analyzed using UPLC/UV. The 0.10 mg/mL formulation was 15.8% above the target concentration. All other formulations were within 10% of the target concentration. Formulation stability was confirmed in a 0.06 mg/mL formulation for up to 22 days at refrigerated (5°C) and room temperatures while protected from light. All chemistry activities were conducted by MRIGlobal (Kansas City, MO).

Clinical Examinations and Sample Collection

Clinical Observations

All rats were observed twice daily for signs of mortality or moribundity. Formal (out of cage) clinical observations were performed daily.

Body and Organ Weights

Animals were weighed during quarantine for randomization on the first day of dosing (study day 0) and on the day of necropsy (study day 5). A gross necropsy was performed on all rats that died spontaneously or were humanely euthanized due to moribund condition. During necropsy for all animals, the heart, liver, and kidneys were removed, and organ weights were recorded; bilateral organs were weighed separately.

Clinical Pathology

Animals were euthanized in random order by CO_2/O_2 (70%/30%) anesthesia 1 day after the final day of dosing. Blood samples were collected from each sex within a 1-hour window and were taken via vena cava or aorta. Blood was collected into tubes containing K_3 EDTA (tripotassium ethylenediaminetetraacetic acid) for hematology analysis and into tubes void of anticoagulant for serum chemistry and thyroid hormone measurements. The following hematology parameters were measured on an Advia® 120 Hematology Analyzer (Siemens Medical Solutions USA, Inc., Malvern, PA): erythrocyte count, hemoglobin, hematocrit, mean cell volume, mean cell hemoglobin, mean cell hemoglobin concentration, white blood cell count and differential, reticulocyte count, platelet count, and nucleated erythrocyte count. Manual hematocrit was determined using a microcentrifuge and capillary reader. Blood smears were prepared, and qualitative evaluation of cellular morphology was performed per study protocol. The following clinical chemistry parameters were measured on a Roche cobas® c501 Chemistry Analyzer (Roche Diagnostics, Indianapolis, IN): alanine aminotransferase (ALT), albumin, alkaline phosphatase (ALP), aspartate aminotransferase (AST), total bile acids, total bilirubin, direct bilirubin, cholesterol, creatine kinase, creatinine, glucose, sorbitol dehydrogenase (SDH), total protein, triglycerides, and urea nitrogen. Globulin, albumin/globulin (A/G) ratio, and indirect bilirubin were calculated based on direct measurements (e.g., indirect bilirubin = total bilirubin − direct bilirubin). Serum concentrations for thyroid stimulating hormone (TSH) and free thyroxine (fT4) were determined by immunoassay using commercially available immunoassay kits from EMD Millipore Corporation (Billerica, MA) for TSH and Biomatik Corporation (Kitchener, Ontario, Canada) for fT4. Serum concentrations of total thyroxine (total T4) and total triiodothyronine (total T3) were determined using a validated method described elsewhere.[10] Individual animal and summary clinical chemistry, hematology, and hormonal data are available in Appendix F.

Internal Dose Assessment

A screening level assessment of the internal dose was performed to determine whether the test chemical had bioaccumulative properties (i.e., if the half-life was >24 hours). Blood was collected from animals dedicated for internal dose assessment in the 4 and 37 mg/kg groups at 2 and 24 hours following the last dose administered on study day 4. At 2 hours postdose, blood was collected from the jugular vein of unanesthetized animals. At 24 hours postdose (study day 5), blood was collected from all study animals and dedicated internal dose assessment animals from the vena cava or abdominal aorta while animals were anesthetized with CO_2/O_2 (70%/30%). Blood was collected into tubes containing K_3 EDTA and kept on wet ice until plasma isolation, within 2 hours of collection. Samples were stored frozen (−85°C to −60°C) until analysis as described in Appendix A.

Transcriptomics

Sample Collection for Transcriptomics

Within 5 minutes of euthanasia, samples from the left liver lobe and right kidney were collected from all study animals for transcriptomic analysis. Half of the left liver lobe and half of the right kidney were processed for RNA isolation. Approximately 250 mg of each tissue was cut into small pieces (approximately 5 mm^3) and placed into cryotubes containing RNA*later*™. The tissue samples were stored at 2°C to 8°C overnight. The RNA*later*™ was then removed and the samples were stored in a −85°C to −60°C freezer until processed for RNA isolation.

RNA Isolation, Library Creation, and Sequencing

RNA isolation was performed on tissue samples preserved in RNA*later*™. Tissues were homogenized in QIAzol buffer (Qiagen Inc., Valencia, CA) using the TissueLyser II bead-beating system followed by RNA extraction using the Rneasy 96 QIAcube HT kits (Cat# 74171, Qiagen Inc., Valencia, CA) with a DNA digestion step. The concentration and purity of all isolated samples were determined from absorbency readings taken at 260 and 280 nm using a NanoDrop ND-8000 Spectrophotometer (NanoDrop Technologies, Wilmington, DE). The readings accurately determined the concentration of each sample while ensuring that an acceptable purity (A_{260}/A_{280} ratio) between 1.80 and 2.20 was achieved. After quantification, RNA was stored at −70°C ± 10°C until further processing.

One microliter of each RNA sample (500–660 ng/µL) was hybridized with the S1500+ beta detector oligo pool mix (2 µL per sample) using the following thermocycler settings: 10 minutes at 70°C, followed by a gradual decrease to 45°C over 49 minutes, and ending with a 45°C hold for 1 minute. Hybridization was followed by nuclease digestion (24 µL nuclease mix addition followed by 90 minutes at 37°C), ligation (24 µL ligation mix addition followed by 60 minutes at 37°C), and heat denaturation (at 80°C for 15 minutes). Ten microliters of each ligation product were then transferred to a 96-well polymerase chain reaction (PCR) amplification microplate with 10 µL of PCR mix per well. Through 25 cycles of amplification, well-specific "barcoded" primer pairs were introduced to templates. Five microliters of the PCR amplification products from each well were then pooled into a single sequencing library. The TempO-Seq library was then processed with a PCR clean-up kit (Machery-Nagel, Mountain View, CA) prior to sequencing. Sequencing was performed using a 50-cycle single-end read flow cell on a HiSeq 2500 Sequencing System (Illumina, San Diego, CA). Processing of sequencing data was conducted using Illumina's BCL2FASTQ software employing default parameter settings.

Sequence Data Processing

FASTQ files of TempO-Seq reads were aligned to the probe sequences from the target platform using Bowtie version 1.2.2[11] with the following parameters: -v 3 -k 1 -m 1 --best --strata. This configuration allows up to three mismatches and reports the single best alignment. After alignment, the total sequenced reads, the percentage of reads aligning to the platform manifest, the alignment rate, and the percentage of expressed probes (≥5 reads per probe) were calculated for each sample.

Sequencing Quality Checks and Outlier Removal

Samples were flagged for values below the following thresholds: sequencing depth <300 K, total alignment rate <40%, unique alignment rate <30%, number of aligned reads <300 K, or

percentage of probes with at least five reads <50%. Filtering on the percentage of expressed probes eliminates biased samples for which the sequenced reads only reflect a small portion of the measured transcriptome. In addition, FastQC was run on all samples to ensure adequate per base quality and per base N content, where N represents bases that could not be identified. All 2,3-BF samples passed the criteria mentioned above.

Principal component (PCA), hierarchical cluster, and inter-replicate correlation analyses were performed. These analyses resulted in none of the samples being removed.

The processing of samples from the study of 2,3-BF was done in parallel with three other chemicals that were studied under a similar protocol, therefore allowing for a more powerful collective assessment of the data. Specifically, the samples from all four studies were distributed over twelve 96-well plates (i.e., one plate per chemical per tissue and four additional plates with overflow samples for three of the chemicals, with nine doses plus vehicle control). For kidney samples, average read depth per chemical varied across plates. Kidney samples on one of the overflow plates also clustered separately (in the PCA and hierarchical cluster analysis) from the other kidney samples for a given chemical. Therefore, kidney samples on that overflow plate were removed, resulting in one plate of data per chemical for the downstream analysis of kidney samples. The exclusion of these data had limited impact on the analysis as the samples from each dose group were randomly sorted into the overflow plates. The final sample counts that were used for benchmark dose (BMD) analysis of the transcriptomics data are shown in Table 1.

Table 1. Final Sample Counts for Benchmark Dose Analysis of the Transcriptomics Data

	0 mg/kg	0.15 mg/kg	0.5 mg/kg	1.4 mg/kg	4 mg/kg	12 mg/kg	37 mg/kg	111 mg/kg	333 mg/kg	1,000 mg/kg
Male										
Liver	10	5	5	5	5	5	5	5	5	5
Kidney	6	4	5	4	5	3	5	3	5	5
Female										
Liver	10	5	5	5	5	5	5	5	5	5
Kidney	8	5	4	5	4	3	4	3	5	4

Data Normalization

The aligned read counts for attenuated probes were properly readjusted to calculate unattenuated equivalent counts using the attenuation factors provided in the platform manifest. To account for between-sample sequencing depth variation, unattenuated read counts were normalized at the probe level by applying reads per million normalization. A pseudo-read-count of 1.0 was added to each normalized expression value, and then the values were log2 transformed to complete the normalization. Principal component-based visualizations of the final expression data set used from modeling are available in Appendix C.

Data Analysis

Statistical Analysis of Body Weights, Organ Weights, and Clinical Pathology

Two approaches were employed to assess the significance of pairwise comparisons between dosed and vehicle control groups in the analysis of continuous variables. Organ and body weight

data, which have approximately normal distributions, were analyzed using the parametric multiple comparison procedures of Williams[12; 13] and Dunnett.[14] Clinical pathology data, which typically have skewed distributions, were analyzed using the nonparametric multiple comparison methods of Shirley[15] and Dunn.[16] The Jonckheere test[17] was used to assess the significance of dose-response trends and to determine whether a trend-sensitive test (Williams or Shirley test) was more appropriate for pairwise comparisons than a test that assumes no monotonic dose response (Dunnett or Dunn test). Trend-sensitive tests were used when the Jonckheere test was significant at $p \leq 0.01$.

Prior to analysis, values identified by the outlier test of Dixon and Massey[18] were examined by National Institute of Environmental Health Sciences (NIEHS) staff. Values from animals suspected of illness due to causes other than experimental exposure and values that the laboratory indicated as inadequate due to measurement problems were eliminated from the analysis.

A no-observed-effect level (NOEL) was identified as the highest dose not showing a significant ($p \leq 0.05$) pairwise difference relative to the vehicle control group. A lowest-observed-effect level (LOEL) was identified as the lowest dose demonstrating a significant ($p \leq 0.05$) pairwise difference relative to the vehicle control group. Throughout the results section for apical endpoints, interpretation of BMDs is made in relationship to NOEL and LOEL values for specific endpoints, as defined here, and are not meant to reflect an overall study NOEL or LOEL.

Benchmark Dose Analysis of Body Weights, Organ Weights, and Clinical Pathology

Clinical pathology, body weight, and organ weight endpoints that exhibited a significant trend and pairwise test were submitted in batch for automated BMD modeling analysis. For body weight, the BMD and benchmark dose lower confidence limit (BMD_L) were presented as not determined when there were no significant results. BMD modeling and analysis was conducted using a modification of Benchmark Dose Modeling Software (BMDS) version 2.7.0. Data sets were executed using the Python BMDS interface (https://pypi.python.org/pypi/bmds; version 0.11), which allows for batch processing of multiple data sets. Data for all endpoints submitted were continuous. A default benchmark response (BMR) of one standard deviation (relative to control) was used for all data sets. The following BMDS 2.7.0 models were used to model the means of the data sets:

- Linear
- Polynomial 2°, 3°, 4°, 5°, 6°, 7°, 8°
- Power
- Hill
- Exponential M2, M3, M4, M5

Multiple versions of the polynomial model were executed, from a polynomial of degree 2 to a polynomial of degree equal to the number of dose groups minus 1 (e.g., if a data set had five dose groups, a 2°, 3°, and 4° polynomial model would be executed). Models were initialized using BMDS 2.7.0 model defaults, including restricting the power parameter of the power model and n-parameter of the Hill model to >1 and the beta parameters of the polynomial model to positive or negative, depending on the mean response direction of the data set. For all models, either a constant or nonconstant variance model was selected as outlined in the Environmental

Protection Agency (EPA) BMD technical guidance[19] and was implemented in the BMDS 2.7.0 software.

After model execution, BMDs were selected using the model recommendation procedures generally described in the EPA BMD technical guidance[19] and the automated decision logic described in Wignall et al.[20] and summarized in Appendix D, Table D-1. Models were placed into one of four possible bins, depending on the results and the bin recommendation logic:

(1) **Failure:** model did not successfully complete

(2) **Nonviable model (NVM):** model successfully completed but failed acceptability criteria

(3) **Not reportable (NR):** model is identified and meets all acceptability criteria with the exception of the estimated BMD being below the lower limit of extrapolation (<1/3 the lowest nonzero dose tested); BMD reported as <1/3 the lowest nonzero dose tested and BMD_L is not reportable

(4) **Viable model:** candidate for recommended model without warning

If only one model was in the viable model bin, it was selected as the best-fitting model. If the viable bin had more than one model, consistent with EPA guidance,[19] either the model with the lowest Akaike information criterion (AIC) or lowest BMD_L was selected. If the range of BMD_L values was sufficiently close (less than threefold difference), the AIC value was used; otherwise, the BMD_L value was used. If no model was recommended, no BMD was presented in the results. Details on the analysis criteria and decision tree are provided in Table D-1 and Figure D-1, respectively. To avoid effects of model extrapolation, BMD values derived from viable models that were threefold lower than the lowest nonzero dose tested were reported as <1/3 the lowest nonzero dose tested, and corresponding BMD_L values were not reported. Finally, all modeling results from apical data yielding a BMD were reviewed by a subject matter expert to determine the validity of the modeling results and potency estimates.

Benchmark Dose Analysis of Transcriptomics Data

The BMD analysis of the transcriptomic data was performed in accordance with the National Toxicology Program (NTP) best practices for genomic dose-response modeling as reviewed by an independent panel of experts in October 2017. These recommendations are described in the 2018 publication, *National Toxicology Program Approach to Genomic Dose Response Modeling*.[21]

Dose-response analyses of normalized gene expression data were performed using BMDExpress 2.30.0507 BETA (https://github.com/auerbachs/BMDExpress-2/releases). A trend test (the Williams trend test[12; 13] $p \leq 0.05$, 10,000 permutations) and fold change filter (1.5-fold change up or down relative to the vehicle control group for probe sets) were applied to the data set to remove probe sets demonstrating no response to chemical exposure from subsequent analysis. These filter criteria were empirically determined with the goal of balancing false discovery with reproducibility. The criteria are consistent with the MicroArray Quality Control recommendations to combine the nominal p value threshold with a fold change filter to maximize replicability of transcriptomic findings across labs.[22] The following dose-response models were fit to the probe sets that passed the trend test and fold change filter:

- Hill

- Power
- Linear
- Polynomial 2°
- Exponential M2, M3, M4, M5

All gene expression data analyzed in BMDExpress were log2 transformed, and thus nearly all probes (also known as detection oligos or DO) were assumed to exhibit constant variance across the doses. For this reason and for efficiency purposes, each model was run assuming constant variance. Lacking any broadly applicable guidance regarding the level of change in gene expression considered biologically significant, a BMR of one standard deviation (relative to the fit at control) was used in this study. This approach enables standardization of the BMR between apical endpoints and transcriptomic endpoints and provides a standard for use across multiple chemicals tested in this rapid screening paradigm. The expression direction (upregulated or downregulated) for each probe was determined by a trend test intrinsic to the model executables (provided by EPA) contained in BMDExpress.

To identify the best-fit model for each fitted probe, the AIC values for each fitted model were compared and the model with the lowest AIC was selected. The best model for each probe was used to calculate the BMD, BMD_L, and BMD upper confidence limit (BMD_U). The specific parameter settings, selected from the BMDExpress software when performing probe-level BMD analysis, were as follows: maximum iterations – 250, confidence level – 0.95, BMR factor – 1 (the multiplier of the standard deviation that defined the BMD), restrict power – no restriction, and constant variance – selected. The specific model selection setting in the BMDExpress software when performing probe set-level BMD analysis was as follows: best poly model test – lowest AIC, flag Hill model with "k" parameters – <1/3 the lowest nonzero dose tested, and best model selection with flagged Hill model – include flagged Hill model. The inclusion of the flagged models is a deviation from EPA BMD analysis guidance.[19] The justification for this deviation relates to subsequent use of the data in which the probe BMD values are grouped into gene sets from which a median BMD is derived. If the probes were removed from the analysis or forced to another model, the probe might not be counted in the gene set analysis and could lead to loss of "active" gene sets. Importantly, most of the probes that produce flagged Hill models show highly potent responses and should therefore be counted in the analysis.

To perform Gene Ontology (GO; annotation accession date: 07/15/2020) gene set analysis, only GO terms with ≥10 and ≤250 annotated genes measured on the gene expression platform were considered. Before sorting genes into the GO terms, the best-fit model for each probe was subjected to a filtering process to remove those probes (1) with a BMD greater than the highest dose tested, (2) that mapped to more than one gene, (3) that had a global goodness-of-fit p value ≤0.1, and (4) with a BMD_U/BMD_L ratio > 40. GO terms that were at least 5% populated and contained three genes that passed the criteria mentioned above were considered "active" (i.e., responsive to chemical exposure). For this report, GO terms populated with identical sets of differentially expressed genes were filtered to limit redundancy in reporting based on the following selection criteria: (1) highest percentage populated and (2) most specific/highest GO level. Redundant GO terms failing to differentiate on the basis of these criteria were retained and reported. A complete list of "active" GO terms can be found in Appendix F. To avoid effects of model extrapolation, GO terms exhibiting BMD values below the lower limit of extrapolation (<1/3 the lowest nonzero dose tested) were reported as <1/3 the lowest nonzero dose tested and corresponding BMD_L and BMD_U values were not reported.

To perform Individual Gene Analysis, the best-fit model for each probe was subjected to a filtering process to remove those probes (1) with a BMD greater than the highest dose tested, (2) that mapped to more than one gene, (3) that had a global goodness-of-fit p value ≤0.1, or (4) with a BMD_U/BMD_L ratio >40. For genes that had more than one probe represented on the platform and passed this filtering process, a median BMD was used to estimate the BMD, BMD_L, and BMD_U values. To ensure only genes with a robust response were assessed for potency, genes with probes that had a median fold change <|2| were removed prior to reporting. A complete list of genes and their corresponding metrics can be found in Appendix F. To avoid effects of model extrapolation, genes exhibiting BMD values below the lower limit of extrapolation (<1/3 the lowest nonzero dose tested) were reported as <1/3 the lowest nonzero dose tested and corresponding BMD_L and BMD_U values were not reported.

A summary of the BMDExpress gene expression analysis pipeline used in this study is shown in Figure D-2.

Empirical False Discovery Rate Determination for Genomic Dose-response Modeling

The genomic dose-response analysis pipeline is a complex multistep process with multiple modeling steps and parameter variables. Because of this complexity, traditional statistical models for determining false discovery rates for the genes and pathways are not straightforward to apply. To overcome this issue, an empirical false discovery rate was determined on the basis of the totality of the analysis pipeline. This was done through the evaluation of synthetic null data sets derived from vehicle control data from four short-term repeat dose toxicogenomic studies including 2,3-BF (each with 10 vehicle control samples). The other toxicogenomic studies, which are reported in separate NIEHS reports, are of perfluorohexanesulfonamide,[23] 6:1 fluorotelomer alcohol,[24] and 1,1,2,2-tetrahydroperfluoro-1-dodecanol.[25] Samples from all four studies were processed as a group and subjected to sequencing at the same time and were visually inspected to ensure there was no batch effect between the different studies.

To create synthetic null data for a given group (tissue per sex combination), up to 40 vehicle control samples from the original studies (10 replicates × 4 chemicals) were used to generate the data sets, with outliers excluded from the analysis. Each computationally generated sample was created by mixing two randomly selected vehicle control samples via a weighted average approach through which weights were obtained from random uniform (0,1) distribution. A total of 55 samples (10 vehicle control samples + 45 dosed samples [9 doses × 5 replicates]) were computationally generated per data set and assigned doses spaced by approximately half-log. A total of 20 data sets were generated per group (i.e., 20 data sets each for female kidney, male kidney, female liver, and male liver) and analyzed using both the individual gene-level and GO biological process (gene set) analysis pipeline employed to analyze the data from each study. The median empirical false discovery rates across the 20 null sets in each group for gene-level analysis across each group were 0.037%, 0.037%, 0%, and 0% (female kidney, male kidney, female liver, and male liver, respectively). The median empirical false discovery rate for each of the 20 null data sets in each group using the GO biological process (gene set) level analysis was 0%. Details of the empirical false discovery rate analysis are available in Appendix C. The associated bm2 analysis file that is the basis of the empirical false discovery rate can be found in Appendix F.

Data Accessibility

Primary and analyzed data used in this study are available to the public at https://doi.org/10.22427/NIEHS-DATA-NIEHS-09.[26]

Results

Animal Condition, Body Weights, and Organ Weights

All male and female rats administered 2,3-benzofluorene (2,3-BF) survived to the end of the study. One male rat in the 12 mg/kg body weight (mg/kg) group and one male rat in the 333 mg/kg group were noted to have soft feces on study day 0; no other clinical observations were noted (Appendix F). There were no significant changes in terminal body weight for male or female rats administered 2,3-BF (Table 2).

In male rats at study termination, absolute and relative liver weights had significant trend and pairwise comparisons. Although a benchmark dose (BMD) was estimated for each of these endpoints, its value was much lower (approximately 85- to 260-fold and 30- to 90-fold for absolute and relative liver weights, respectively) than would be expected given the endpoint-specific no-observed-effect level (NOEL) and lowest-observed-effect level (LOEL) values, suggesting that the BMD estimate did not accurately reflect the true potency of the effect and was likely an anomalous product of the BMD modeling approach (Table 3). The BMDs for all organ weights were reviewed by a subject matter expert for anomalous modeling results (i.e., when the traditional statistics are notably different from the estimated BMD values). Significant trend and pairwise comparisons were not observed in absolute or relative heart, right kidney, or left kidney weights (Appendix F).

In female rats at study termination, a significant increase in absolute and relative liver weights occurred in dose groups ≥37 mg/kg; both endpoints had positive trends (Table 3). The BMD and benchmark dose lower confidence limit (BMD_L) for increased absolute liver weight was 24.928 (7.768) mg/kg. A BMD (BMD_L) for increased relative liver weights was not determined because no viable model was available. Significant trend and pairwise comparisons were not observed in absolute or relative heart, right kidney, or left kidney weights (Appendix F).

Table 2. Summary of Body Weights of Male and Female Rats Administered 2,3-Benzofluorene for Five Days

Study Day[a,b]	0 mg/kg	0.15 mg/kg	0.5 mg/kg	1.4 mg/kg	4 mg/kg	12 mg/kg	37 mg/kg	111 mg/kg	333 mg/kg	1,000 mg/kg	BMD_{1Std} (mg/kg)	BMD_{L1Std} (mg/kg)
Male												
n	10	5	5	5	5	5	5	5	5	5	NA	NA
0	307.8 ± 5.7	306.6 ± 3.9	313.6 ± 4.8	311.9 ± 3.0	305.7 ± 7.4	307.4 ± 6.7	302.4 ± 9.4	302.0 ± 5.4	305.6 ± 5.7	305.4 ± 5.6	ND	ND
5	324.0 ± 6.3	320.2 ± 3.9	325.9 ± 3.2	328.0 ± 3.4	326.4 ± 8.4	319.0 ± 7.6	315.9 ± 9.2	310.8 ± 6.0	318.8 ± 6.7	316.2 ± 6.6	ND	ND
Female												
n	10	5	5	5	5	5	5	5	5	5	NA	NA
0	210.5 ± 5.9	210.1 ± 7.4	211.2 ± 4.4	220.8 ± 5.4	211.6 ± 7.7	214.8 ± 6.4	211.4 ± 6.1	214.0 ± 0.9	206.5 ± 4.2	209.6 ± 3.0	ND	ND
5	215.4 ± 5.7	213.2 ± 8.4	216.0 ± 6.7	228.2 ± 4.9	216.3 ± 9.2	218.6 ± 5.9	215.5 ± 5.6	220.7 ± 3.3	210.1 ± 5.8	211.2 ± 2.1	ND	ND

BMD_{1Std} = benchmark dose corresponding to a benchmark response set to one standard deviation from the mean; BMD_{L1Std} = benchmark dose lower confidence limit corresponding to a benchmark response set to one standard deviation from the mean; NA = not applicable; ND = not determined.
[a]Data are displayed as mean ± standard error of the mean; body weight data are presented in grams.
[b]Statistical analysis performed by the Jonckheere (trend) and Williams or Dunnett (pairwise) tests.

Table 3. Summary of Liver Weights of Male and Female Rats Administered 2,3-Benzofluorene for Five Days

Endpoint[a,b,c]	0 mg/kg	0.15 mg/kg	0.5 mg/kg	1.4 mg/kg	4 mg/kg	12 mg/kg	37 mg/kg	111 mg/kg	333 mg/kg	1,000 mg/kg	BMD_{1Std} (mg/kg)	BMD_{L1Std} (mg/kg)
Male												
n	10	5	5	5	5	5	5	5	5	5	NA	NA
Terminal Body Wt. (g)	324.0 ± 6.3	320.2 ± 3.9	325.9 ± 3.2	328.0 ± 3.4	326.4 ± 8.4	319.0 ± 7.6	315.9 ± 9.2	310.8 ± 6.0	318.8 ± 6.7	316.2 ± 6.6	ND	ND
Liver												
Absolute (g)	12.68 ± 0.38**	12.46 ± 0.43	12.14 ± 0.33	14.42 ± 0.39	13.16 ± 0.46	12.84 ± 0.73	12.82 ± 0.58	13.19 ± 0.23	15.48 ± 0.51**	14.89 ± 0.66**	1.283[d]	0.821[d]
Relative (mg/g)[e]	39.11 ± 0.75**	38.88 ± 0.98	37.25 ± 0.87	43.96 ± 1.16	40.33 ± 0.86	40.14 ± 1.40	40.51 ± 0.84	42.47 ± 0.45*	48.53 ± 0.78**	47.02 ± 1.31**	1.254[d]	0.844[d]
Female												
n	10	5	5	5	5	5	5	5	5	5	NA	NA
Terminal Body Wt. (g)	215.4 ± 5.7	213.2 ± 8.4	216.0 ± 6.7	228.2 ± 4.9	216.3 ± 9.2	218.6 ± 5.9	215.5 ± 5.6	220.7 ± 3.3	210.1 ± 5.8	211.2 ± 2.1	ND	ND
Liver												
Absolute (g)	7.66 ± 0.25**	7.63 ± 0.63	7.90 ± 0.36	8.44 ± 0.38	7.99 ± 0.44	8.05 ± 0.31	8.92 ± 0.48*	9.28 ± 0.28**	8.73 ± 0.37**	9.38 ± 0.12**	24.928	7.768
Relative (mg/g)	35.55 ± 0.51**	35.56 ± 1.72	36.53 ± 0.64	36.91 ± 1.13	36.88 ± 0.69	36.80 ± 0.50	41.39 ± 1.99**	42.01 ± 0.68**	41.53 ± 1.17**	44.40 ± 0.36**	NVM	NVM

Statistical significance for a dosed group indicates a significant pairwise test compared to the vehicle control group. Statistical significance for the vehicle control group indicates a significant trend test.
*Statistically significant at $p \leq 0.05$; **$p \leq 0.01$.
BMD_{1Std} = benchmark dose corresponding to a benchmark response set to one standard deviation from the mean; BMD_{L1Std} = benchmark dose lower confidence limit corresponding to a benchmark response set to one standard deviation from the mean; NA = not applicable; ND = not determined; NVM = nonviable model.
[a]Descriptions of organ weight endpoints and changes are provided in Appendix E.
[b]Data are displayed as mean ± standard error of the mean.
[c]Statistical analysis performed by the Jonckheere (trend) and Williams or Dunnett (pairwise) tests.
[d]BMD values are much lower than would be expected given the lowest-observed-effect level and no-observed-effect level values, suggesting that the BMD estimates do not accurately reflect the true potency of the effect of these endpoints and are likely an anomalous product of the BMD modeling approach.
[e]Relative organ weights (organ weight-to-body weight ratios) are given as mg organ weight/g body weight.

Clinical Pathology

Cholesterol concentration in male and female rats had a positive trend with significant pairwise comparisons in the ≥333 mg/kg and the 1,000 mg/kg groups, respectively, with a BMD (BMD_L) of 288.242 (226.534) mg/kg in female rats (Table 4). In male rats, a BMD (BMD_L) was not determined because no viable model was available. Globulin concentration had a positive trend with significant pairwise comparisons in the ≥333 mg/kg male rats; a BMD (BMD_L) was not determined because no viable model was available. In female rats, alkaline phosphatase activity had a positive trend with significant pairwise comparisons in dose groups ≥111 mg/kg; a BMD (BMD_L) was not determined because no viable model was available. In female rats, globulin concentration had a positive trend with a significant decrease in the lowest dose group; these changes were minimal and considered to be due to biological variability. The BMDs for all clinical pathology endpoints were reviewed by a subject matter expert for anomalous modeling results (i.e., when the traditional statistics are notably different from the estimated BMD values).

In both male and female rats, the reticulocyte count had a negative trend and significant pairwise comparisons in dose groups ≥37 mg/kg and ≥111 mg/kg, respectively, with a BMD (BMD_L) of 11.837 (6.978) mg/kg in male rats (Table 5). In female rats, a BMD (BMD_L) was not determined because no viable model was available. In addition, platelet count had a positive trend with a significant pairwise comparison in the 1,000 mg/kg male rats; a BMD (BMD_L) was not determined because no viable model was available. Eosinophil counts in both male and female rats had significant trend and pairwise comparisons. Although a BMD was estimated for each of these endpoints, these values were much lower (approximately 90- to 280-fold and 25- to 75-fold in male and female rats, respectively) than would be expected given the endpoint-specific NOEL and LOEL values, suggesting that the BMD estimate did not accurately reflect the true potency of the effect and was likely an anomalous product of the BMD modeling approach.

In male rats, total thyroxine concentration had a negative trend and significant pairwise comparisons in the ≥333 mg/kg groups with a BMD (BMD_L) of 61.426 (24.276) mg/kg (Table 6). Thyroid stimulating hormone concentration (TSH) had a positive trend and significant pairwise comparisons in dose groups ≥111 mg/kg with a BMD (BMD_L) of 44.526 (19.298) mg/kg. In female rats, TSH had a positive trend and significant pairwise comparisons in the ≥37 mg/kg groups with a BMD (BMD_L) of 1.078 (0.267) mg/kg.

Table 4. Summary of Select Clinical Chemistry Data for Male and Female Rats Administered 2,3-Benzofluorene for Five Days

Endpoint[a,b]	0 mg/kg	0.15 mg/kg	0.5 mg/kg	1.4 mg/kg	4 mg/kg	12 mg/kg	37 mg/kg	111 mg/kg	333 mg/kg	1,000 mg/kg	BMD_{1Std} (mg/kg)	BMD_{L1Std} (mg/kg)
Male												
n	10	5	5	5	5	5	5	5	5	5	NA	NA
Globulin (g/dL)	2.15 ± 0.07**	2.16 ± 0.05	2.24 ± 0.15	2.12 ± 0.10	2.18 ± 0.02	2.20 ± 0.04	2.26 ± 0.04	2.26 ± 0.07	2.30 ± 0.06*	2.30 ± 0.04*	NVM	NVM
Cholesterol (mg/dL)	114.9 ± 5.9**	115.2 ± 2.2	119.6 ± 13.6	112.2 ± 8.0	123.0 ± 4.8	114.2 ± 3.4	117.8 ± 9.3	123.4 ± 5.9	131.0 ± 3.4*	163.6 ± 7.1**	NVM	NVM
Female												
n	10	5	5	5	5	5	5	5	5	5	NA	NA
Globulin (g/dL)	1.93 ± 0.07*	1.66 ± 0.02*	1.88 ± 0.05	1.88 ± 0.04	1.86 ± 0.08	1.84 ± 0.05	2.04 ± 0.09	1.94 ± 0.05	1.90 ± 0.09	1.98 ± 0.05	36.678	13.695
Cholesterol (mg/dL)	105.0 ± 5.3**	97.8 ± 5.8	100.8 ± 7.1	88.6 ± 4.7	101.0 ± 3.8	109.0 ± 12.2	123.8 ± 10.4	105.6 ± 5.5	120.8 ± 6.0	162.4 ± 8.5**	288.242	226.543
Alkaline Phosphatase (IU/L)	201.3 ± 13.1**	198.8 ± 11.9	216.2 ± 38.8	210.0 ± 19.9	218.4 ± 10.1	208.4 ± 7.4	222.8 ± 25.0	240.0 ± 9.3*	241.4 ± 5.7*	272.2 ± 18.2**	NVM	NVM

Statistical significance for a dosed group indicates a significant pairwise test compared to the vehicle control group. Statistical significance for the vehicle control group indicates a significant trend test.
*Statistically significant at $p \leq 0.05$; **$p \leq 0.01$.
BMD_{1Std} = benchmark dose corresponding to a benchmark response set to one standard deviation from the mean; BMD_{L1Std} = benchmark dose lower confidence limit corresponding to a benchmark response set to one standard deviation from the mean; NA = not applicable; NVM = nonviable model.
[a]Data are displayed as mean ± standard error of the mean.
[b]Statistical analysis performed by the Jonckheere (trend) and Shirley or Dunn (pairwise) tests.

Table 5. Summary of Select Hematology Data for Male and Female Rats Administered 2,3-Benzofluorene for Five Days

Endpoint[a,b]	0 mg/kg	0.15 mg/kg	0.5 mg/kg	1.4 mg/kg	4 mg/kg	12 mg/kg	37 mg/kg	111 mg/kg	333 mg/kg	1,000 mg/kg	BMD_{1Std} (mg/kg)	BMD_{L1Std} (mg/kg)
Male												
n	9[c]	5	5	5	5	5	5	5	5	4[d]	NA	NA
Reticulocytes (10^3/µL)	244.7 ± 7.2**	247.2 ± 21.3	232.6 ± 12.8	212.3 ± 12.5	258.3 ± 14.2	210.8 ± 14.1	168.7 ± 8.8**	147.0 ± 11.0**	138.5 ± 6.7**	122.4 ± 14.9**	11.837	6.978
Platelets (10^3/µL)	869 ± 50*	1,029 ± 59	926 ± 24	954 ± 80	904 ± 159	975 ± 27	877 ± 85	883 ± 65	1,061 ± 42[e]	1,178 ± 30**	NVM	NVM
Eosinophils (10^3/µL)	0.10 ± 0.02**	0.07 ± 0.01	0.09 ± 0.02	0.22 ± 0.14[f]	0.10 ± 0.01	0.06 ± 0.01	0.08 ± 0.03	0.06 ± 0.02	0.05 ± 0.01*	0.04 ± 0.00**	1.194[g]	0.522[g]
Female												
n	8[h]	5	5	5	5	5	5	5	4[c]	5	NA	NA
Reticulocytes (10^3/µL)	227.2 ± 15.8**	254.5 ± 12.1	210.6 ± 15.5	210.8 ± 25.0	225.4 ± 17.0	209.2 ± 3.8	188.0 ± 11.4	177.3 ± 10.9*	134.5 ± 16.0**	138.8 ± 15.9**	NVM	NVM
Eosinophils (10^3/µL)	0.08 ± 0.01**	0.08 ± 0.02	0.08 ± 0.01	0.09 ± 0.02	0.07 ± 0.02	0.05 ± 0.01	0.04 ± 0.01	0.08 ± 0.02	0.03 ± 0.01**	0.04 ± 0.01*	4.428[g]	1.564[g]

Statistical significance for a dosed group indicates a significant pairwise test compared to the vehicle control group. Statistical significance for the vehicle control group indicates a significant trend test.
*Statistically significant at $p \leq 0.05$; **$p \leq 0.01$.
BMD_{1Std} = benchmark dose corresponding to a benchmark response set to one standard deviation from the mean; BMD_{L1Std} = benchmark dose lower confidence limit corresponding to a benchmark response set to one standard deviation from the mean; NA = not applicable; NVM = nonviable model.
[a]Data are displayed as mean ± standard error of the mean.
[b]Statistical analysis performed by the Jonckheere (trend) and Shirley or Dunn (pairwise) tests.
[c]One sample from the indicated dose groups had a clot present and was not analyzed.
[d]One sample in the indicated dose group was empty.
[e]One value for platelets in the 333 mg/kg group was excluded; it was an outlier.
[f]One value for eosinophils in the 1.4 mg/kg group was excluded due to analysis concerns.
[g]BMD values are much lower than would be expected given the lowest-observed-effect level and no-observed-effect level values, suggesting that the BMD estimates do not accurately reflect the true potency of the effect of these endpoints and are likely an anomalous product of the BMD modeling approach.
[h]Two samples in the indicated dose group had a clot present and were not analyzed.

Table 6. Summary of Select Hormone Data for Male and Female Rats Administered 2,3-Benzofluorene for Five Days

Endpoint[a,b]	0 mg/kg	0.15 mg/kg	0.5 mg/kg	1.4 mg/kg	4 mg/kg	12 mg/kg	37 mg/kg	111 mg/kg	333 mg/kg	1,000 mg/kg	BMD_{1Std} (mg/kg)	BMD_{L1Std} (mg/kg)
Male												
n	8[c]	5	5	4[d]	5	5	4[d]	3[c]	4[d]	3[c]	NA	NA
TSH (ng/mL)	2.950 ± 0.617**	3.760 ± 1.448	4.260 ± 0.701	3.275 ± 1.121	2.760 ± 0.354	3.900 ± 1.020	4.525 ± 0.945	7.033 ± 0.639**	7.500 ± 1.073**	7.233 ± 1.011*	44.526	19.298
Total T4 (μg/dL)	2.80 ± 0.20**	2.59 ± 0.24	2.71 ± 0.22	3.16 ± 0.25	2.82 ± 0.39	2.72 ± 0.28	2.53 ± 0.35	1.97 ± 0.23	1.65 ± 0.12**	1.72 ± 0.16*	61.426	24.276
Female												
n	6[e]	5	5	5	4[d]	5	4[d]	5	4[d]	5	NA	NA
TSH (ng/mL)	2.783 ± 0.326**	3.360 ± 0.853	2.940 ± 0.687	4.200 ± 0.476	4.025 ± 0.333	4.260 ± 0.493	4.475 ± 0.239*	5.480 ± 1.102*	4.900 ± 1.360*	8.600 ± 1.762**	1.078	0.267

Statistical significance for a dosed group indicates a significant pairwise test compared to the vehicle control group. Statistical significance for the vehicle control group indicates a significant trend test.
*Statistically significant at $p \leq 0.05$; **$p \leq 0.01$.
BMD_{1Std} = benchmark dose corresponding to a benchmark response set to one standard deviation from the mean; BMD_{L1Std} = benchmark dose lower confidence limit corresponding to a benchmark response set to one standard deviation from the mean; NA = not applicable; TSH = thyroid stimulating hormone; total T4 = total thyroxine.
[a]Data are displayed as mean ± standard error of the mean.
[b]Statistical analysis performed by the Jonckheere (trend) and Shirley or Dunn (pairwise) tests.
[c]Two samples in the indicated dose groups did not have sufficient specimen volume available for analysis.
[d]One sample in the indicated dose groups did not have sufficient specimen volume available for analysis.
[e]Four samples in the indicated dose group did not have sufficient specimen volume available for analysis.

Internal Dose Assessment

For the 4 and 37 mg/kg groups, 2,3-BF plasma concentrations were determined at 2 and 24 hours following the last dose administered on study day 4 to male and female rats. Average 2,3-BF concentrations are given in Table 7. In general, average plasma concentrations in male rats were higher than those in female rats, demonstrating some sex differences. At 2 hours following administration to male and female rats—as the administered dose increased from 4 to 37 mg/kg (a ninefold increase)—there was a less-than-proportional increase (approximately four- to sixfold) in the average 2,3-BF plasma concentration, suggesting changes in the absorption, distribution, metabolism, and excretion processes (e.g., lower absorption and/or induction of metabolism and clearance pathways) as the dose increased. At 24 hours postdose, the concentration decreased across each dosed group, with values falling below or close to the limit of detection (LOD = 1.8 ng/mL) of the analytical method in female and male rats, respectively. Half-lives estimated using the data from these two time points for male rats were 25.3 and 4.4 hours, respectively, for the 4 and 37 mg/kg groups. Half-lives could not be estimated for female rats because the concentration at 24 hours in both dosed groups was below LOD.

Table 7. Summary of Plasma Concentration Data for Male and Female Rats Administered 2,3-Benzofluorene for Five Days[a]

	4 mg/kg	37 mg/kg
n	3	3
Male		
2 Hours Postdose (ng/mL)	8.52 ± 1.64	49.3 ± 17.5
24 Hours Postdose (ng/mL)	4.67 ± 3.77	1.53 ± 0.630
Female		
2 Hours Postdose (ng/mL)	3.62 ± 1.27	15.5 ± 3.20
24 Hours Postdose (ng/mL)	BD	BD

If over 20% of the animals in a group are above the limit of detection, then half the limit of detection value is substituted for values that are below it.
BD = below detection; group did not have over 20% of its values above the limit of detection so mean and standard error were not calculated.
[a]Data are displayed as mean ± standard error of the mean.

Apical Endpoint Benchmark Dose Summary

A summary of the calculated BMDs for each toxicological endpoint is provided in Table 8. The endpoint-specific LOEL and NOEL are included and could be informative for endpoints that lack a calculated BMD either because no viable model was available or because the estimated BMD was below the lower limit of extrapolation (<0.050 mg/kg).

Table 8. BMD, BMD_L, LOEL, and NOEL Summary for Apical Endpoints, Sorted by BMD or LOEL from Low to High

Endpoint	BMD_{1Std} (mg/kg)	BMD_{L1Std} (mg/kg)	LOEL (mg/kg)[a]	NOEL (mg/kg)	Direction of Change
Male					
Reticulocytes	11.837	6.978	37	12	DOWN

Endpoint	BMD_{1Std} (mg/kg)	BMD_{L1Std} (mg/kg)	LOEL (mg/kg)[a]	NOEL (mg/kg)	Direction of Change
Thyroid Stimulating Hormone	44.526	19.298	111	37	UP
Total Thyroxine	61.426	24.276	333	111	DOWN
Relative Liver Weight	UREP[b]	UREP[b]	**111**	37	–[b]
Absolute Liver Weight	UREP	UREP	**333**	111	–
Cholesterol	NVM	NVM	**333**	111	UP
Eosinophils	UREP	UREP	**333**	111	–
Globulin	NVM	NVM	**333**	111	UP
Platelets	NVM	NVM	**1,000**	333	UP
Female					
Thyroid Stimulating Hormone	1.078	0.267	37	12	UP
Absolute Liver Weight	24.928	7.768	37	12	UP
Globulin	36.678	13.695	0.15	ND	–[c]
Cholesterol	288.242	226.543	1,000	333	UP
Relative Liver Weight	NVM	NVM	**37**	12	UP
Alkaline Phosphatase	NVM	NVM	**111**	37	UP
Reticulocytes	NVM	NVM	**111**	37	DOWN
Eosinophils	UREP	UREP	**333**	111	–

BMD_{1Std} = benchmark dose corresponding to a benchmark response set to one standard deviation from the mean; BMD_{L1Std} = benchmark dose lower confidence limit corresponding to a benchmark response set to one standard deviation from the mean; LOEL = lowest-observed-effect level; NOEL = no-observed-effect level; UREP = unreliable estimate of potency is a label based on review by a subject matter expert and rejection of BMD modeling results; NVM = nonviable model, defined as a modeling result that does not meet prespecified fit criteria and hence is deemed unreliable; ND = not determined.
[a]Values in bold text indicate the LOEL of endpoints for which a BMD could not be calculated.
[b]BMD values are much lower than would be expected given the endpoint-specific LOEL and NOEL values, suggesting that the BMD estimates do not accurately reflect the true potency of the effect of these endpoints and are likely an anomalous product of the BMD modeling approach.
[c]Statistically significant finding was not attributed to chemical exposure.

Gene Set Benchmark Dose Analysis

Chemical-induced alterations in liver and kidney gene transcript expression were examined to determine those gene sets most sensitive to 2,3-BF exposure. To that end, BMD analysis of transcripts and gene sets (Gene Ontology [GO] biological process) was conducted to determine the potency of the chemical to elicit gene expression changes in the liver and kidney. This analysis used transcript-level BMD data to assess an aggregate score of gene set potency (median transcript BMD) and enrichment.

The “active” gene sets in the liver and kidney with the lowest BMD median values are shown in Table 9 and Table 10, respectively. The gene sets in Table 9 and Table 10 should be interpreted with caution from the standpoint of the underlying biological mechanism and any relationship to toxicity or toxic agents referenced in the GO term definitions. The data primarily should be considered a metric of potency for chemical-induced transcriptional changes (i.e., a concerted biological change) that could serve as a surrogate of estimated biological potency and, by extension, toxicological potency when more definitive toxicological data are unavailable.

No gene sets in the liver of male or female rats had estimated BMD median values <0.050 mg/kg. In male rats, the most sensitive GO biological processes for which a BMD value could be reliably calculated were regulation of ossification (GO:0030278) and kidney development (GO:0001822) with median BMDs (BMD_Ls) of 5.660 (2.158) and 5.765 (1.618) mg/kg, respectively. In female rats, the most sensitive GO biological processes for which a BMD value could be reliably calculated were DNA conformation change (GO:0071103) and chromosome organization (GO:0051276), both with a median BMD (BMD_L) of 1.874 (0.497) mg/kg.

No gene sets in the kidney of male or female rats had estimated BMD median values <0.050 mg/kg. In male rats, the most sensitive GO biological processes for which a BMD value could be reliably calculated were brain development (GO:0007420) and cellular process involved in reproduction in multicellular organism (GO:0022412) with median BMDs (BMD_Ls) of 6.167 (1.732) and 12.334 (3.464) mg/kg, respectively. In female rats, the most sensitive GO biological processes for which a BMD value could be reliably calculated were regulation of fibroblast proliferation (GO:0048145) and negative regulation of fibroblast proliferation (GO:0048147) with median BMDs (BMD_Ls) of 14.574 (7.161) and 14.763 (9.430) mg/kg, respectively. The full list of affected gene sets in the liver and kidney of male and female rats can be found in Appendix F.

Table 9. Top 10 Liver Gene Ontology Biological Process Gene Sets Ranked by Potency of Perturbation, Sorted by Benchmark Dose Median[a]

Category Name	No. of Active Genes/ Platform Genes in Gene Set	% Gene Set Coverage	Active Genes	BMD_{1std} Median of Gene Set Transcripts (mg/kg)	Median BMD_{L1Std}–BMD_{U1Std} (mg/kg)	Genes with Changed Direction Up	Genes with Changed Direction Down
Male							
GO:0030278 regulation of ossification	3/58	5%	*Mgp*; *Id2*; *Cebpd*	5.660	2.158–16.350	1	2
GO:0001822 kidney development	4/53	8%	*Zfp354a*; *Id2*; *Egr1*; *Aldh1a1*	5.765	1.618–28.410	2	2
GO:1903707 negative regulation of hemopoiesis	3/48	6%	*Pf4*; *Nfe2l2*; *Id2*	6.642	3.406–13.468	3	0
GO:0071372 cellular response to follicle-stimulating hormone stimulus	3/19	16%	*Inhba*; *Id2*; *Egr1*	8.263	1.517–45.905	1	2
GO:0014910 regulation of smooth muscle cell migration	3/50	6%	*Nfe2l2*; *Igfbp3*; *Egr1*	8.263	3.406–45.905	1	2

Category Name	No. of Active Genes/ Platform Genes in Gene Set	% Gene Set Coverage	Active Genes	BMD_{1std} Median of Gene Set Transcripts (mg/kg)	Median BMD_{L1Std}–BMD_{U1Std} (mg/kg)	Genes with Changed Direction Up	Genes with Changed Direction Down
GO:0097237 cellular response to toxic substance	4/80	5%	*Ugt2b1*; *Nqo1*; *Nfe2l2*; *Egr1*	16.188	7.373–41.474	3	1
GO:0045598 regulation of fat cell differentiation	3/42	7%	*Trib3*; *Lpl*; *Id2*	16.895	6.465–58.991	2	1
GO:0034976 response to endoplasmic reticulum stress	3/58	5%	*Trib3*; *Nfe2l2*; *Ccnd1*	16.895	6.465–58.991	2	1
GO:0009404 toxin metabolic process	3/17	18%	*Nfe2l2*; *Cyp1a1*; *Akr7a3*	19.850	12.797–32.354	3	0
GO:0098754 detoxification	5/58	9%	*Nqo1*; *Nfe2l2*; *Gstm2*; *Gsr*; *Akr7a3*	19.850	12.797–32.354	5	0
Female							
GO:0071103 DNA conformation change	3/32	9%	*Top2a*; *Mcm6*; *Mcm2*	1.874	0.497–9.530	3	0
GO:0051276 chromosome organization	5/90	6%	*Top2a*; *Mcm6*; *Mcm2*; *Kif22*; *Gar1*	1.874	0.497–9.530	5	0
GO:0006281 DNA repair	4/74	5%	*Mms22l*; *Mcm6*; *Mcm2*; *Kif22*	2.822	0.727–15.213	4	0
GO:0000724 double-strand break repair via homologous recombination	3/15	20%	*Mms22l*; *Mcm6*; *Mcm2*	3.769	0.956–20.896	3	0
GO:0006259 DNA metabolic process	7/119	6%	*Top2a*; *Mms22l*; *Mcm6*; *Mcm2*; *Kif22*; *Gar1*; *Cyp1b1*	3.769	0.956–20.896	7	0
GO:0009066 aspartate family amino acid metabolic process	4/14	29%	*Phgdh*; *Bhmt*; *Asns*; *Aass*	5.933	2.674–26.084	2	2

Category Name	No. of Active Genes/ Platform Genes in Gene Set	% Gene Set Coverage	Active Genes	BMD_{1std} Median of Gene Set Transcripts (mg/kg)	Median BMD_{L1Std}–BMD_{U1Std} (mg/kg)	Genes with Changed Direction Up	Genes with Changed Direction Down
GO: 0042178 xenobiotic catabolic process	5/60	8%	*Pck2*; *Hba-A1*; *Hba-A2*; *Gpx1*; *Aass*	8.004	2.700–37.943	1	4
GO:0010639 negative regulation of organelle organization	5/89	6%	*Top2a*; *Mcm2*; *Insig1*; *Gpx1*; *Gclc*	8.004	2.700–25.225	4	1
GO:0045833 negative regulation of lipid metabolic process	3/34	9%	*Insig1*; *Esr1*; *Apoc3*	12.540	3.750–51.297	1	2
GO:1901607 alpha-amino acid biosynthetic process	6/19	32%	*Pycr1*; *Psat1*; *Phgdh*; *Bhmt*; *Asns*; *Aass*	16.607	6.379–70.854	4	2

BMD_{1Std} = benchmark dose corresponding to a benchmark response set to one standard deviation from the mean; BMD_{L1Std} = benchmark dose lower confidence limit corresponding to a benchmark response set to one standard deviation from the mean; BMD_{U1Std} = benchmark dose upper confidence limit corresponding to a benchmark response set to one standard deviation from the mean; GO = Gene Ontology.

[a]Definitions of GO terms were adapted from the Gene Ontology Resource.[27] Official gene symbols from the Rat Genome Database[28] are shown in the "Active Genes" column.

GO process description version: https://doi.org/10.22427/NTP-DATA-002-00600-0002-000-0.

GO:0030278 regulation of ossification: Any process that modulates the frequency, rate, or extent of ossification, the formation of bone or of a bony substance or the conversion of fibrous tissue or of cartilage into bone or a bony substance.

GO:0001822 kidney development: The process whose specific outcome is the progression of the kidney over time, from its formation to the mature structure. The kidney is an organ that filters the blood and/or excretes the end products of body metabolism in the form of urine.

GO:1903707 negative regulation of hemopoiesis: Any process that stops, prevents, or reduces the frequency, rate, or extent of hemopoiesis.

GO:0071372 cellular response to follicle-stimulating hormone stimulus: Any process that results in a change in state or activity of a cell (in terms of movement, secretion, enzyme production, gene expression, etc.) as a result of a follicle-stimulating hormone stimulus.

GO:0014910 regulation of smooth muscle cell migration: Any process that modulates the frequency, rate, or extent of smooth muscle cell migration.

GO:0097237 cellular response to toxic substance: Any process that results in a change in state or activity of a cell (in terms of movement, secretion, enzyme production, gene expression, etc.) as a result of a toxic stimulus.

GO:0045598 regulation of fat cell differentiation: Any process that modulates the frequency, rate, or extent of adipocyte differentiation.

GO:0034976 response to endoplasmic reticulum stress: Any process that results in a change in state or activity of a cell (in terms of movement, secretion, enzyme production, gene expression, etc.) as a result of a stress acting at the endoplasmic reticulum. ER stress usually results from the accumulation of unfolded or misfolded proteins in the ER lumen.

GO:0009404 toxin metabolic process: The chemical reactions and pathways involving a toxin, a poisonous compound (typically a protein) that is produced by cells or organisms and that can cause disease when introduced into the body or tissues of an organism.

GO:0098754 detoxification: Any process that reduces or removes the toxicity of a toxic substance. These may include transport of the toxic substance away from sensitive areas and to compartments or complexes whose purpose is sequestration of the toxic substance.

GO:0071103 DNA conformation change: A cellular process that results in a change in the spatial configuration of a DNA molecule. A conformation change can bend DNA, or alter the twist, writhe, or linking number of a DNA molecule.

GO:0051276 chromosome organization: A process that is carried out at the cellular level that results in the assembly, arrangement of constituent parts, or disassembly of chromosomes, structures composed of a very long molecule of DNA and associated proteins that carries hereditary information. This term covers covalent modifications at the molecular level as well as spatial relationships among the major components of a chromosome.
GO:0006281 DNA repair: The process of restoring DNA after damage. Genomes are subject to damage by chemical and physical agents in the environment (e.g., UV and ionizing radiations, chemical mutagens, fungal and bacterial toxins) and by free radicals or alkylating agents endogenously generated in metabolism. DNA is also damaged because of errors during its replication. A variety of different DNA repair pathways have been reported that include direct reversal, base excision repair, nucleotide excision repair, photoreactivation, bypass, double-strand break repair pathway, and mismatch repair pathway.
GO:0000724 double-strand break repair via homologous recombination: The error-free repair of a double-strand break in DNA in which the broken DNA molecule is repaired using homologous sequences. A strand in the broken DNA searches for a homologous region in an intact chromosome to serve as the template for DNA synthesis. The restoration of two intact DNA molecules results in the exchange, reciprocal or nonreciprocal, of genetic material between the intact DNA molecule and the broken DNA molecule.
GO:0006259 DNA metabolic process: Any cellular metabolic process involving deoxyribonucleic acid. This is one of the two main types of nucleic acid, consisting of a long, unbranched macromolecule formed from one, or more commonly, two, strands of linked deoxyribonucleotides.
GO:0009066 aspartate family amino acid metabolic process: The chemical reactions and pathways involving amino acids of the aspartate family, comprising asparagine, aspartate, lysine, methionine and threonine.
GO: 0042178 xenobiotic catabolic process: The chemical reactions and pathways resulting in the breakdown of a xenobiotic compound (a compound foreign to the organism exposed to it). It may be synthesized by another organism (like ampicillin) or it can be a synthetic chemical.
GO:0010639 negative regulation of organelle organization: Any process that decreases the frequency, rate, or extent of a process involved in the formation, arrangement of constituent parts, or disassembly of an organelle.
GO:0045833 negative regulation of lipid metabolic process: Any process that stops, prevents, or reduces the frequency, rate, or extent of the chemical reactions and pathways involving lipids.
GO:1901607 alpha-amino acid biosynthetic process: The chemical reactions and pathways resulting in the formation of an alpha-amino acid.

Table 10. Top 10 Kidney Gene Ontology Biological Process Gene Sets Ranked by Potency of Perturbation, Sorted by Benchmark Dose Median[a]

Category Name	No. of Active Genes/ Platform Genes in Gene Set	% Gene Set Coverage	Active Genes	BMD_{1std} Median of Gene Set Transcripts (mg/kg)	Median BMD_{L1Std}–BMD_{U1Std} (mg/kg)	Genes with Changed Direction Up	Genes with Changed Direction Down
Male							
GO:0007420 brain development	4/79	5%	*Top2a*; *Nefh*; *Hmgcs2*; *Cxcr4*	6.167	1.732–23.263	0	4
GO:0022412 cellular process involved in reproduction in multicellular organism	3/60	5%	*Top2a*; *Kif20a*; *Cxcr4*	12.334	3.464–46.527	0	3
GO:1903046 meiotic cell-cycle process	3/29	10%	*Top2a*; *Nuf2*; *Kif20a*	12.334	4.279–46.527	0	3
GO:0051301 cell division	4/79	5%	*Top2a*; *Nuf2*; *Mcm5*; *Kif20a*	12.417	6.977–42.166	0	4
GO:0000281 mitotic cytokinesis	3/16	19%	*Kif23*; *Kif20a*; *Ect2*	31.232	15.546–67.195	0	3
GO:0046685 response to arsenic-containing substance	3/20	15%	*Zfand2a*; *Nefh*; *Cyp1a1*	49.045	39.236–64.853	2	1
GO:0098754 detoxification	3/58	5%	*Nqo1*; *Mt1*; *Akr7a3*	62.795	48.749–87.647	2	1
GO:0001822 kidney development	4/53	8%	*Zfp354a*; *Rgn*; *Hmgcs2*; *Cyp4a8*	102.787	65.463–185.933	1	3
GO:1901570 fatty acid derivative biosynthetic process	3/23	13%	*Hmgcs2*; *Cyp4a8*; *Cyp2c11*	106.351	59.870–208.329	1	2
GO:0031099 regeneration	7/120	6%	*Socs3*; *Rgn*; *Nrep*; *Nefh*; *Dmbt1*; *Cebpb*; *Alas2*	114.178	79.082–204.229	2	5
Female							
GO:0048145 regulation of fibroblast proliferation	4/41	10%	*Thy1*; *Mmp9*; *Gstp1*; *Ccna2*	14.574	7.161–41.985	1	3

Category Name	No. of Active Genes/ Platform Genes in Gene Set	% Gene Set Coverage	Active Genes	BMD_{1std} Median of Gene Set Transcripts (mg/kg)	Median BMD_{L1Std}–BMD_{U1Std} (mg/kg)	Genes with Changed Direction Up	Genes with Changed Direction Down
GO:0048147 negative regulation of fibroblast proliferation	3/11	27%	*Thy1*; *Mmp9*; *Gstp1*	14.763	9.430–25.720	1	2
GO:0001523 retinoid metabolic process	4/19	21%	*Ppard*; *Cyp26b1*; *Cyp1a1*; *Ces1d*	15.537	9.574–28.025	2	2
GO:0006694 steroid biosynthetic process	4/49	8%	*Dhcr7*; *Cyp26b1*; *Cyp1a1*; *Ces1d*	15.537	9.574–28.025	2	2
GO:0031100 animal organ regeneration	4/80	5%	*Vwf*; *Mki67*; *Gstp1*; *Ccna2*	17.220	5.859–67.215	1	3
GO:0008610 lipid biosynthetic process	7/122	6%	*Ppard*; *Gstp1*; *Dhcr7*; *Cyp26b1*; *Cyp1a1*; *Ces1d*; *Alox15*	18.187	10.018–36.727	3	4
GO:0016101 diterpenoid metabolic process	5/26	19%	*Ppard*; *Pgr*; *Cyp26b1*; *Cyp1a1*; *Ces1d*	18.187	10.018–36.727	2	3
GO:0034754 cellular hormone metabolic process	3/41	7%	*Ugt2b7*; *Cyp26b1*; *Cyp1a1*	18.187	10.018–36.727	3	0
GO:1902653 secondary alcohol biosynthetic process	3/22	14%	*Dhcr7*; *Cyp26b1*; *Ces1d*	18.187	10.018–36.727	1	2
GO:0071241 cellular response to inorganic substance	6/113	5%	*Nqo1*; *Mmp9*; *Ect2*; *Cyp1a1*; *Ccna2*; *Alox15*	20.033	8.435–72.186	2	4

BMD_{1Std} = benchmark dose corresponding to a benchmark response set to one standard deviation from the mean; BMD_{L1Std} = benchmark dose lower confidence limit corresponding to a benchmark response set to one standard deviation from the mean; BMD_{U1Std} = benchmark dose upper confidence limit corresponding to a benchmark response set to one standard deviation from the mean; GO = Gene Ontology.

[a]Definitions of GO terms were adapted from the Gene Ontology Resource.[27] Official gene symbols from the Rat Genome Database[28] are shown in the "Active Genes" column.

GO process description version: https://doi.org/10.22427/NTP-DATA-002-00600-0002-000-0.

GO:0007420 brain development: The process whose specific outcome is the progression of the brain over time, from its formation to the mature structure. Brain development begins with patterning events in the neural tube and ends with the mature

structure that is the center of thought and emotion. The brain is responsible for the coordination and control of bodily activities and the interpretation of information from the senses (sight, hearing, smell, etc.).
GO:0022412 cellular process involved in reproduction in multicellular organism: A process, occurring at the cellular level, which is involved in the reproductive function of a multicellular organism.
GO:1903046 meiotic cell-cycle process: A process that is part of the meiotic cell cycle.
GO:0051301 cell division: The process resulting in division and partitioning of components of a cell to form more cells; may or may not be accompanied by the physical separation of a cell into distinct, individually membrane-bounded daughter cells.
GO:0000281 mitotic cytokinesis: A cell-cycle process that results in the division of the cytoplasm of a cell after mitosis, resulting in the separation of the original cell into two daughter cells.
GO:0046685 response to arsenic-containing substance: Any process that results in a change in state or activity of a cell or an organism (in terms of movement, secretion, enzyme production, gene expression, etc.) as a result of an arsenic stimulus from compounds containing arsenic, including arsenates, arsenites, and arsenides.
GO:0098754 detoxification: Any process that reduces or removes the toxicity of a toxic substance. These may include transport of the toxic substance away from sensitive areas and to compartments or complexes whose purpose is sequestration of the toxic substance.
GO:0001822 kidney development: The process whose specific outcome is the progression of the kidney over time, from its formation to the mature structure. The kidney is an organ that filters the blood and/or excretes the end products of body metabolism in the form of urine.
GO:1901570 fatty acid derivative biosynthetic process: The chemical reactions and pathways resulting in the formation of fatty acid derivative.
GO:0031099 regeneration: The regrowth of a lost or destroyed body part, such as an organ or tissue. This process may occur via renewal, repair, and/or growth alone (i.e., increase in size or mass).
GO:0048145 regulation of fibroblast proliferation: Any process that modulates the frequency, rate, or extent of multiplication or reproduction of fibroblast cells.
GO:0048147 negative regulation of fibroblast proliferation: Any process that stops, prevents, or reduces the frequency, rate, or extent of multiplication or reproduction of fibroblast cells.
GO:0001523 retinoid metabolic process: The chemical reactions and pathways involving retinoids, any member of a class of isoprenoids that contain or are derived from four prenyl groups linked head-to-tail. Retinoids include retinol and retinal and structurally similar natural derivatives or synthetic compounds but need not have vitamin A activity.
GO:0006694 steroid biosynthetic process: The chemical reactions and pathways resulting in the formation of steroids, compounds with a 1,2,cyclopentanoperhydrophenanthrene nucleus; includes de novo formation and steroid interconversion by modification.
GO:0031100 animal organ regeneration: The regrowth of a lost or destroyed animal organ.
GO:0008610 lipid biosynthetic process: The chemical reactions and pathways resulting in the formation of lipids, compounds soluble in an organic solvent but not, or sparingly, in an aqueous solvent.
GO:0016101 diterpenoid metabolic process: The chemical reactions and pathways involving diterpenoid compounds, which are terpenoids with four isoprene units.
GO:0034754 cellular hormone metabolic process: The chemical reactions and pathways involving any hormone, naturally occurring substances secreted by specialized cells that affect the metabolism or behavior of other cells possessing functional receptors for the hormone, as carried out by individual cells.
GO:1902653 secondary alcohol biosynthetic process: The chemical reactions and pathways resulting in the formation of secondary alcohol.
GO:0071241 cellular response to inorganic substance: Any process that results in a change in state or activity of a cell (in terms of movement, secretion, enzyme production, gene expression, etc.) as a result of an inorganic substance stimulus.

Gene Benchmark Dose Analysis

The top 10 genes based on BMD potency in the liver and kidney (fold change >|2|, significant Williams trend test, global goodness-of-fit p value >0.1, and $BMD_U/BMD_L \leq 40$) are shown in Table 11 and Table 12. As with the GO analysis, the biological or toxicological significance of the changes in gene expression shown in Table 11 and Table 12 should be interpreted with caution. The data primarily should be considered a metric of potency for chemical-induced transcriptional changes that could serve as a conservative surrogate of estimated biological potency, and by extension toxicological potency, when more definitive toxicological data are unavailable.

No liver genes in male or female rats had estimated BMD median values <0.050 mg/kg. In male rats, the most sensitive upregulated genes with a calculated BMD were *G0s2* (G0/G1switch 2), *Trib3* (tribbles pseudokinase 3), *Akr7a3* (aldo-keto reductase family 7 member A3), *Nqo1* (NAD(P)H quinone dehydrogenase 1), and *Ephx1* (epoxide hydrolase 1) with BMDs (BMD_Ls) of

3.451 (1.074), 16.895 (6.465), 19.850 (12.797), 24.112 (16.415), and 24.878 (15.487) mg/kg, respectively. The most sensitive genes exhibiting a decrease in expression were *Zfp354a* (zinc finger protein 354A), *Tsku* (tsukushi, small leucine rich proteoglycan), *Egr1* (early growth response 1), *C7* (complement C7), and *Loc100911558*/*Spink1l* (serine peptidase inhibitor, Kazal type 1-like) with BMDs (BMD_{LS}) of 3.267 (1.720), 6.126 (1.466), 8.263 (1.517), 13.843 (5.329), and 26.630 (12.428) mg/kg, respectively.

In female rats, the most sensitive upregulated liver genes with a calculated BMD were *Kif22* (kinesin family member 22), *Anln* (anillin, actin binding protein), *Anlnl1* (anillin, actin binding protein-like 1), *Asns* (asparagine synthetase [glutamine-hydrolyzing]), and *Nr1d2* (nuclear receptor subfamily 1, group D, member 2) with BMDs (BMD_{LS}) of 0.962 (0.282), 3.325 (1.105), 3.325 (1.105), 6.056 (2.744), and 9.460 (2.213) mg/kg, respectively. The most sensitive genes exhibiting a decrease in expression were *Car3* (carbonic anhydrase 3), *Aass* (aminoadipate-semialdehyde synthase), *A2m* (alpha-2-macroglobulin), *Loc100911545*/*A2m* (alpha-2-macroglobulin), and *Sez6* (seizure-related 6 homolog) with BMDs (BMD_{LS}) of 3.449 (2.131), 5.811 (2.605), 8.459 (1.870), 8.459 (1.870), and 10.639 (3.960) mg/kg, respectively.

The most sensitive kidney gene in male rats, exhibiting a decrease in expression, was *Nefh* (neurofilament heavy chain) with an estimated BMD median value <0.050 mg/kg. The most sensitive downregulated genes with a calculated BMD were *Top2a* (DNA topoisomerase II alpha), *Ect2* (epithelial cell transforming 2), *Hmgcs2* (3-hydroxy-3-methylglutaryl-CoA synthase 2), *Nfil3* (nuclear factor, interleukin 3 regulated), *Mt1* (metallothionein 1), and *Cyp2c11* (cytochrome P450, subfamily 2, polypeptide 11) with BMDs (BMD_{LS}) of 12.334 (3.464), 31.232 (16.473), 106.351 (59.870), 121.321 (82.552), 168.588 (103.554), and 216.743 (139.563) mg/kg, respectively. The most sensitive upregulated genes with a calculated BMD were *Nqo1* (NAD(P)H quinone dehydrogenase 1), *Cyp1a1* (cytochrome P450, family 1, subfamily a, polypeptide 1), and *Rassf1* (Ras association domain family member 1) with BMDs (BMD_{LS}) of 40.551 (21.583), 49.045 (39.236), and 903.848 (608.514) mg/kg, respectively.

None of the top 10 most sensitive kidney genes in female rats had estimated BMD median values <0.050 mg/kg. The most sensitive upregulated genes with a calculated BMD were *Cyp1a1* (cytochrome P450, family 1, subfamily a, polypeptide 1), *Gstp1* (glutathione S-transferase pi 1), *Cyp26b1* (cytochrome P450, family 26, subfamily b, polypeptide 1), and *Nqo1* (NAD(P)H quinone dehydrogenase 1) with BMDs (BMD_{LS}) of 12.886 (9.131), 14.763 (9.430), 18.187 (10.018), and 25.681 (7.739) mg/kg, respectively. The most sensitive genes exhibiting a decrease in expression were *Vwf* (von Willebrand factor), *Abcb1b* (ATP-binding cassette, subfamily B (MDR/TAP), member 1B), *Npas2* (neuronal PAS domain protein 2), *Arntl* (aryl hydrocarbon receptor nuclear translocator-like), *C4a* (complement C4A), and *Loc103689965*/*C4a* (complement C4A) with BMDs (BMD_{LS}) of 19.676 (4.116), 20.794 (8.254), 21.088 (11.331), 22.913 (11.412), 24.209 (8.100), and 24.209 (8.100) mg/kg, respectively.

Table 11. Top 10 Liver Genes Ranked by Potency of Perturbation, Sorted by Benchmark Dose Median[a]

Gene Symbol	Entrez Gene IDs	Probe IDs[b]	BMD_{1Std} (BMD_{L1std}–BMD_{U1std}) in mg/kg	Maximum Fold Change	Direction of Expression Change
Male					
Zfp354a	24522	ZFP354A_10203	3.267 (1.720–6.668)	6.5	DOWN
G0s2	289388	G0S2_32729	3.451 (1.074–14.322)	2.1	UP
Tsku	308843	TSKU_10094	6.126 (1.466–41.334)	2.4	DOWN
Egr1	24330	EGR1_8533	8.263 (1.517–45.905)	5.3	DOWN
C7	117517	C7_8179	13.843 (5.329–41.896)	2.5	DOWN
Trib3	246273	TRIB3_10079	16.895 (6.465–58.991)	2.3	UP
Akr7a3	26760	AKR7A3_8015	19.850 (12.797–32.354)	4.1	UP
Nqo1	24314	NQO1_33055	24.112 (16.415–37.043)	4.8	UP
Ephx1	25315	EPHX1_8567	24.878 (15.487–41.380)	2.6	UP
Loc100911558/Spink1l	100911558	SPINK1_32461	26.630 (12.428–61.587)	2.0	DOWN
Female					
Kif22	293502	KIF22_8963	0.962 (0.282–4.473)	2.1	UP
Anln	363031	ANLN_32599	3.325 (1.105–12.281)	2.1	UP
Anlnl1	307056	ANLN_32599	3.325 (1.105–12.281)	2.1	UP
Car3	54232	CAR3_8196	3.449 (2.131–6.021)	6.8	DOWN
Aass	296925	AASS_7936	5.811 (2.605–14.079)	2.3	DOWN
Asns	25612	ASNS_8091	6.056 (2.744–14.335)	3.5	UP
A2m	24153	A2M_7932	8.459 (1.870–42.023)	2.8	DOWN
Loc100911545/A2m	100911545	A2M_7932	8.459 (1.870–42.023)	2.8	DOWN
Nr1d2	259241	NR1D2_9358	9.460 (2.213–49.422)	2.2	UP
Sez6	192247	SEZ6_9819	10.639 (3.960–29.500)	3.7	DOWN

BMD_{1Std} = benchmark dose corresponding to a benchmark response set to one standard deviation from the mean; BMD_{L1Std} = benchmark dose lower confidence limit corresponding to a benchmark response set to one standard deviation from the mean; BMD_{U1Std} = benchmark dose upper confidence limit corresponding to a benchmark response set to one standard deviation from the mean.

[a]Descriptions of orthologous human genes are shown due to the increased detail available in public resources such as UniprotKB[29] and Entrez Gene.[30] Gene definitions adapted from Human UniprotKB were used as the primary resource due to the greater breadth of annotation and depth of functional detail provided. Gene definitions adapted from Rat UniprotKB were used as the secondary resource if the primary source did not provide a detailed description of function. Human Entrez Gene was used as the third resource. Rat Entrez Gene was used as the fourth resource.

[b]In some cases, a probe may map to more than one gene, resulting in duplicate reporting of that probe mapped to different genes.

Gene definition version: https://doi.org/10.22427/NTP-DATA-002-00600-0002-000-0.

***Zfp354a*:** Rat Uniprot function (Human *ZNF354A*): It may play a role in renal development and may also be involved in the repair of the kidney after ischemia-reperfusion or folic acid administration.

***G0s2*:** Human Uniprot function (Human *G0S2*): Promotes apoptosis by binding to BCL2, hence preventing the formation of protective BCL2-BAX heterodimers. {ECO0000269|PubMed19706769}.

***Tsku*:** Human Uniprot function (Human *TSKU*): Contributes to various developmental events and other processes such as wound healing and cholesterol homeostasis through its interactions with multiple signaling pathways. Wnt signaling inhibitor, which competes with WNT2B for binding to Wnt receptor FZD4 and represses WNT2B-dependent development of the peripheral eye. Plays a role in regulating the hair cycle by controlling TGFB1 signaling. Required for the development of the anterior commissure in the brain by inhibiting neurite outgrowth. Essential for terminal differentiation of hippocampal neural stem cells.

Plays a role in regulating bone elongation and bone mass by modulating growth plate chondrocyte function and overall body size. Required for development of the inner ear through its involvement in stereocilia formation in inner hair cells. Facilitates wound healing by inhibiting secretion of TGFB1 from macrophages, which prevents myofibroblast differentiation, maintaining inflammatory cell quiescence. Plays a role in cholesterol homeostasis by reducing circulating high-density lipoprotein cholesterol, lowering cholesterol efflux capacity and decreasing cholesterol-to-bile acid conversion in the liver. In one study, shown to negatively regulate sympathetic innervation in brown fat, leading to reduced energy expenditure. In another study, shown not to affect brown fat thermogenic capacity, body weight gain, or glucose homeostasis.
***Egr1*:** Human Uniprot function (Human *EGR1*): Transcriptional regulator (PubMed20121949). Recognizes and binds to the DNA sequence 5'-GCG(T/G)GGGCG-3'(EGR-site) in the promoter region of target genes (by similarity). Binds double-stranded target DNA, irrespective of the cytosine methylation status (PubMed25258363, PubMed25999311). Regulates the transcription of numerous target genes, and thereby plays an important role in regulating the response to growth factors, DNA damage, and ischemia. Plays a role in the regulation of cell survival, proliferation and cell death. Activates expression of p53/TP53 and TGFB1, and thereby helps prevent tumor formation. Required for normal progress through mitosis and normal proliferation of hepatocytes after partial hepatectomy. Mediates responses to ischemia and hypoxia; regulates the expression of proteins such as IL1B and CXCL2 that are involved in inflammatory processes and development of tissue damage after ischemia. Regulates biosynthesis of luteinizing hormone (LHB) in the pituitary (by similarity). Regulates the amplitude of the expression rhythms of clock genes ARNTL/BMAL1, PER2 and NR1D1 in the liver via the activation of PER1 (clock repressor) transcription. Regulates the rhythmic expression of core clock gene ARNTL/BMAL1 in the suprachiasmatic nucleus (SCN) (by similarity). {ECO0000250|UniProtKBP08046, ECO0000269|PubMed20121949, ECO0000269|PubMed25258363, ECO0000269|PubMed25999311}.
***C7*:** Human Uniprot function (Human *C7*): Constituent of the membrane attack complex (MAC) that plays a key role in the innate and adaptive immune response by forming pores in the plasma membrane of target cells. C7 serves as a membrane anchor.
***Trib3*:** Human Uniprot function (Human *TRIB3*): Inactive protein kinase which acts as a regulator of the integrated stress response (ISR), a process for adaptation to various stress (PubMed15781252, PubMed15775988). Inhibits the transcriptional activity of DDIT3/CHOP and is involved in DDIT3/CHOP-dependent cell death during ER stress (PubMed15781252, PubMed15775988). May play a role in programmed neuronal cell death but does not appear to affect nonneuronal cells (PubMed15781252, PubMed15775988). Acts as a negative feedback regulator of the ATF4-dependent transcription during the ISR, while TRIB3 expression is promoted by ATF4, TRIB3 protein interacts with ATF4 and inhibits ATF4 transcription activity (by similarity). Disrupts insulin signaling by binding directly to Akt kinases and blocking their activation (by similarity). May bind directly to and mask the 'Thr-308' phosphorylation site in AKT1 (by similarity). Interacts with the NF-kappa-B transactivator p65 RELA and inhibits its phosphorylation and thus its transcriptional activation activity (PubMed12736262). Interacts with MAPK kinases and regulates activation of MAP kinases (PubMed15299019). Can inhibit APOBEC3A editing of nuclear DNA (PubMed22977230). {ECO0000250|UniProtKBQ8K4K2, ECO0000269|PubMed12736262, ECO0000269|PubMed15299019, ECO0000269|PubMed15775988, ECO0000269|PubMed15781252, ECO0000269|PubMed22977230}.
***Akr7a3*:** Human Uniprot function (Human *AKR7A3*): Can reduce the dialdehyde protein-binding form of aflatoxin B1 (AFB1) to the nonbinding AFB1 dialcohol. May be involved in protection of liver against the toxic and carcinogenic effects of AFB1, a potent hepatocarcinogen. {ECO0000269|PubMed18416522}.
***Nqo1*:** Human Uniprot function (Human *NQO1*): The enzyme apparently serves as a quinone reductase in connection with conjugation reactions of hydroquinons involved in detoxification pathways as well as in biosynthetic processes such as the vitamin K-dependent gamma-carboxylation of glutamate residues in prothrombin synthesis.
***Ephx1*:** Human Uniprot function (Human *EPHX1*): Biotransformation enzyme that catalyzes the hydrolysis of arene and aliphatic epoxides to less reactive and more water soluble dihydrodiols by the trans addition of water (by similarity). Plays a role in the metabolism of endogenous lipids such as epoxide-containing fatty acids (PubMed22798687). Metabolizes the abundant endocannabinoid 2-arachidonoylglycerol (2-AG) to free arachidonic acid (AA) and glycerol (PubMed24958911). {ECO0000250|UniProtKBP07687, ECO0000269|PubMed22798687, ECO0000269|PubMed24958911}.
***LOC100911558*/*Spink1l*:** Human Uniprot function (Human *SPINK1*): Serine protease inhibitor which exhibits anti-trypsin activity (PubMed7142173). In the pancreas, protects against trypsin-catalyzed premature activation of zymogens (by similarity). {ECO0000250|UniProtKBP09036, ECO0000269|PubMed7142173}. FUNCTION In the male reproductive tract, binds to sperm heads where it modulates sperm capacitance by inhibiting calcium uptake and nitrogen oxide (NO) production. {ECO0000250|UniProtKBP09036}.
***Kif22*:** Human Uniprot function (Human *KIF22*): Kinesin family member that is involved in spindle formation and the movements of chromosomes during mitosis and meiosis. Binds to microtubules and to DNA (by similarity). Plays a role in congression of laterally attached chromosomes in NDC80-depleted cells (PubMed25743205). {ECO0000250|UniProtKBQ9I869, ECO0000269|PubMed25743205}.
***Anln*:** Human Uniprot function (Human *ANLN*): Required for cytokinesis (PubMed16040610). Essential for the structural integrity of the cleavage furrow and for completion of cleavage furrow ingression. Plays a role in bleb assembly during metaphase and anaphase of mitosis (PubMed23870127). May play a significant role in podocyte cell migration (PubMed24676636). {ECO0000269|PubMed10931866, ECO0000269|PubMed12479805, ECO0000269|PubMed15496454, ECO0000269|PubMed16040610, ECO0000269|PubMed16357138, ECO0000269|PubMed23870127, ECO0000269|PubMed24676636}.
***Anlnl1*:** Human Uniprot function (Human *ANLN*): Required for cytokinesis (PubMed16040610). Essential for the structural integrity of the cleavage furrow and for completion of cleavage furrow ingression. Plays a role in bleb assembly during metaphase and anaphase of mitosis (PubMed23870127). May play a significant role in podocyte cell migration (PubMed24676636). {ECO0000269|PubMed10931866, ECO0000269|PubMed12479805, ECO0000269|PubMed15496454,

ECO0000269|PubMed16040610, ECO0000269|PubMed16357138, ECO0000269|PubMed23870127, ECO0000269|PubMed24676636}.
***Car3*:** Human Uniprot function (Human *CA3*): Reversible hydration of carbon dioxide.
***Aass*:** Human Uniprot function (Human *AASS*): Bifunctional enzyme that catalyzes the first two steps in lysine degradation. The N-terminal and the C-terminal contain lysine-ketoglutarate reductase and saccharopine dehydrogenase activity, respectively.
***Asns*:** Human Entrez Gene Summary (Human *ASNS*): The protein encoded by this gene is involved in the synthesis of asparagine. This gene complements a mutation in the temperature-sensitive hamster mutant ts11, which blocks progression through the G1 phase of the cell cycle at nonpermissive temperature. Alternatively spliced transcript variants have been described for this gene. [provided by RefSeq, May 2010]
***A2m*:** Human Uniprot function (Human *A2M*): Is able to inhibit all four classes of proteinases by a unique 'trapping' mechanism. This protein has a peptide stretch, called the 'bait region' which contains specific cleavage sites for different proteinases. When a proteinase cleaves the bait region, a conformational change is induced in the protein which traps the proteinase. The entrapped enzyme remains active against low molecular weight substrates (activity against high molecular weight substrates is greatly reduced). Following cleavage in the bait region, a thioester bond is hydrolyzed and mediates the covalent binding of the protein to the proteinase.
***LOC100911545*/*A2m*:** Human Uniprot function (Human *A2M*): Is able to inhibit all four classes of proteinases by a unique 'trapping' mechanism. This protein has a peptide stretch, called the 'bait region' which contains specific cleavage sites for different proteinases. When a proteinase cleaves the bait region, a conformational change is induced in the protein which traps the proteinase. The entrapped enzyme remains active against low molecular weight substrates (activity against high molecular weight substrates is greatly reduced). Following cleavage in the bait region, a thioester bond is hydrolyzed and mediates the covalent binding of the protein to the proteinase.
***Nr1d2*:** Human Uniprot function (Human *NR1D2*): Transcriptional repressor which coordinates circadian rhythm and metabolic pathways in a heme-dependent manner. Integral component of the complex transcription machinery that governs circadian rhythmicity and forms a critical negative limb of the circadian clock by directly repressing the expression of core clock components ARNTL/BMAL1 and CLOCK. Also regulates genes involved in metabolic functions, including lipid metabolism and the inflammatory response. Acts as a receptor for heme which stimulates its interaction with the NCOR1/HDAC3 corepressor complex, enhancing transcriptional repression. Recognizes two classes of DNA response elements within the promoter of its target genes and can bind to DNA as either monomers or homodimers, depending on the nature of the response element. Binds as a monomer to a response element composed of the consensus half-site motif 5'-[A/G]GGTCA-3' preceded by an A/T-rich 5' sequence (RevRE), or as a homodimer to a direct repeat of the core motif spaced by two nuclegotides (RevDR-2). Acts as a potent competitive repressor of ROR alpha (RORA) function and also negatively regulates the expression of NR1D1. Regulates lipid and energy homeostasis in the skeletal muscle via repression of genes involved in lipid metabolism and myogenesis including CD36, FABP3, FABP4, UCP3, SCD1 and MSTN. Regulates hepatic lipid metabolism via the repression of APOC3. Represses gene expression at a distance in macrophages by inhibiting the transcription of enhancer-derived RNAs (eRNAs). In addition to its activity as a repressor, can also act as a transcriptional activator. Acts as a transcriptional activator of the sterol regulatory element-binding protein 1 (SREBF1) and the inflammatory mediator interleukin-6 (IL6) in the skeletal muscle (by similarity). Plays a role in the regulation of circadian sleep/wake cycle; essential for maintaining wakefulness during the dark phase or active period (by similarity). Key regulator of skeletal muscle mitochondrial function; negatively regulates the skeletal muscle expression of core clock genes and genes involved in mitochondrial biogenesis, fatty acid beta-oxidation and lipid metabolism (by similarity). May play a role in the circadian control of neutrophilic inflammation in the lung (by similarity). {ECO0000250|UniProtKBQ60674, ECO0000269|PubMed17892483, ECO0000269|PubMed17996965}.
***Sez6*:** Human Uniprot function (Human *SEZ6*): May play a role in cell-cell recognition and in neuronal membrane signaling. Seems to be important for the achievement of the necessary balance between dendrite elongation and branching during the elaboration of a complex dendritic arbor. Involved in the development of appropriate excitatory synaptic connectivity (by similarity). {ECO0000250}.

Table 12. Top 10 Kidney Genes Ranked by Potency of Perturbation, Sorted by Benchmark Dose Median[a]

Gene Symbol	Entrez Gene IDs	Probe IDs	BMD_{1Std} (BMD_{L1std}–BMD_{U1std}) in mg/kg	Maximum Fold Change	Direction of Expression Change
Male					
Nefh	24587	NEFH_33218	<0.050[b] (NR)	2.4	DOWN
Top2a	360243	TOP2A_10059	12.334 (3.464-46.527)	2.8	DOWN
Ect2	361921	ECT2_8523	31.232 (16.473-67.195)	2.2	DOWN
Nqo1	24314	NQO1_33055	40.551 (21.583-79.355)	2.6	UP
Cyp1a1	24296	CYP1A1_8415	49.045 (39.236-64.853)	8.8	UP
Hmgcs2	24450	HMGCS2_8812	106.351 (59.870-208.329)	2.6	DOWN
Nfil3	114519	NFIL3_9304	121.321 (82.552-229.790)	2.2	DOWN
Mt1	24567	MT1A_9255	168.588 (103.554-1208.950)	2.1	DOWN
Cyp2c11	29277	CYP2C11_32593	216.743 (139.563-368.944)	8.4	DOWN
Rassf1	363140	RASSF1_32475	903.848 (608.514-1171.720)	2.7	UP
Female					
Cyp1a1	24296	CYP1A1_8415	12.886 (9.131-19.323)	15.5	UP
Gstp1	24426	GSTP1_8762	14.763 (9.430-25.720)	3.5	UP
Cyp26b1	312495	CYP26B1_8418	18.187 (10.018-36.727)	2.1	UP
Vwf	116669	VWF_32396	19.676 (4.116-94.078)	2.1	DOWN
Abcb1b	24646	ABCB1B_7939	20.794 (8.254-57.212)	6.2	DOWN
Npas2	316351	NPAS2_9350	21.088 (11.331-43.562)	3.1	DOWN
Arntl	29657	ARNTL_8086	22.913 (11.412-50.159)	3.4	DOWN
C4a	24233	C4A_8176	24.209 (8.100-89.537)	2.3	DOWN
Loc103689965/C4a	103689965	C4A_8176	24.209 (8.100-89.537)	2.3	DOWN
Nqo1	24314	NQO1_33055	25.681 (7.739-86.121)	2.2	UP

BMD_{1Std} = benchmark dose corresponding to a benchmark response set to one standard deviation from the mean; BMD_{L1Std} = benchmark dose lower confidence limit corresponding to a benchmark response set to one standard deviation from the mean; BMD_{U1Std} = benchmark dose upper confidence limit corresponding to a benchmark response set to one standard deviation from the mean; NR = the BMD_{L1Std}–BMD_{U1Std} range is not reportable because the BMD median is below the lower limit of extrapolation (<1/3 of the lowest nonzero dose tested).

[a]Descriptions of orthologous human genes are shown due to the increased detail available in public resources such as UniprotKB[29] and Entrez Gene.[30] Gene definitions adapted from Human UniprotKB were used as the primary resource due to the greater breadth of annotation and depth of functional detail provided. Gene definitions adapted from Rat UniprotKB were used as the secondary resource if the primary source did not provide a detailed description of function. Human Entrez Gene was used as the third resource. Rat Entrez Gene was used as the fourth resource.

[b]<0.050 = a best-fit model was identified and a BMD was estimated that was <1/3 of the lowest nonzero dose tested.

Gene definition version: https://doi.org/10.22427/NTP-DATA-002-00600-0002-000-0.

***Nefh*:** Human Uniprot function (Human *NEFH*): Neurofilaments usually contain three intermediate filament proteins NEFL, NEFM, and NEFH which are involved in the maintenance of neuronal caliber. NEFH has an important function in mature axons that is not subserved by the two smaller NF proteins. May additionally cooperate with the neuronal intermediate filament proteins PRPH and INA to form neuronal filamentous networks (by similarity). {ECO0000250|UniProtKBP19246}.

***Top2a*:** Human Uniprot function (Human *TOP2A*): Key decatenating enzyme that alters DNA topology by binding to two double-stranded DNA molecules, generating a double-stranded break in one of the strands, passing the intact strand through the broken strand, and religating the broken strand (PubMed17567603, PubMed18790802, PubMed22013166, PubMed22323612). May play a role in regulating the period length of ARNTL/BMAL1 transcriptional oscillation (by similarity).

{ECO0000250|UniProtKBQ01320, ECO0000269|PubMed17567603, ECO0000269|PubMed18790802, ECO0000269|PubMed22013166, ECO0000269|PubMed22323612}.
***Ect2*:** Human Uniprot function (Human *ECT2*): Guanine nucleotide exchange factor (GEF) that catalyzes the exchange of GDP for GTP. Promotes guanine nucleotide exchange on the Rho family members of small GTPases, like RHOA, RHOC, RAC1, and CDC42. Required for signal transduction pathways involved in the regulation of cytokinesis. Component of the centralspindlin complex that serves as a microtubule-dependent and Rho-mediated signaling required for the myosin contractile ring formation during the cell-cycle cytokinesis. Regulates the translocation of RHOA from the central spindle to the equatorial region. Plays a role in the control of mitotic spindle assembly; regulates the activation of CDC42 in metaphase for the process of spindle fibers attachment to kinetochores before chromosome congression. Involved in the regulation of epithelial cell polarity; participates in the formation of epithelial tight junctions in a polarity complex PARD3-PARD6-protein kinase PRKCQ-dependent manner. Plays a role in the regulation of neurite outgrowth. Inhibits phenobarbital (PB)-induced NR1I3 nuclear translocation. Stimulates the activity of RAC1 through its association with the oncogenic PARD6A-PRKCI complex in cancer cells, thereby acting to coordinately drive tumor cell proliferation and invasion. Also stimulates genotoxic stress-induced RHOB activity in breast cancer cells leading to their cell death. {ECO0000269|PubMed10579713, ECO0000269|PubMed14645260, ECO0000269|PubMed15254234, ECO0000269|PubMed15545273, ECO0000269|PubMed15642749, ECO0000269|PubMed16103226, ECO0000269|PubMed16170345, ECO0000269|PubMed16236794, ECO0000269|PubMed16495035, ECO0000269|PubMed19129481, ECO0000269|PubMed19468300, ECO0000269|PubMed19617897, ECO0000269|PubMed21189248, ECO0000269|PubMed21373644, ECO0000269|PubMed25068414, ECO0000269|PubMed31888991}.
***Nqo1*:** Human Uniprot function (Human *NQO1*): The enzyme apparently serves as a quinone reductase in connection with conjugation reactions of hydroquinons involved in detoxification pathways as well as in biosynthetic processes, such as the vitamin K-dependent gamma-carboxylation of glutamate residues in prothrombin synthesis.
***Cyp1a1*:** Human Uniprot function (Human *CYP1A1*): A cytochrome P450 monooxygenase involved in the metabolism of various endogenous substrates, including fatty acids, steroid hormones and vitamins (PubMed11555828, PubMed14559847, PubMed12865317, PubMed15805301, PubMed15041462, PubMed18577768, PubMed19965576, PubMed20972997, PubMed10681376). Mechanistically, uses molecular oxygen inserting one oxygen atom into a substrate, and reducing the second into a water molecule, with two electrons provided by NADPH via cytochrome P450 reductase (NADPH–hemoprotein reductase) (PubMed11555828, PubMed14559847, PubMed12865317, PubMed15805301, PubMed15041462, PubMed18577768, PubMed19965576, PubMed20972997, PubMed10681376). Catalyzes the hydroxylation of carbon-hydrogen bonds. Exhibits high catalytic activity for the formation of hydroxyestrogens from estrone (E1) and 17beta-estradiol (E2), namely 2-hydroxy E1 and E2, as well as D-ring hydroxylated E1 and E2 at the C15-alpha and C16-alpha positions (PubMed11555828, PubMed14559847, PubMed12865317, PubMed15805301). Displays different regioselectivities for polyunsaturated fatty acids (PUFA) hydroxylation (PubMed15041462, PubMed18577768). Catalyzes the epoxidation of double bonds of certain PUFA (PubMed15041462, PubMed19965576, PubMed20972997). Converts arachidonic acid toward epoxyeicosatrienoic acid (EET) regioisomers, 8,9-, 11,12-, and 14,15-EET that function as lipid mediators in the vascular system (PubMed20972997). Displays an absolute stereoselectivity in the epoxidation of eicosapentaenoic acid producing the 17(R),18(S) enantiomer (PubMed15041462). May play an important role in all-*trans* retinoic acid biosynthesis in extrahepatic tissues. Catalyzes two successive oxidative transformation of all-*trans*-retinol to all-*trans*-retinal and then to the active form all-*trans* retinoic acid (PubMed10681376). May also participate in eicosanoids metabolism by converting hydroperoxide species into oxo metabolites (lipoxygenase-like reaction, NADPH-independent) (PubMed21068195). {ECO0000269|PubMed10681376, ECO0000269|PubMed11555828, ECO0000269|PubMed12865317, ECO0000269|PubMed14559847, ECO0000269|PubMed15041462, ECO0000269|PubMed15805301, ECO0000269|PubMed18577768, ECO0000269|PubMed19965576, ECO0000269|PubMed20972997, ECO0000269|PubMed21068195}.
***Hmgcs2*:** Human Uniprot function (Human *HMGCS2*): Catalyzes the first irreversible step in ketogenesis, condensing acetyl-CoA to acetoacetyl-CoA to form HMG-CoA, which is converted by HMG-CoA reductase (HMGCR) into mevalonate. {ECO0000269|PubMed11228257, ECO0000269|PubMed23751782, ECO0000269|PubMed29597274}.
***Nfil3*:** Human Uniprot function (Human *NFIL3*): Acts as a transcriptional regulator that recognizes and binds to the sequence 5'-[GA]TTA[CT]GTAA[CT]-3', a sequence present in many cellular and viral promoters. Represses transcription from promoters with activating transcription factor (ATF) sites. Represses promoter activity in osteoblasts (by similarity). Represses transcriptional activity of PER1 (by similarity). Represses transcriptional activity of PER2 via the B-site on the promoter (by similarity). Activates transcription from the interleukin-3 promoter in T-cells. Competes for the same consensus-binding site with PAR DNA-binding factors (DBP, HLF, and TEF) (by similarity). Component of the circadian clock that acts as a negative regulator for the circadian expression of PER2 oscillation in the cell-autonomous core clock (by similarity). Protects pro-B cells from programmed cell death (by similarity). Represses the transcription of CYP2A5 (by similarity). Positively regulates the expression and activity of CES2 by antagonizing the repressive action of NR1D1 on CES2 (by similarity). {ECO0000250|UniProtKBO08750, ECO0000269|PubMed1620116, ECO0000269|PubMed7565758, ECO0000269|PubMed8836190}.
***Mt1*:** Human Uniprot function (Human *MT1A*): Metallothioneins have a high content of cysteine residues that bind various heavy metals; these proteins are transcriptionally regulated by both heavy metals and glucocorticoids.
***Cyp2c11*:** Human Uniprot function (Human *CYP2C9*): A cytochrome P450 monooxygenase involved in the metabolism of various endogenous substrates, including fatty acids and steroids (PubMed7574697, PubMed9866708, PubMed9435160, PubMed12865317, PubMed15766564, PubMed19965576, PubMed21576599). Mechanistically, uses molecular oxygen inserting one oxygen atom into a substrate, and reducing the second into a water molecule, with two electrons provided by NADPH via cytochrome P450 reductase (NADPH--hemoprotein reductase) (PubMed7574697, PubMed9866708, PubMed9435160, PubMed12865317, PubMed15766564, PubMed19965576, PubMed21576599). Catalyzes the epoxidation of double bonds of

polyunsaturated fatty acids (PUFA) (PubMed7574697, PubMed15766564, PubMed19965576, PubMed9866708). Catalyzes the hydroxylation of carbon-hydrogen bonds. Metabolizes cholesterol toward 25-hydroxycholesterol, a physiological regulator of cellular cholesterol homeostasis (PubMed21576599). Exhibits low catalytic activity for the formation of catechol estrogens from 17beta-estradiol (E2) and estrone (E1), namely 2-hydroxy E1 and E2 (PubMed12865317). Catalyzes bisallylic hydroxylation and hydroxylation with double-bond migration of polyunsaturated fatty acids (PUFA) (PubMed9866708, PubMed9435160). Also metabolizes plant monoterpenes such as limonene. Oxygenates (R)- and (S)-limonene to produce carveol and perillyl alcohol (PubMed11950794). Contributes to the wide pharmacokinetics variability of the metabolism of drugs such as S-warfarin, diclofenac, phenytoin, tolbutamide, and losartan (PubMed25994031). {ECO0000269|PubMed11950794, ECO0000269|PubMed12865317, ECO0000269|PubMed15766564, ECO0000269|PubMed19965576, ECO0000269|PubMed21576599, ECO0000269|PubMed25994031, ECO0000269|PubMed7574697, ECO0000269|PubMed9435160, ECO0000269|PubMed9866708}.

***Rassf1*:** Human Uniprot function (Human *RASSF1*): Potential tumor suppressor. Required for death receptor-dependent apoptosis. Mediates activation of STK3/MST2 and STK4/MST1 during Fas-induced apoptosis by preventing their dephosphorylation. When associated with MOAP1, promotes BAX conformational change and translocation to mitochondrial membranes in response to TNF and TNFSF10 stimulation. Isoform A interacts with CDC20, an activator of the anaphase-promoting complex, APC, resulting in the inhibition of APC activity and mitotic progression. Inhibits proliferation by negatively regulating cell-cycle progression at the level of G1/S-phase transition by regulating accumulation of cyclin D1 protein. Isoform C has been shown not to perform these roles, no function has been identified for this isoform. Isoform A disrupts interactions among MDM2, DAXX, and USP7, thus contributing to the efficient activation of TP53 by promoting MDM2 self-ubiquitination in cell-cycle checkpoint control in response to DNA damage. {ECO0000269|PubMed10888881, ECO0000269|PubMed11333291, ECO0000269|PubMed12024041, ECO0000269|PubMed14743218, ECO0000269|PubMed15109305, ECO0000269|PubMed15949439, ECO0000269|PubMed16510573, ECO0000269|PubMed18566590, ECO0000269|PubMed21199877}.

***Gstp1*:** Human Uniprot function (Human *GSTP1*): Conjugation of reduced glutathione to a wide number of exogenous and endogenous hydrophobic electrophiles. Involved in the formation of glutathione conjugates of both prostaglandin A2 (PGA2) and prostaglandin J2 (PGJ2) (PubMed9084911). Participates in the formation of novel hepoxilin regioisomers (PubMed21046276). Regulates negatively CDK5 activity via p25/p35 translocation to prevent neurodegeneration. {ECO0000269|PubMed21046276, ECO0000269|PubMed21668448, ECO0000269|PubMed9084911}.

***Cyp26b1*:** Human Uniprot function (Human *CYP26B1*): Involved in the metabolism of retinoic acid (RA), rendering this classical morphogen inactive through oxidation (PubMed10823918, PubMed22020119). Involved in the specific inactivation of all-*trans* retinoic acid (all-*trans* RA), with a preference for the following substrates all-*trans* RA > 9-*cis* RA > 13-*cis* RA (PubMed10823918, PubMed22020119). Generates several hydroxylated forms of RA, including 4-OH-RA, 4-oxo-RA, and 18-OH-RA (PubMed10823918). Catalyzes the hydroxylation of carbon-hydrogen bonds of atRA primarily at C-4 (PubMed10823918, PubMed22020119). Essential for postnatal survival (by similarity). Plays a central role in germ cell development acts by degrading RA in the developing testis, preventing STRA8 expression, thereby leading to delay of meiosis (by similarity). Required for the maintenance of the undifferentiated state of male germ cells during embryonic development in Sertoli cells, inducing arrest in G0 phase of the cell cycle and preventing meiotic entry (by similarity). Plays a role in skeletal development, both at the level of patterning and in the ossification of bone and the establishment of some synovial joints (PubMed22019272). {ECO0000250|UniProtKBQ811W2, ECO0000269|PubMed10823918, ECO0000269|PubMed22019272, ECO0000269|PubMed22020119}. FUNCTION Has also a significant activity in oxidation of tazarotenic acid and may therefore metabolize that xenobiotic in vivo. {ECO0000269|PubMed26937021}.

***Vwf*:** Human Uniprot function (Human *VWF*): Important in the maintenance of hemostasis, it promotes adhesion of platelets to the sites of vascular injury by forming a molecular bridge between sub-endothelial collagen matrix and platelet-surface receptor complex GPIb-IX-V. Also acts as a chaperone for coagulation factor VIII, delivering it to the site of injury, stabilizing its heterodimeric structure, and protecting it from premature clearance from plasma.

***Abcb1b*:** Human Uniprot function (Human *ABCB1*): Translocates drugs and phospholipids across the membrane (PubMed8898203, PubMed2897240, PubMed9038218). Catalyzes the flop of phospholipids from the cytoplasmic to the exoplasmic leaflet of the apical membrane. Participates mainly to the flop of phosphatidylcholine, phosphatidylethanolamine, beta-D-glucosylceramides, and sphingomyelins (PubMed8898203). Energy-dependent efflux pump responsible for decreased drug accumulation in multidrug-resistant cells (PubMed2897240, PubMed9038218). {ECO0000269|PubMed2897240, ECO0000269|PubMed8898203, ECO0000269|PubMed9038218}.

***Npas2*:** Human Uniprot function (Human *NPAS2*): Transcriptional activator that forms a core component of the circadian clock. The circadian clock, an internal time-keeping system, regulates various physiological processes through the generation of approximately 24-hour circadian rhythms in gene expression, which are translated into rhythms in metabolism and behavior. It is derived from the Latin roots ‘circa’ (about) and ‘diem’ (day) and acts as an important regulator of a wide array of physiological functions including metabolism, sleep, body temperature, blood pressure, endocrine, immune, cardiovascular, and renal function. Consists of two major components the central clock, residing in the suprachiasmatic nucleus (SCN) of the brain, and the peripheral clocks that are present in nearly every tissue and organ system. Both the central and peripheral clocks can be reset by environmental cues, also known as Zeitgebers (German for “timegivers”). The predominant Zeitgeber for the central clock is light, which is sensed by retina and signals directly to the SCN. The central clock entrains the peripheral clocks through neuronal and hormonal signals, body temperature and feeding-related cues, aligning all clocks with the external light/dark cycle. Circadian rhythms allow an organism to achieve temporal homeostasis with its environment at the molecular level by regulating gene expression to create a peak of protein expression once every 24 hours to control when a particular physiological process is most active with respect to the solar day. Transcription and translation of core clock components (CLOCK, NPAS2, ARNTL/BMAL1, ARNTL2/BMAL2, PER1, PER2, PER3, CRY1, and CRY2) plays a critical role in rhythm generation, whereas delays imposed

by post-translational modifications (PTMs) are important for determining the period (tau) of the rhythms (tau refers to the period of a rhythm and is the length, in time, of one complete cycle). A diurnal rhythm is synchronized with the day/night cycle, while the ultradian and infradian rhythms have a period shorter and longer than 24 hours, respectively. Disruptions in the circadian rhythms contribute to the pathology of cardiovascular diseases, cancer, metabolic syndromes, and aging. A transcription/translation feedback loop (TTFL) forms the core of the molecular circadian clock mechanism. Transcription factors, CLOCK or NPAS2 and ARNTL/BMAL1 or ARNTL2/BMAL2, form the positive limb of the feedback loop, act in the form of a heterodimer, and activate the transcription of core clock genes and clock-controlled genes (involved in key metabolic processes), harboring E-box elements (5'-CACGTG-3') within their promoters. The core clock genes PER1/2/3 and CRY1/2, which are transcriptional repressors, form the negative limb of the feedback loop and interact with the CLOCK|NPAS2-ARNTL/BMAL1|ARNTL2/BMAL2 heterodimer inhibiting its activity and thereby negatively regulating their own expression. This heterodimer also activates nuclear receptors NR1D1/2 and RORA/B/G, which form a second feedback loop and which activate and repress ARNTL/BMAL1 transcription, respectively. The NPAS2-ARNTL/BMAL1 heterodimer positively regulates the expression of MAOA, F7, and LDHA and modulates the circadian rhythm of daytime contrast sensitivity by regulating the rhythmic expression of adenylate cyclase type 1 (ADCY1) in the retina. NPAS2 plays an important role in sleep homeostasis and in maintaining circadian behaviors in normal light/dark and feeding conditions and in the effective synchronization of feeding behavior with scheduled food availability. Regulates the gene transcription of key metabolic pathways in the liver and is involved in DNA damage response by regulating several cell cycle and DNA repair genes. Controls the circadian rhythm of NR0B2 expression by binding rhythmically to its promoter (by similarity). Mediates the diurnal variation in the expression of GABARA1 receptor in the brain and contributes to the regulation of anxiety-like behaviors and GABAergic neurotransmission in the ventral striatum (by similarity). {ECO0000250|UniProtKBP97460, ECO0000269|PubMed11441146, ECO0000269|PubMed11441147, ECO0000269|PubMed14645221, ECO0000269|PubMed18439826, ECO0000269|PubMed18819933}.
***Arntl*:** Human Uniprot function (Human *ARNTL*): Transcriptional activator that forms a core component of the circadian clock. The circadian clock, an internal time-keeping system, regulates various physiological processes through the generation of approximately 24-hour circadian rhythms in gene expression, which are translated into rhythms in metabolism and behavior. It is derived from the Latin roots 'circa' (about) and 'diem' (day) and acts as an important regulator of a wide array of physiological functions including metabolism, sleep, body temperature, blood pressure, endocrine, immune, cardiovascular, and renal function. Consists of two major components the central clock, residing in the suprachiasmatic nucleus (SCN) of the brain, and the peripheral clocks that are present in nearly every tissue and organ system. Both the central and peripheral clocks can be reset by environmental cues, also known as Zeitgebers (German for 'timegivers'). The predominant Zeitgeber for the central clock is light, which is sensed by retina and signals directly to the SCN. The central clock entrains the peripheral clocks through neuronal and hormonal signals, body temperature, and feeding-related cues, aligning all clocks with the external light/dark cycle. Circadian rhythms allow an organism to achieve temporal homeostasis with its environment at the molecular level by regulating gene expression to create a peak of protein expression once every 24 hours to control when a particular physiological process is most active with respect to the solar day. Transcription and translation of core clock components (CLOCK, NPAS2, ARNTL/BMAL1, ARNTL2/BMAL2, PER1, PER2, PER3, CRY1, and CRY2) plays a critical role in rhythm generation, whereas delays imposed by post-translational modifications (PTMs) are important for determining the period (tau) of the rhythms (tau refers to the period of a rhythm and is the length, in time, of one complete cycle). A diurnal rhythm is synchronized with the day/night cycle, while the ultradian and infradian rhythms have a period shorter and longer than 24 hours, respectively. Disruptions in the circadian rhythms contribute to the pathology of cardiovascular diseases, cancer, metabolic syndromes, and aging. A transcription/translation feedback loop (TTFL) forms the core of the molecular circadian clock mechanism. Transcription factors, CLOCK or NPAS2 and ARNTL/BMAL1 or ARNTL2/BMAL2, form the positive limb of the feedback loop, act in the form of a heterodimer, and activate the transcription of core clock genes and clock-controlled genes (involved in key metabolic processes), harboring E-box elements (5'-CACGTG-3') within their promoters. The core clock genes PER1/2/3 and CRY1/2, which are transcriptional repressors, form the negative limb of the feedback loop and interact with the CLOCK|NPAS2-ARNTL/BMAL1|ARNTL2/BMAL2 heterodimer inhibiting its activity and thereby negatively regulating their own expression. This heterodimer also activates nuclear receptors NR1D1/2 and RORA/B/G, which form a second feedback loop and which activate and repress ARNTL/BMAL1 transcription, respectively. ARNTL/BMAL1 positively regulates myogenesis and negatively regulates adipogenesis via the transcriptional control of the genes of the canonical Wnt signaling pathway. Plays a role in normal pancreatic beta-cell function; regulates glucose-stimulated insulin secretion via the regulation of antioxidant genes NFE2L2/NRF2 and its targets SESN2, PRDX3, CCLC, and CCLM. Negatively regulates the mTORC1 signaling pathway; regulates the expression of MTOR and DEPTOR. Controls diurnal oscillations of Ly6C inflammatory monocytes; rhythmic recruitment of the PRC2 complex imparts diurnal variation to chemokine expression that is necessary to sustain Ly6C monocyte rhythms. Regulates the expression of HSD3B2, STAR, PTGS2, CYP11A1, CYP19A1, and LHCGR in the ovary and also the genes involved in hair growth. Plays an important role in adult hippocampal neurogenesis by regulating the timely entry of neural stem/progenitor cells (NSPCs) into the cell cycle and the number of cell divisions that take place prior to cell-cycle exit. Regulates the circadian expression of CIART and KLF11. The CLOCK-ARNTL/BMAL1 heterodimer regulates the circadian expression of SERPINE1/PAI1, VWF, B3, CCRN4L/NOC, NAMPT, DBP, MYOD1, PPARGC1A, PPARGC1B, SIRT1, GYS2, F7, NGFR, GNRHR, BHLHE40/DEC1, ATF4, MTA1, KLF10, and also genes implicated in glucose and lipid metabolism. Promotes rhythmic chromatin opening, regulating the DNA accessibility of other transcription factors. The NPAS2-ARNTL/BMAL1 heterodimer positively regulates the expression of MAOA, F7, and LDHA and modulates the circadian rhythm of daytime contrast sensitivity by regulating the rhythmic expression of adenylate cyclase type 1 (ADCY1) in the retina. The preferred binding motif for the CLOCK-ARNTL/BMAL1 heterodimer is 5'-CACGTGA-3', which contains a flanking Ala residue in addition to the canonical 6-nucleotide E-box sequence (PubMed23229515). CLOCK specifically binds to the half-site 5'-CAC-3', while ARNTL binds to the half-site 5'-GTGA-3' (PubMed23229515). The CLOCK-ARNTL/BMAL1 heterodimer also recognizes the noncanonical E-box motifs 5'-AACGTGA-3' and 5'-CATGTGA-3' (PubMed23229515). Essential for the

rhythmic interaction of CLOCK with ASS1 and plays a critical role in positively regulating CLOCK-mediated acetylation of ASS1 (PubMed28985504). Plays a role in protecting against lethal sepsis by limiting the expression of immune checkpoint protein CD274 in macrophages in a PKM2-dependent manner (by similarity). Regulates the diurnal rhythms of skeletal muscle metabolism via transcriptional activation of genes promoting triglyceride synthesis (DGAT2) and metabolic efficiency (COQ10B) (by similarity). {ECO0000250|UniProtKBQ9WTL8, ECO0000269|PubMed11441146, ECO0000269|PubMed12738229, ECO0000269|PubMed18587630, ECO0000269|PubMed23785138, ECO0000269|PubMed23955654, ECO0000269|PubMed24005054, ECO0000269|PubMed28985504}.
***C4a*:** Human Uniprot function (Human *C4A*): Nonenzymatic component of C3 and C5 convertases and thus essential for the propagation of the classical complement pathway. Covalently binds to immunoglobulins and immune complexes and enhances the solubilization of immune aggregates and the clearance of IC through CR1 on erythrocytes. C4A isotype is responsible for effective binding to form amide bonds with immune aggregates or protein antigens, while C4B isotype catalyzes the transacylation of the thioester carbonyl group to form ester bonds with carbohydrate antigens. Derived from proteolytic degradation of complement C4, C4a anaphylatoxin is a mediator of local inflammatory process. It induces the contraction of smooth muscle, increases vascular permeability, and causes histamine release from mast cells and basophilic leukocytes.
***LOC103689965/C4a*:** Human Uniprot function (Human *C4A*): Nonenzymatic component of C3 and C5 convertases and thus essential for the propagation of the classical complement pathway. Covalently binds to immunoglobulins and immune complexes and enhances the solubilization of immune aggregates and the clearance of IC through CR1 on erythrocytes. C4A isotype is responsible for effective binding to form amide bonds with immune aggregates or protein antigens, while C4B isotype catalyzes the transacylation of the thioester carbonyl group to form ester bonds with carbohydrate antigens. Derived from proteolytic degradation of complement C4, C4a anaphylatoxin is a mediator of local inflammatory process. It induces the contraction of smooth muscle, increases vascular permeability and causes histamine release from mast cells and basophilic leukocytes.

Summary

2,3-Benzofluorene (2,3-BF) is a member of the polycyclic aromatic hydrocarbon class of compounds to which humans are widely exposed. A review of the literature did not identify toxicological data for estimating the potential adverse health effects of 2,3-BF. This study used a transcriptomic approach and standard toxicological endpoints to estimate the in vivo biological potency of 2,3-BF.

A subset of standard toxicological endpoints (absolute liver weight, relative liver weight, and eosinophil count in male rats; eosinophil count in female rats) exhibited benchmark dose (BMD) values much lower than would be expected given the endpoint-specific no-observed-effect level and lowest-observed-effect level values. Expert review of the data suggests that the BMD estimates do not accurately reflect the true potency of the effect of these endpoints and were likely an anomalous product of the BMD modeling approach.

Taking this into account, the most sensitive apical endpoint in male rats was a decrease in reticulocyte count with an estimated BMD and benchmark dose lower confidence limit (BMD_L) of 11.837 (6.978) mg/kg. An increase in thyroid stimulating hormone concentration and a decrease in total thyroxine concentration were the next most sensitive apical endpoint changes observed in male rats with BMDs (BMD_Ls) of 44.526 (19.298) and 61.426 (24.276) mg/kg, respectively. In female rats, the most sensitive apical endpoint was an increase in thyroid stimulating hormone concentration with a BMD (BMD_L) of 1.078 (0.267) mg/kg. The next most sensitive apical endpoints observed were an increase in absolute liver weight and an increase in cholesterol concentration with BMDs (BMD_Ls) of 24.928 (7.768) and 288.242 (226.543) mg/kg, respectively.

Gene set-level transcriptional changes in the liver following 2,3-BF exposure were estimated to occur at a BMD (BMD_L) as low as 5.660 (2.158) mg/kg in male rats, corresponding to regulation of ossification (GO:0030278), and as low as 1.874 (0.497) mg/kg in female rats, corresponding to DNA conformation change (GO:0071103) and chromosome organization (GO:0051276). The most sensitive liver gene for which a reliable BMD could be determined was *Zfp354a*, with a BMD (BMD_L) of 3.267 (1.720) mg/kg in male rats, and *Kif22*, with a BMD (BMD_L) of 0.962 (0.282) mg/kg, in female rats.

Gene set-level transcriptional changes in the kidney were estimated to occur at a BMD (BMD_L) as low as 6.167 (1.732) mg/kg in male rats, corresponding to brain development (GO:0007420), and as low as 14.574 (7.161) mg/kg in female rats, corresponding to regulation of fibroblast proliferation (GO:0048145). One kidney gene in male rats had a BMD estimate below the lower limit of extrapolation (<0.050 mg/kg). The most sensitive kidney gene for which a reliable BMD could be determined was *Top2a*, with a BMD (BMD_L) of 12.334 (3.464) mg/kg, in male rats and *Cyp1a1*, with a BMD (BMD_L) of 12.886 (9.131) mg/kg, in female rats.

Under the conditions of this short-duration transcriptomic study in Sprague Dawley (Hsd:Sprague Dawley® SD®) rats, the most sensitive point of departure with a reliable estimate in male rats was a transcriptional change in a gene, *Zfp354a*, with a BMD (BMD_L) of 3.267 (1.720) mg/kg. Gene set transcriptional changes and apical endpoints provided potency estimates slightly higher than *Zfp354a*. In female rats, the most sensitive point of departure with a reliable estimate was a transcriptional change in a gene, *Kif22*, with a BMD (BMD_L) of 0.962

(0.282) mg/kg. Gene set transcriptional changes provided potency estimates that were slightly higher, whereas apical endpoints provided potency estimates in the same range as *Kif22*.

References

1. U.S. Environmental Protection Agency (USEPA). CompTox Chemicals Dashboard: 11H-Benzo[b]fluorene 243-17-4 | DTXSID1022477. 2021. https://comptox.epa.gov/dashboard/chemical/details/DTXSID1022477

2. National Center for Biotechnology Information (NCBI). PubChem Compound Summary for CID 9201, 2,3-Benzofluorene. 2021. https://pubchem.ncbi.nlm.nih.gov/compound/9201

3. European Chemicals Agency (ECHA). Substance Infocard: Benzo[b]fluorene. 2021. https://echa.europa.eu/substance-information/-/substanceinfo/100.005.412

4. Patel AB, Shaikh S, Jain KR, Desai C, Madamwar D. Polycyclic aromatic hydrocarbons: Sources, toxicity, and remediation approaches. Front Microbiol. 2020; 11:562813. https://doi.org/10.3389/fmicb.2020.562813

5. U.S. Environmental Protection Agency (USEPA). CompTox Chemicals Dashboard: 11H-Benzo[b]fluorene 243-17-4 | DTXSID1022477: Executive Summary. 2021. https://comptox.epa.gov/dashboard/chemical/executive-summary/DTXSID1022477

6. National Center for Biotechnology Information (NCBI). PubChem Compound Summary for CID 9201, 2,3-Benzofluorene: 8.1.1 Carcinogen Classification. 2021. https://pubchem.ncbi.nlm.nih.gov/compound/2_3-Benzofluorene#section=Carcinogen-Classification

7. Gwinn WM, Auerbach SS, Parham F, Stout MD, Waidyanatha S, Mutlu E, Collins B, Paules RS, Merrick BA, Ferguson S et al. Evaluation of 5-day in vivo rat liver and kidney with high-throughput transcriptomics for estimating benchmark doses of apical outcomes. Toxicol Sci. 2020; 176(2):343-354. https://doi.org/10.1093/toxsci/kfaa081

8. Mansouri K, Karmaus AL, Fitzpatrick J, Patlewicz G, Pradeep P, Alberga D, Alepee N, Allen TEH, Allen D, Alves VM et al. CATMoS: Collaborative Acute Toxicity Modeling Suite. Environ Health Perspect. 2021; 129(4):47013. https://doi.org/10.1289/EHP8495

9. Mansouri K, Grulke CM, Judson RS, Williams AJ. OPERA models for predicting physicochemical properties and environmental fate endpoints. J Cheminform. 2018; 10(1):10. https://doi.org/10.1186/s13321-018-0263-1

10. Waidyanatha S, Fletcher BL, Fernando RA, Cora MC, Silinski MAR. Development and validation of an ultraperformance liquid chromatography-tandem mass spectrometry method for quantitation of total 3,3',5-triiodo-L-thyronine and 3,3',5,5'-tetraiodo-L-thyronine in rodent serum. Anal Lett. 2021; 55(5):796-811. https://doi.org/10.1080/00032719.2021.1967969

11. Langmead B, Trapnell C, Pop M, Salzberg SL. Ultrafast and memory-efficient alignment of short DNA sequences to the human genome. Genome Biol. 2009; 10(3):R25. https://doi.org/10.1186/gb-2009-10-3-r25

12. Williams DA. A test for differences between treatment means when several dose levels are compared with a zero dose control. Biometrics. 1971; 27(1):103-117. http://dx.doi.org/10.2307/2528930

13. Williams DA. The comparison of several dose levels with a zero dose control. Biometrics. 1972; 28(2):519-531. http://dx.doi.org/10.2307/2556164

14. Dunnett CW. A multiple comparison procedure for comparing several treatments with a control. J Am Stat Assoc. 1955; 50(272):1096-1121. http://dx.doi.org/10.1080/01621459.1955.10501294

15. Shirley E. A non-parametric equivalent of Williams' test for contrasting increasing dose levels of a treatment. Biometrics. 1977; 33(2):386-389. http://dx.doi.org/10.2307/2529789

16. Dunn OJ. Multiple comparisons using rank sums. Technometrics. 1964; 6(3):241-252. http://dx.doi.org/10.1080/00401706.1964.10490181

17. Jonckheere AR. A distribution-free k-sample test against ordered alternatives. Biometrika. 1954; 41(1/2):133-145. http://dx.doi.org/10.2307/2333011

18. Dixon WJ, Massey FJ. Introduction to Statistical Analysis. New York,: McGraw-Hill; 1951.

19. U.S. Environmental Protection Agency (USEPA). Benchmark dose technical guidance. Washington, DC: U.S. Environmental Protection Agency, Risk Assessment Forum; 2012. https://www.epa.gov/sites/production/files/2015-01/documents/benchmark_dose_guidance.pdf

20. Wignall JA, Shapiro AJ, Wright FA, Woodruff TJ, Chiu WA, Guyton KZ, Rusyn I. Standardizing benchmark dose calculations to improve science-based decisions in human health assessments. Environ Health Perspect. 2014; 122(5):499-505. http://dx.doi.org/10.1289/ehp.1307539

21. National Toxicology Program (NTP). NTP research report on National Toxicology Program approach to genomic dose-response modeling. Research Triangle Park, NC: U.S. Department of Health and Human Services, National Institute of Environmental Health Sciences, National Toxicology Program; 2018. NTP Research Report No. 5.

22. Shi L, Jones WD, Jensen RV, Harris SC, Perkins RG, Goodsaid FM, Guo L, Croner LJ, Boysen C, Fang H et al. The balance of reproducibility, sensitivity, and specificity of lists of differentially expressed genes in microarray studies. BMC Bioinformatics. 2008; 9:S10. https://doi.org/10.1186/1471-2105-9-s9-s10

23. Auerbach SS, Ballin JD, Blake JC, Browning DB, Collins BJ, Cora MC, Fernando RA, Fostel JM, Liu YF, Luh J et al. NIEHS report on the in vivo repeat dose biological potency study of perfluorohexanesulfonamide (CASRN 41997-13-1) in Sprague Dawley (Hsd:Sprague Dawley® SD®) rats (gavage studies). Research Triangle Park, NC: U.S. Department of Health and Human Services, Public Health Service, National Institute of Environmental Health Sciences; 2023. NIEHS Report 10. https://doi.org/10.22427/NIEHS-10

24. Auerbach SS, Aillon KL, Ballin JD, Collins BJ, Cora MC, Duncan NS, Fostel JM, Liu YF, Luh J, Machesky NJ et al. NIEHS report on the in vivo repeat dose biological potency study of 6:1 fluorotelomer alcohol (CASRN 375-82-6) in Sprague Dawley (Hsd:Sprague Dawley® SD®) rats (gavage studies). Research Triangle Park, NC: U.S. Department of Health and Human Services, Public Health Service, National Institute of Environmental Health Sciences; 2023. NIEHS Report 07. https://doi.org/10.22427/NIEHS-07

25. Auerbach SS, Ballin JD, Blake JC, Browning DB, Collins BJ, Cora MC, Fernando RA, Fostel JM, Liu YF, Luh J et al. NIEHS report on the in vivo repeat dose biological potency study of 1,1,2,2-tetrahydroperfluoro-1-dodecanol (CASRN 865-86-1) in Sprague Dawley (Hsd:Sprague Dawley® SD®) rats (gavage studies). Research Triangle Park, NC: U.S. Department of Health and Human Services, Public Health Service, National Institute of Environmental Health Sciences; 2023. NIEHS Report 08. https://doi.org/10.22427/NIEHS-08

26. National Toxicology Program (NTP). NIEHS 09: Chemical Effects in Biological Systems (CEBS) data repository. Research Triangle Park, NC: U.S. Department of Health and Human Services, National Institute of Environmental Health Sciences, National Toxicology Program; 2023. https://doi.org/10.22427/NIEHS-DATA-NIEHS-09

27. Geneontology. The gene ontology resource. 2021. http://geneontology.org/

28. Medical College of Wisconsin. Rat Genome Database. 2021. https://rgd.mcw.edu/

29. UniProt. UniProtKB results. 2021. https://www.uniprot.org/uniprot/

30. Entrez Gene. Gene. 2021. https://www.ncbi.nlm.nih.gov/gene/

31. Thomas RS, Allen BC, Nong A, Yang L, Bermudez E, Clewell HJ, III, Andersen ME. A method to integrate benchmark dose estimates with genomic data to assess the functional effects of chemical exposure. Toxicol Sci. 2007; 98(1):240-248. http://dx.doi.org/10.1093/toxsci/kfm092

Appendix A. Internal Dose Assessment

Table of Contents

A.1. Quantitation of 2,3-Benzofluorene in Plasma

Quantification of 2,3-benzofluorene (2,3-BF) in plasma samples was completed by MRIGlobal (Kansas City, MO). A gas chromatography mass spectroscopy (GC/MS) method was developed to determine 2,3-BF concentrations in rat plasma. A six-point matrix calibration curve, in the range of 10–100 ng/mL, was prepared by adding 10 µL of an appropriate spiking solution of 2,3-BF in methanol to 100 µL of control matrix (adult male Sprague Dawley rat plasma). Quality control (QC) samples were prepared similarly at a target concentration of 52.5 ng/mL in plasma. Blanks and study samples were prepared like standards, except 10 µL of methanol was used in place of spiking solution. Each sample was extracted with 1,000 µL of hexane, vortex-mixed for 60 seconds, and then centrifuged at approximately 842 × g for 2 minutes. A 900 µL aliquot of the supernatant was removed, evaporatively dried at 25°C, and then reconstituted and mixed with 100 µL of extraction solvent.

All samples were analyzed using an Agilent 6890N GC with an Agilent 5975 MS (Santa Clara, CA). A Restek Rxi 5Sil MS column (30 m × 0.25 mm, 0.25 µm) was used with a helium carrier gas. A flow rate of 1 mL/min was run with a temperature program starting at 50°C for 3 minutes, a linear ramp at 25°C/min to 150°C, then a linear ramp at 10°C/min to 330°C, and then held at 330°C for 10 minutes. Electron impact ionization was used with an ionization voltage of 70 eV and a source temperature of 200°C. Single ion monitoring was used at m/z 216 and 215 (2,3-BF), and m/z 166 and 169 (internal standard).

A linear regression with 1/X weighting was used to relate peak area ratio of matrix calibration standards to their analyte concentration. Calibration curves were linear ($r > 0.99$). The limit of detection (LOD; 1.8 ng/mL) was estimated as three times the standard deviation of the lower limit of quantitation (LOQ; 10.0 ng/mL), expressed as concentration. For QC samples, the accuracy measured as percent relative error was within ±28.4% of the nominal concentration with relative standard deviations ≤24.4%. The concentrations (ng/mL) of 2,3-BF in study samples were calculated using peak areas and the regression equation. All values above LOD were reported.

Appendix B. Animal Identifiers

Tables

Table B-1. Animal Numbers and FASTQ Data File Names

Animal Number	Sex	Group	Dose (mg/kg)	Survived to Study Termination	Tissue	FASTQ File ID
431	Male	Vehicle control	0	Yes	Kidney	Plate7-431
431	Male	Vehicle control	0	Yes	Liver	Plate3-431
432	Male	Vehicle control	0	Yes	Kidney	Plate8-432[a]
432	Male	Vehicle control	0	Yes	Liver	Plate3-432
433	Male	Vehicle control	0	Yes	Kidney	Plate7-433
433	Male	Vehicle control	0	Yes	Liver	Plate4-433
434	Male	Vehicle control	0	Yes	Kidney	Plate8-434[a]
434	Male	Vehicle control	0	Yes	Liver	Plate3-434
435	Male	Vehicle control	0	Yes	Kidney	Plate8-435[a]
435	Male	Vehicle control	0	Yes	Liver	Plate3-435
436	Male	Vehicle control	0	Yes	Kidney	Plate8-436[a]
436	Male	Vehicle control	0	Yes	Liver	Plate3-436
437	Male	Vehicle control	0	Yes	Kidney	Plate7-437
437	Male	Vehicle control	0	Yes	Liver	Plate3-437
438	Male	Vehicle control	0	Yes	Kidney	Plate7-438
438	Male	Vehicle control	0	Yes	Liver	Plate3-438
439	Male	Vehicle control	0	Yes	Kidney	Plate7-439
439	Male	Vehicle control	0	Yes	Liver	Plate3-439
440	Male	Vehicle control	0	Yes	Kidney	Plate7-440
440	Male	Vehicle control	0	Yes	Liver	Plate3-440
441	Female	Vehicle control	0	Yes	Kidney	Plate7-441
441	Female	Vehicle control	0	Yes	Liver	Plate3-441
442	Female	Vehicle control	0	Yes	Kidney	Plate7-442
442	Female	Vehicle control	0	Yes	Liver	Plate3-442
443	Female	Vehicle control	0	Yes	Kidney	Plate7-443
443	Female	Vehicle control	0	Yes	Liver	Plate4-443
444	Female	Vehicle control	0	Yes	Kidney	Plate7-444
444	Female	Vehicle control	0	Yes	Liver	Plate3-444
445	Female	Vehicle control	0	Yes	Kidney	Plate7-445
445	Female	Vehicle control	0	Yes	Liver	Plate4-445
446	Female	Vehicle control	0	Yes	Kidney	Plate7-446
446	Female	Vehicle control	0	Yes	Liver	Plate4-446
447	Female	Vehicle control	0	Yes	Kidney	Plate7-447
447	Female	Vehicle control	0	Yes	Liver	Plate4-447
448	Female	Vehicle control	0	Yes	Kidney	Plate7-448
448	Female	Vehicle control	0	Yes	Liver	Plate3-448
449	Female	Vehicle control	0	Yes	Kidney	Plate8-449[a]
449	Female	Vehicle control	0	Yes	Liver	Plate3-449

Animal Number	Sex	Group	Dose (mg/kg)	Survived to Study Termination	Tissue	FASTQ File ID
450	Female	Vehicle control	0	Yes	Kidney	Plate8-450[a]
450	Female	Vehicle control	0	Yes	Liver	Plate3-450
451	Male	2,3-Benzofluorene	0.15	Yes	Kidney	Plate7-451
451	Male	2,3-Benzofluorene	0.15	Yes	Liver	Plate3-451
452	Male	2,3-Benzofluorene	0.15	Yes	Kidney	Plate8-452[a]
452	Male	2,3-Benzofluorene	0.15	Yes	Liver	Plate3-452
453	Male	2,3-Benzofluorene	0.15	Yes	Kidney	Plate7-453
453	Male	2,3-Benzofluorene	0.15	Yes	Liver	Plate4-453
454	Male	2,3-Benzofluorene	0.15	Yes	Kidney	Plate7-454
454	Male	2,3-Benzofluorene	0.15	Yes	Liver	Plate3-454
455	Male	2,3-Benzofluorene	0.15	Yes	Kidney	Plate7-455
455	Male	2,3-Benzofluorene	0.15	Yes	Liver	Plate4-455
456	Female	2,3-Benzofluorene	0.15	Yes	Kidney	Plate7-456
456	Female	2,3-Benzofluorene	0.15	Yes	Liver	Plate3-456
457	Female	2,3-Benzofluorene	0.15	Yes	Kidney	Plate7-457
457	Female	2,3-Benzofluorene	0.15	Yes	Liver	Plate3-457
458	Female	2,3-Benzofluorene	0.15	Yes	Kidney	Plate7-458
458	Female	2,3-Benzofluorene	0.15	Yes	Liver	Plate3-458
459	Female	2,3-Benzofluorene	0.15	Yes	Kidney	Plate7-459
459	Female	2,3-Benzofluorene	0.15	Yes	Liver	Plate3-459
460	Female	2,3-Benzofluorene	0.15	Yes	Kidney	Plate7-460
460	Female	2,3-Benzofluorene	0.15	Yes	Liver	Plate3-460
461	Male	2,3-Benzofluorene	0.5	Yes	Kidney	Plate7-461
461	Male	2,3-Benzofluorene	0.5	Yes	Liver	Plate3-461
462	Male	2,3-Benzofluorene	0.5	Yes	Kidney	Plate7-462
462	Male	2,3-Benzofluorene	0.5	Yes	Liver	Plate3-462
463	Male	2,3-Benzofluorene	0.5	Yes	Kidney	Plate7-463
463	Male	2,3-Benzofluorene	0.5	Yes	Liver	Plate3-463
464	Male	2,3-Benzofluorene	0.5	Yes	Kidney	Plate7-464
464	Male	2,3-Benzofluorene	0.5	Yes	Liver	Plate3-464
465	Male	2,3-Benzofluorene	0.5	Yes	Kidney	Plate7-465
465	Male	2,3-Benzofluorene	0.5	Yes	Liver	Plate3-465
466	Female	2,3-Benzofluorene	0.5	Yes	Kidney	Plate7-466
466	Female	2,3-Benzofluorene	0.5	Yes	Liver	Plate3-466
467	Female	2,3-Benzofluorene	0.5	Yes	Kidney	Plate8-467[a]
467	Female	2,3-Benzofluorene	0.5	Yes	Liver	Plate3-467
468	Female	2,3-Benzofluorene	0.5	Yes	Kidney	Plate7-468
468	Female	2,3-Benzofluorene	0.5	Yes	Liver	Plate3-468
469	Female	2,3-Benzofluorene	0.5	Yes	Kidney	Plate7-469

Animal Number	Sex	Group	Dose (mg/kg)	Survived to Study Termination	Tissue	FASTQ File ID
469	Female	2,3-Benzofluorene	0.5	Yes	Liver	Plate3-469
470	Female	2,3-Benzofluorene	0.5	Yes	Kidney	Plate7-470
470	Female	2,3-Benzofluorene	0.5	Yes	Liver	Plate3-470
471	Male	2,3-Benzofluorene	1.4	Yes	Kidney	Plate7-471
471	Male	2,3-Benzofluorene	1.4	Yes	Liver	Plate4-471
472	Male	2,3-Benzofluorene	1.4	Yes	Kidney	Plate7-472
472	Male	2,3-Benzofluorene	1.4	Yes	Liver	Plate3-472
473	Male	2,3-Benzofluorene	1.4	Yes	Kidney	Plate7-473
473	Male	2,3-Benzofluorene	1.4	Yes	Liver	Plate3-473
474	Male	2,3-Benzofluorene	1.4	Yes	Kidney	Plate8-474[a]
474	Male	2,3-Benzofluorene	1.4	Yes	Liver	Plate3-474
475	Male	2,3-Benzofluorene	1.4	Yes	Kidney	Plate7-475
475	Male	2,3-Benzofluorene	1.4	Yes	Liver	Plate3-475
476	Female	2,3-Benzofluorene	1.4	Yes	Kidney	Plate7-476
476	Female	2,3-Benzofluorene	1.4	Yes	Liver	Plate3-476
477	Female	2,3-Benzofluorene	1.4	Yes	Kidney	Plate7-477
477	Female	2,3-Benzofluorene	1.4	Yes	Liver	Plate3-477
478	Female	2,3-Benzofluorene	1.4	Yes	Kidney	Plate7-478
478	Female	2,3-Benzofluorene	1.4	Yes	Liver	Plate3-478
479	Female	2,3-Benzofluorene	1.4	Yes	Kidney	Plate7-479
479	Female	2,3-Benzofluorene	1.4	Yes	Liver	Plate4-479
480	Female	2,3-Benzofluorene	1.4	Yes	Kidney	Plate7-480
480	Female	2,3-Benzofluorene	1.4	Yes	Liver	Plate3-480
481	Male	2,3-Benzofluorene	4.0	Yes	Kidney	Plate7-481
481	Male	2,3-Benzofluorene	4.0	Yes	Liver	Plate3-481
482	Male	2,3-Benzofluorene	4.0	Yes	Kidney	Plate7-482
482	Male	2,3-Benzofluorene	4.0	Yes	Liver	Plate3-482
483	Male	2,3-Benzofluorene	4.0	Yes	Kidney	Plate7-483
483	Male	2,3-Benzofluorene	4.0	Yes	Liver	Plate3-483
484	Male	2,3-Benzofluorene	4.0	Yes	Kidney	Plate7-484
484	Male	2,3-Benzofluorene	4.0	Yes	Liver	Plate3-484
485	Male	2,3-Benzofluorene	4.0	Yes	Kidney	Plate7-485
485	Male	2,3-Benzofluorene	4.0	Yes	Liver	Plate3-485
486	Female	2,3-Benzofluorene	4.0	Yes	Kidney	Plate7-486
486	Female	2,3-Benzofluorene	4.0	Yes	Liver	Plate3-486
487	Female	2,3-Benzofluorene	4.0	Yes	Kidney	Plate7-487
487	Female	2,3-Benzofluorene	4.0	Yes	Liver	Plate3-487
488	Female	2,3-Benzofluorene	4.0	Yes	Kidney	Plate7-488
488	Female	2,3-Benzofluorene	4.0	Yes	Liver	Plate3-488

Animal Number	Sex	Group	Dose (mg/kg)	Survived to Study Termination	Tissue	FASTQ File ID
489	Female	2,3-Benzofluorene	4.0	Yes	Kidney	Plate7-489
489	Female	2,3-Benzofluorene	4.0	Yes	Liver	Plate4-489
490	Female	2,3-Benzofluorene	4.0	Yes	Kidney	Plate8-490[a]
490	Female	2,3-Benzofluorene	4.0	Yes	Liver	Plate3-490
491	Male	2,3-Benzofluorene	12.0	Yes	Kidney	Plate7-491
491	Male	2,3-Benzofluorene	12.0	Yes	Liver	Plate4-491
492	Male	2,3-Benzofluorene	12.0	Yes	Kidney	Plate7-492
492	Male	2,3-Benzofluorene	12.0	Yes	Liver	Plate3-492
493	Male	2,3-Benzofluorene	12.0	Yes	Kidney	Plate8-493[a]
493	Male	2,3-Benzofluorene	12.0	Yes	Liver	Plate3-493
494	Male	2,3-Benzofluorene	12.0	Yes	Kidney	Plate8-494[a]
494	Male	2,3-Benzofluorene	12.0	Yes	Liver	Plate4-494
495	Male	2,3-Benzofluorene	12.0	Yes	Kidney	Plate7-495
495	Male	2,3-Benzofluorene	12.0	Yes	Liver	Plate3-495
496	Female	2,3-Benzofluorene	12.0	Yes	Kidney	Plate7-496
496	Female	2,3-Benzofluorene	12.0	Yes	Liver	Plate3-496
497	Female	2,3-Benzofluorene	12.0	Yes	Kidney	Plate7-497
497	Female	2,3-Benzofluorene	12.0	Yes	Liver	Plate3-497
498	Female	2,3-Benzofluorene	12.0	Yes	Kidney	Plate7-498
498	Female	2,3-Benzofluorene	12.0	Yes	Liver	Plate3-498
499	Female	2,3-Benzofluorene	12.0	Yes	Kidney	Plate8-499[a]
499	Female	2,3-Benzofluorene	12.0	Yes	Liver	Plate4-499
500	Female	2,3-Benzofluorene	12.0	Yes	Kidney	Plate8-500[a]
500	Female	2,3-Benzofluorene	12.0	Yes	Liver	Plate3-500
501	Male	2,3-Benzofluorene	37.0	Yes	Kidney	Plate7-501
501	Male	2,3-Benzofluorene	37.0	Yes	Liver	Plate3-501
502	Male	2,3-Benzofluorene	37.0	Yes	Kidney	Plate7-502
502	Male	2,3-Benzofluorene	37.0	Yes	Liver	Plate4-502
503	Male	2,3-Benzofluorene	37.0	Yes	Kidney	Plate7-503
503	Male	2,3-Benzofluorene	37.0	Yes	Liver	Plate3-503
504	Male	2,3-Benzofluorene	37.0	Yes	Kidney	Plate7-504
504	Male	2,3-Benzofluorene	37.0	Yes	Liver	Plate4-504
505	Male	2,3-Benzofluorene	37.0	Yes	Kidney	Plate7-505
505	Male	2,3-Benzofluorene	37.0	Yes	Liver	Plate3-505
506	Female	2,3-Benzofluorene	37.0	Yes	Kidney	Plate8-506
506	Female	2,3-Benzofluorene	37.0	Yes	Liver	Plate3-506
507	Female	2,3-Benzofluorene	37.0	Yes	Kidney	Plate7-507
507	Female	2,3-Benzofluorene	37.0	Yes	Liver	Plate3-507
508	Female	2,3-Benzofluorene	37.0	Yes	Kidney	Plate7-508

Animal Number	Sex	Group	Dose (mg/kg)	Survived to Study Termination	Tissue	FASTQ File ID
508	Female	2,3-Benzofluorene	37.0	Yes	Liver	Plate3-508
509	Female	2,3-Benzofluorene	37.0	Yes	Kidney	Plate7-509
509	Female	2,3-Benzofluorene	37.0	Yes	Liver	Plate3-509
510	Female	2,3-Benzofluorene	37.0	Yes	Kidney	Plate7-510
510	Female	2,3-Benzofluorene	37.0	Yes	Liver	Plate3-510
511	Male	2,3-Benzofluorene	111.0	Yes	Kidney	Plate7-511
511	Male	2,3-Benzofluorene	111.0	Yes	Liver	Plate3-511
512	Male	2,3-Benzofluorene	111.0	Yes	Kidney	Plate8-512[a]
512	Male	2,3-Benzofluorene	111.0	Yes	Liver	Plate3-512
513	Male	2,3-Benzofluorene	111.0	Yes	Kidney	Plate8-513[a]
513	Male	2,3-Benzofluorene	111.0	Yes	Liver	Plate3-513
514	Male	2,3-Benzofluorene	111.0	Yes	Kidney	Plate7-514
514	Male	2,3-Benzofluorene	111.0	Yes	Liver	Plate3-514
515	Male	2,3-Benzofluorene	111.0	Yes	Kidney	Plate7-515
515	Male	2,3-Benzofluorene	111.0	Yes	Liver	Plate3-515
516	Female	2,3-Benzofluorene	111.0	Yes	Kidney	Plate8-516[a]
516	Female	2,3-Benzofluorene	111.0	Yes	Liver	Plate3-516
517	Female	2,3-Benzofluorene	111.0	Yes	Kidney	Plate8-517[a]
517	Female	2,3-Benzofluorene	111.0	Yes	Liver	Plate3-517
518	Female	2,3-Benzofluorene	111.0	Yes	Kidney	Plate7-518
518	Female	2,3-Benzofluorene	111.0	Yes	Liver	Plate3-518
519	Female	2,3-Benzofluorene	111.0	Yes	Kidney	Plate7-519
519	Female	2,3-Benzofluorene	111.0	Yes	Liver	Plate3-519
520	Female	2,3-Benzofluorene	111.0	Yes	Kidney	Plate7-520
520	Female	2,3-Benzofluorene	111.0	Yes	Liver	Plate3-520
521	Male	2,3-Benzofluorene	333.0	Yes	Kidney	Plate7-521
521	Male	2,3-Benzofluorene	333.0	Yes	Liver	Plate3-521
522	Male	2,3-Benzofluorene	333.0	Yes	Kidney	Plate7-522
522	Male	2,3-Benzofluorene	333.0	Yes	Liver	Plate3-522
523	Male	2,3-Benzofluorene	333.0	Yes	Kidney	Plate7-523
523	Male	2,3-Benzofluorene	333.0	Yes	Liver	Plate3-523
524	Male	2,3-Benzofluorene	333.0	Yes	Kidney	Plate7-524
524	Male	2,3-Benzofluorene	333.0	Yes	Liver	Plate3-524
525	Male	2,3-Benzofluorene	333.0	Yes	Kidney	Plate7-525
525	Male	2,3-Benzofluorene	333.0	Yes	Liver	Plate4-525
526	Female	2,3-Benzofluorene	333.0	Yes	Kidney	Plate7-526
526	Female	2,3-Benzofluorene	333.0	Yes	Liver	Plate3-526
527	Female	2,3-Benzofluorene	333.0	Yes	Kidney	Plate7-527
527	Female	2,3-Benzofluorene	333.0	Yes	Liver	Plate3-527

Animal Number	Sex	Group	Dose (mg/kg)	Survived to Study Termination	Tissue	FASTQ File ID
528	Female	2,3-Benzofluorene	333.0	Yes	Kidney	Plate7-528
528	Female	2,3-Benzofluorene	333.0	Yes	Liver	Plate3-528
529	Female	2,3-Benzofluorene	333.0	Yes	Kidney	Plate7-529
529	Female	2,3-Benzofluorene	333.0	Yes	Liver	Plate3-529
530	Female	2,3-Benzofluorene	333.0	Yes	Kidney	Plate7-530
530	Female	2,3-Benzofluorene	333.0	Yes	Liver	Plate3-530
531	Male	2,3-Benzofluorene	1,000.0	Yes	Kidney	Plate7-531
531	Male	2,3-Benzofluorene	1,000.0	Yes	Liver	Plate4-531
532	Male	2,3-Benzofluorene	1,000.0	Yes	Kidney	Plate7-532
532	Male	2,3-Benzofluorene	1,000.0	Yes	Liver	Plate4-532
533	Male	2,3-Benzofluorene	1,000.0	Yes	Kidney	Plate7-533
533	Male	2,3-Benzofluorene	1,000.0	Yes	Liver	Plate3-533
534	Male	2,3-Benzofluorene	1,000.0	Yes	Kidney	Plate7-534
534	Male	2,3-Benzofluorene	1,000.0	Yes	Liver	Plate3-534
535	Male	2,3-Benzofluorene	1,000.0	Yes	Kidney	Plate7-535
535	Male	2,3-Benzofluorene	1,000.0	Yes	Liver	Plate3-535
536	Female	2,3-Benzofluorene	1,000.0	Yes	Kidney	Plate7-536
536	Female	2,3-Benzofluorene	1,000.0	Yes	Liver	Plate3-536
537	Female	2,3-Benzofluorene	1,000.0	Yes	Kidney	Plate8-537[a]
537	Female	2,3-Benzofluorene	1,000.0	Yes	Liver	Plate3-537
538	Female	2,3-Benzofluorene	1,000.0	Yes	Kidney	Plate7-538
538	Female	2,3-Benzofluorene	1,000.0	Yes	Liver	Plate4-538
539	Female	2,3-Benzofluorene	1,000.0	Yes	Kidney	Plate7-539
539	Female	2,3-Benzofluorene	1,000.0	Yes	Liver	Plate3-539
540	Female	2,3-Benzofluorene	1,000.0	Yes	Kidney	Plate7-540
540	Female	2,3-Benzofluorene	1,000.0	Yes	Liver	Plate4-540

[a]Removed due to plate/batch effect.

Appendix C. Transcriptomic Quality Control and Empirical False Discovery Rate

Table of Contents

Tables

Figures

C.1. Gene Expression Quality Control

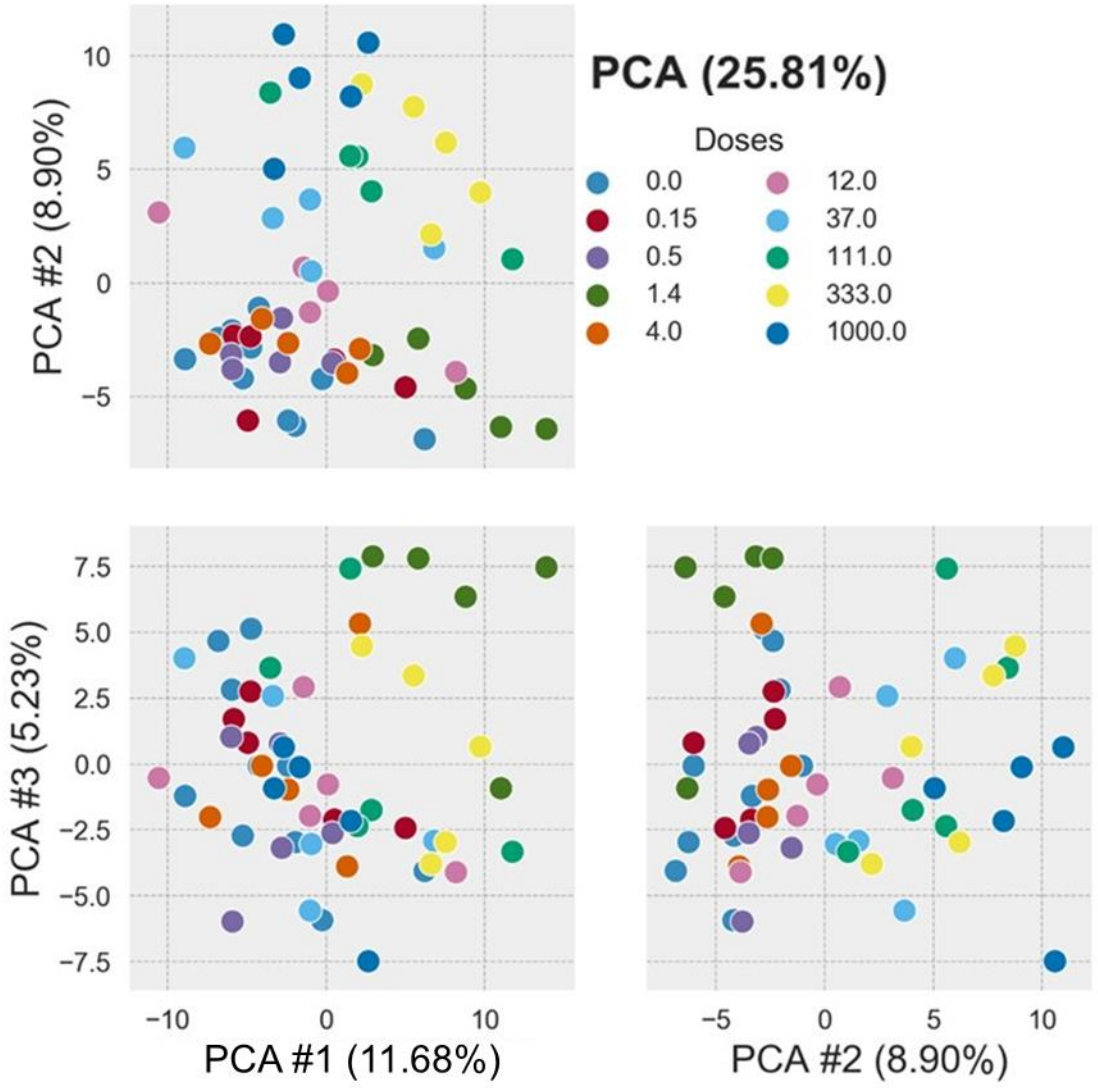

Figure C-1. A Principal Component Analysis of the Normalized Data from the Liver of Male Rats

A principal component analysis (PCA) plot enables visualization of global transcriptional changes in two dimensions, with each plot showing a different angle on the basis of the principal components plotted. Global transcript data are shown for individual animals (dots) within each dose group (designated by color). Dots that are spatially closer to each other indicate more similarity in global expression profiles; dots that are farther apart indicate dissimilarity in global expression profiles for those animals. The data represented in the plot are those employed in dose response modeling (i.e., if outliers were identified in the quality control process, they were removed from the data set and are not present in the plot). Visual inspection does not suggest subgrouping of the data other than dose-related changes, which indicates any technical batch-related effects are minimal.

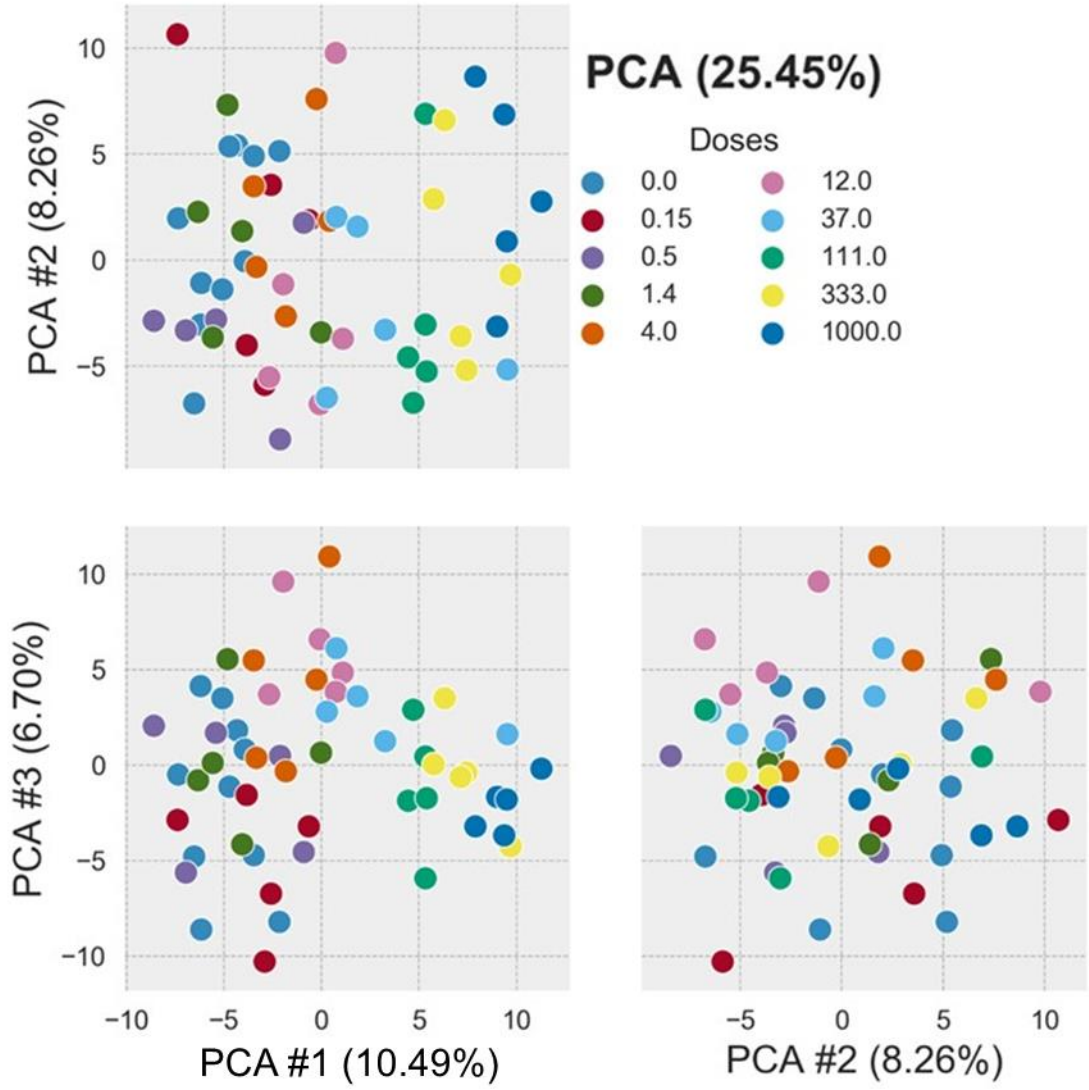

Figure C-2. A Principal Component Analysis of the Normalized Data from the Liver of Female Rats

A principal component analysis (PCA) plot enables visualization of global transcriptional changes in two dimensions, with each plot showing a different angle on the basis of the principal components plotted. Global transcript data are shown for individual animals (dots) within each dose group (designated by color). Dots that are spatially closer to each other indicate more similarity in global expression profiles; dots that are farther apart indicate dissimilarity in global expression profiles for those animals. The data represented in the plot are those employed in dose response modeling (i.e., if outliers were identified in the quality control process, they were removed from the data set and are not present in the plot). Visual inspection does not suggest subgrouping of the data other than dose-related changes, which indicates any technical batch-related effects are minimal.

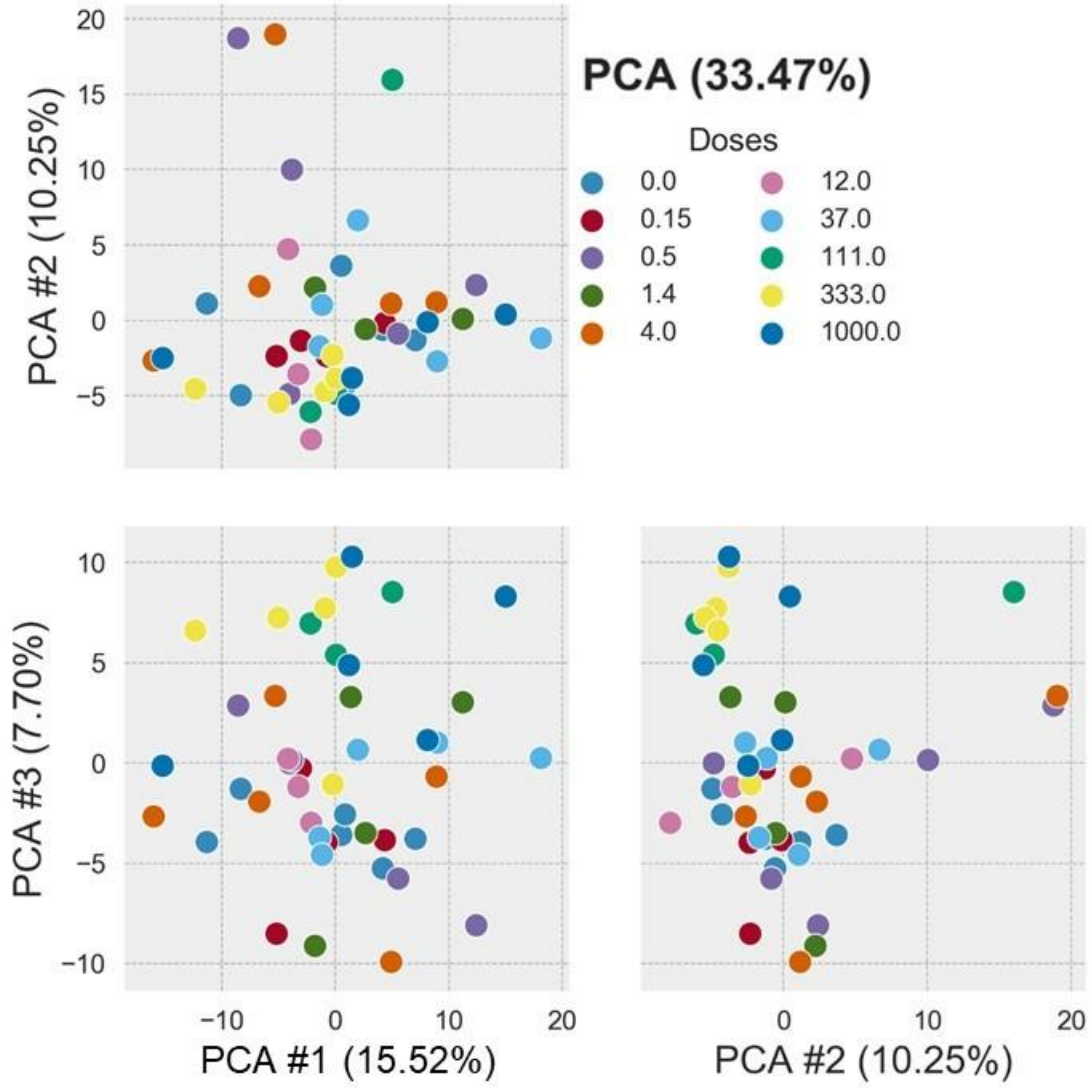

Figure C-3. A Principal Component Analysis of the Normalized Data from the Kidney of Male Rats

A principal component analysis (PCA) plot enables visualization of global transcriptional changes in two dimensions, with each plot showing a different angle on the basis of the principal components plotted. Global transcript data are shown for individual animals (dots) within each dose group (designated by color). Dots that are spatially closer to each other indicate more similarity in global expression profiles; dots that are farther apart indicate dissimilarity in global expression profiles for those animals. The data represented in the plot are those employed in dose response modeling (i.e., if outliers were identified in the quality control process, they were removed from the data set and are not present in the plot). Visual inspection does not suggest subgrouping of the data and shows limited dose-related changes, which indicates any technical batch-related effects are minimal.

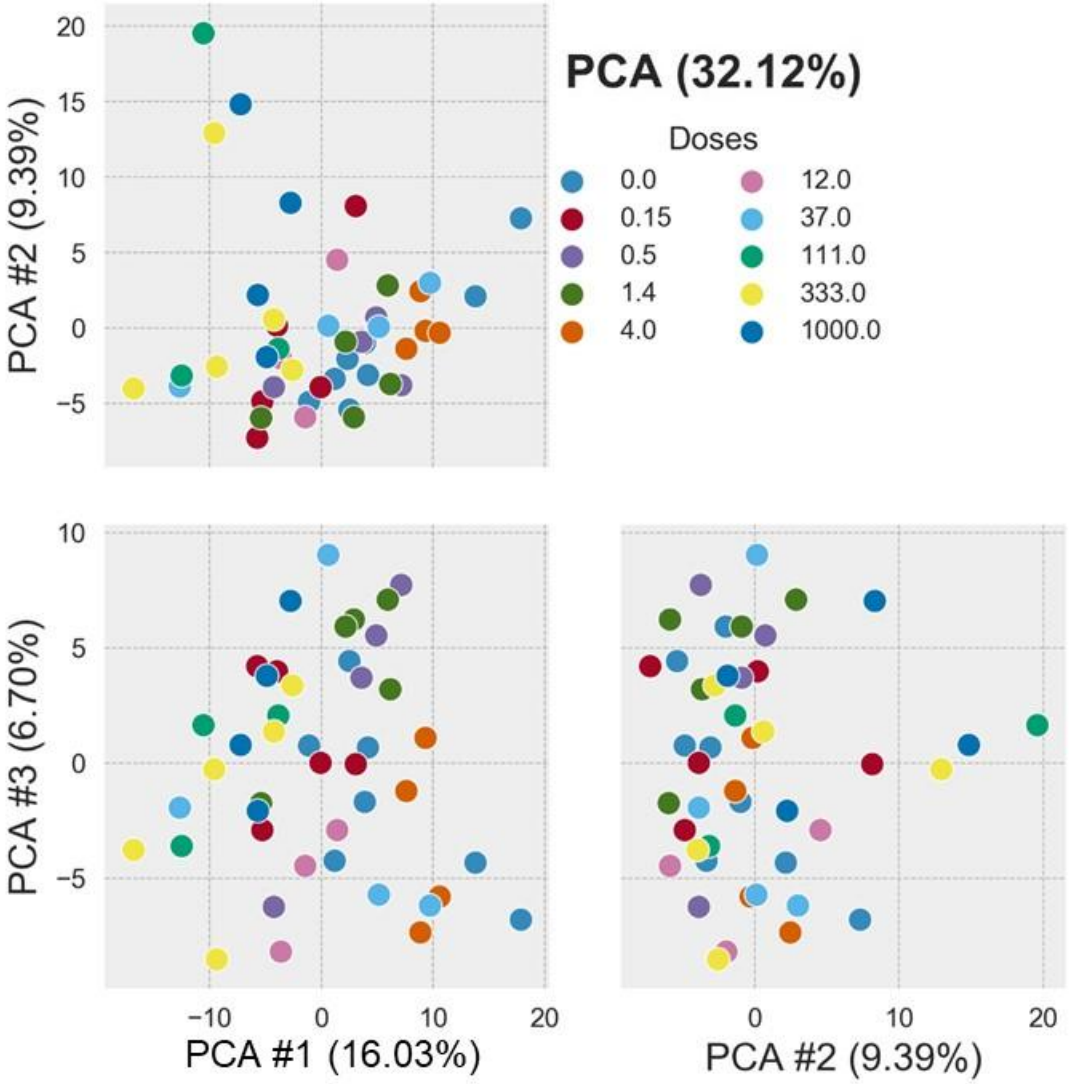

Figure C-4. A Principal Component Analysis of the Normalized Data from the Kidney of Female Rats

A principal component analysis (PCA) plot enables visualization of global transcriptional changes in two dimensions, with each plot showing a different angle on the basis of the principal components plotted. Global transcript data are shown for individual animals (dots) within each dose group (designated by color). Dots that are spatially closer to each other indicate more similarity in global expression profiles; dots that are farther apart indicate dissimilarity in global expression profiles for those animals. The data represented in the plot are those employed in dose response modeling (i.e., if outliers were identified in the quality control process, they were removed from the data set and are not present in the plot). Visual inspection does not suggest subgrouping of the data and shows limited dose-related changes, which indicates any technical batch-related effects are minimal.

C.2. Empirical False Discovery Rate

C.2.1. Methods

Empirical false discovery assessment was performed to evaluate the performance of the benchmark dose (BMD) analysis technique and underlining probe/pathway filtering criteria. Toward this goal, 20 computationally generated data sets were used with this study design (each data set containing 10 vehicle control replicates and 5 replicates per dose), and equivalent BMD analysis was performed using the same parameter configurations. The 20 data sets were generated from the original 2,3-benzofluorene (2,3-BF) study data, along with data from three other chemicals that were studied in parallel under a similar protocol.[23-25]

For a given group (tissue per sex combination), up to 40 vehicle control samples from the original studies (10 replicates × 4 chemicals) were used for this analysis. The previously identified outlier vehicle control samples and overflow plate control samples exhibiting a batch effect were excluded from this analysis.

Each computationally generated sample was created by randomly mixing the normalized expression signal from two randomly selected vehicle control samples using a weighted average approach. The weights utilized during per-probe mixing were randomly simulated from uniform (0,1) distribution. A total of 55 samples (10 vehicle control samples + 45 dosed samples [9 doses × 5 replicates]) were computationally generated per data set and assigned to either vehicle control or 1 of the 9 dosed groups that were separated by approximately half-log spacing, consistent with the dose spacing used in the original studies. For each group, 20 such data sets were generated. Because each of the 20 generated data sets used in the empirical false discovery analysis was derived from actual vehicle control samples, none of the data sets should have any true dose-responsive genes.

Each data set was then analyzed using the same parameter settings and significance criteria that were implemented in the original study. At the gene level, genes that passed the following criteria were considered false positive discoveries: fold change ≥|2|, Williams's trend p value ≤0.05, global goodness-of-fit p value >0.1, BMD upper confidence limit/BMD lower confidence limit (BMD_U/BMD_L) ≤40, and BMD <highest dose tested. Categorical analysis on Gene Ontology (GO) gene sets was performed using the genes that passed the gene-level criteria with maximum absolute fold change ≥1.5. At the gene set GO level, GO biological processes that passed the following criteria were considered false positive discoveries: ≥3 genes that pass all filters, totaling at least 5% of the genes in a gene set.

False positive discovery rates were assessed for each computationally generated data set using the following equations:

$$\text{False Positive Gene Rate} = \frac{\text{\# False Positive Entrez Gene IDs}}{2{,}680} \times 100 \quad (1)$$

$$\text{False Positive GO Biological Process Rate} = \frac{\text{\# False Positive GO Biological Processes}}{5{,}667} \times 100 \quad (2)$$

where 2,680 is the number of unique Entrez Gene IDs on the rat S1500+ platform and 5,667 is the number of GO biological processes that have at least three genes in rat S1500+.

Mean and median false discovery rates across all 20 computationally generated data sets were calculated for each tissue per sex in the study.

C.2.2. Results

The number of false positives for genes and GO biological processes are given in Table C-1. Mean and median false positive rates were <0.1% for genes and <0.5% for GO biological processes for all tissue per sex group (Figure C-5 and Figure C-6). The maximum false positive rates for any of the 80 computationally generated control data sets were 0.3% (gene) and 4.4% (GO biological process).

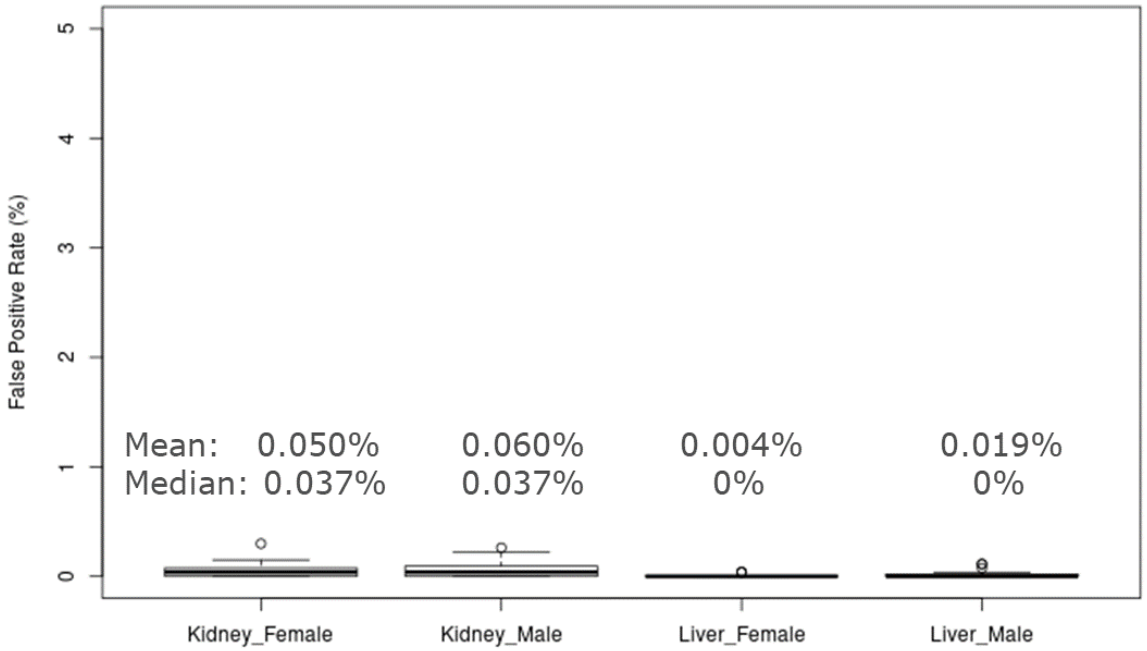

Figure C-5. Boxplots of the False Positive Gene Rate for Each Tissue per Sex Combination

Each boxplot displays the distribution of the false positive rates for 20 computationally generated data sets.

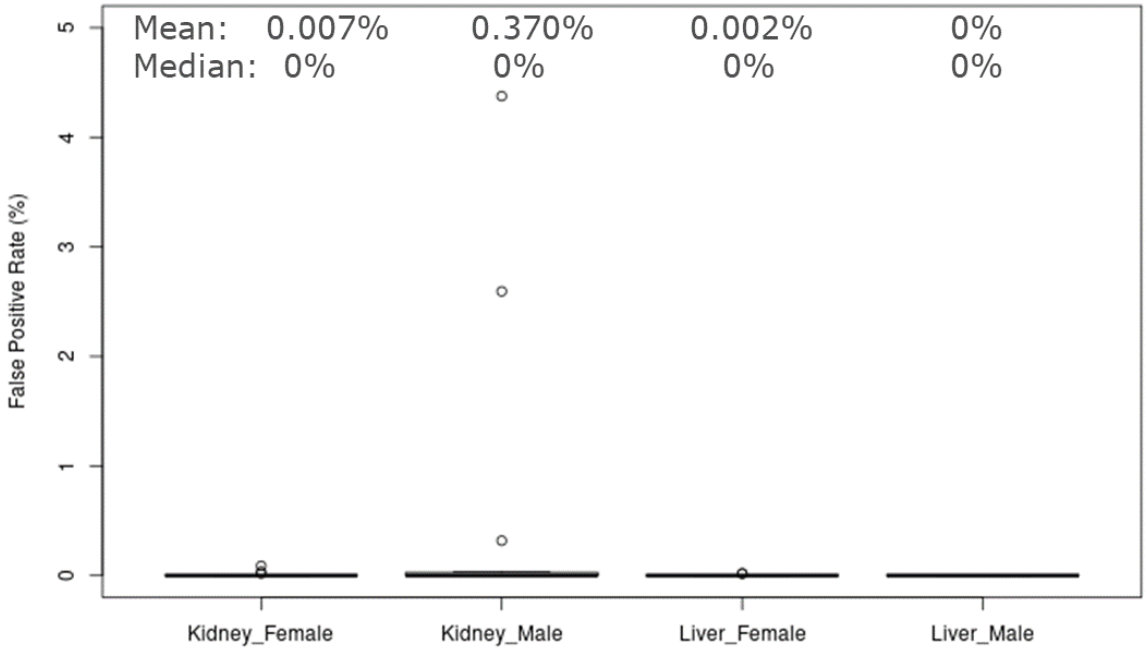

Figure C-6. Boxplots of the False Positive Gene Ontology Biological Process Rate for Each Tissue per Sex Combination

Each boxplot displays the distribution of the false positive rates for 20 computationally generated data sets.

Table C-1. Number of False Positives

Generated Data Set	# False Positive Genes				# False Positive GO Biological Process			
	Kidney Female	Kidney Male	Liver Female	Liver Male	Kidney Female	Kidney Male	Liver Female	Liver Male
01	3	0	0	0	0	0	0	0
02	4	0	0	0	2	1	0	0
03	0	2	0	0	0	1	1	0
04	2	1	0	0	0	0	0	0
05	2	3	0	0	0	0	0	0
06	1	0	0	3	0	0	1	0
07	1	6	0	0	0	18	0	0
08	0	0	0	0	0	0	0	0
09	3	0	0	0	0	0	0	0
10	0	0	0	0	0	0	0	0
11	0	1	0	1	0	0	0	0
12	1	4	0	3	1	147	0	0
13	0	2	0	0	0	2	0	0
14	1	0	0	2	0	0	0	0
15	0	3	0	0	0	2	0	0
16	0	1	1	0	0	0	0	0
17	0	0	1	0	0	0	0	0
18	0	2	0	0	0	0	0	0
19	1	0	0	1	0	0	0	0
20	8	7	0	0	5	248	0	0

GO = Gene Ontology.

Appendix D. Benchmark Dose Model Recommendation and Selection Methodologies

Tables

Figures

Table D-1. Benchmark Dose Model Recommendation/Selection Rules for Apical Endpoints

Rule	Criteria for "Viable"	Numerical Threshold	Bin Placement for Rule Failure
BMD Existence	A BMD exists.	NA	Failure
BMD_L Existence	A BMD_L exists.	NA	Failure
AIC Existence	An AIC exists.	NA	Failure
Residual of Interest Existence	The residual at the dose group closest to the BMD (i.e., the residual of interest) exists.	NA	Failure
Variance Model Fit	The variance model used fits the data.	NA	Nonviable
Variance Model Selection	The variance model is appropriate.	NA	Nonviable
Global Goodness of Fit	The mean model fits the data means sufficiently well (BMDS 2.7.0 Test 4 p value >N).	0.1	Nonviable
Degrees of Freedom	There is at least 1 degree of freedom (i.e., more dose groups than model parameters).	NA	Nonviable
BMD-to-BMD_L Ratio	The ratio of BMD to BMD_L is not large (BMD/BMD_L <N).	20	Viable
High BMD_L	The BMD_L is <N times higher than the maximum dose.	1	Viable
High BMD	The BMD is <N times higher than the maximum dose.	1	Viable
Low BMD	The BMD is <N times lower than the minimum nonzero dose.	3	Nonreportable
Control Residual	The residual at control is small (residual <N).	2	Nonviable
Control Standard Deviation	The modeled standard deviation is similar to the actual (<N times different).	1.5	Nonviable
Residual of Interest	The residual at the dose group closest to the BMD (i.e., the residual of interest) is small (residual <N).	2	Nonviable
No Warnings Reported	No warnings in the BMD model system were reported.	NA	Viable

BMD = benchmark dose; NA = not applicable; BMD_L = benchmark dose lower confidence limit; AIC = Akaike information criterion; BMDS = Benchmark Dose Software; N = numerical threshold.

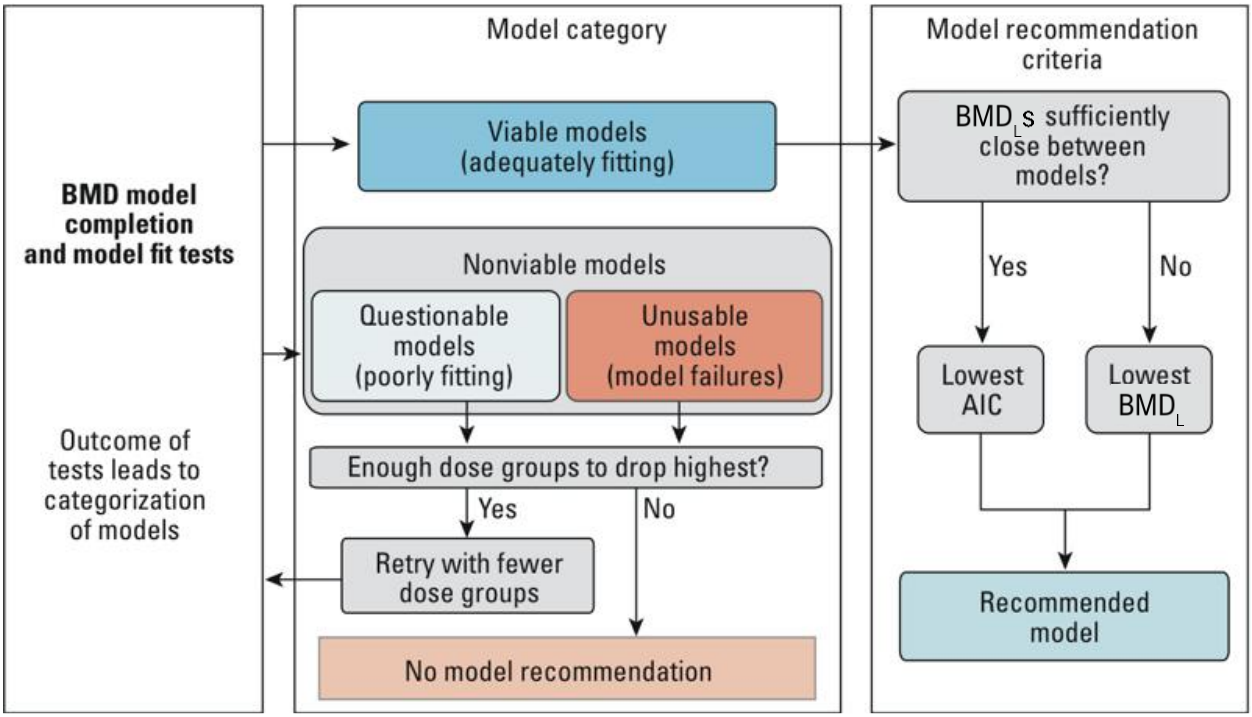

Figure D-1. Benchmark Dose Model Recommendation/Selection Methodology for Automated Benchmark Dose Execution of Apical Endpoints

Source: Figure adapted from Wignall et al. (2014)[20]
BMD = benchmark dose; BMD_L = benchmark dose lower confidence limit; AIC = Akaike information criterion.

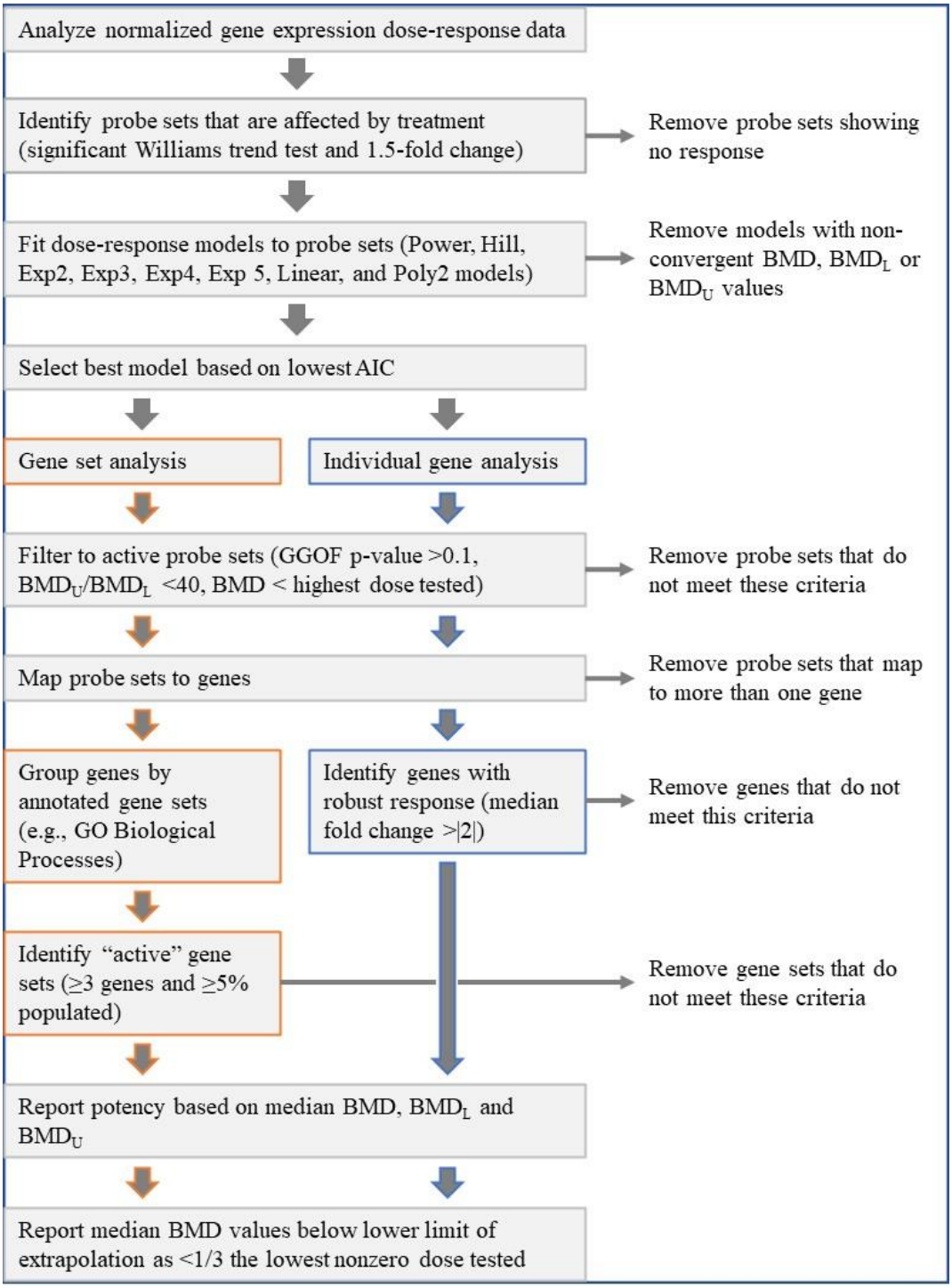

Figure D-2. Benchmark Dose Model Recommendation/Selection Methodology for Benchmark Dose Execution of Gene Sets with Expression Changes Enacted by Chemical Exposure

Adapted from Thomas et al. (2007)[31]
Exp = exponential; Poly = polynomial; BMD = benchmark dose; BMD_L = benchmark dose lower confidence limit; BMD_U = benchmark dose upper confidence limit; AIC = Akaike information criterion; GGOF = global goodness of fit; GO = Gene Ontology.

Appendix E. Organ Weight Descriptions

Table of Contents

E.1. Organ Weight Descriptions

Liver: The liver carries out biotransformation and excretion of endogenous and xenobiotic substances, regulation of blood sugar, enzymatic transformation of essential nutrients, generation of blood proteins involved in fluid balance and clotting, and bile production for digestion and absorption of fats. Liver weight changes can be an indication of chemical-induced stress. Specifically, in subacute studies, increases in liver weight in response to low doses of toxicants typically stem from increases in xenobiotic metabolizing enzymes and associated hepatocyte hypertrophy or peroxisome proliferation. Increased liver weight, particularly when accompanied by evidence of leakage of liver-specific enzymes into blood, likely reflects hemodynamic changes related to severe hepatotoxicity. Higher liver weight relative to body weight may also occur at any dose level that causes a slowed rate of body growth and does not necessarily indicate liver toxicity. Decreased liver weight in subacute studies is typically of unknown toxicological significance but in rare cases may be related to glycogen depletion.

Kidney: The kidneys remove waste products and xenobiotics from the body, balance blood electrolytes, regulate blood pressure through the release of hormones, synthesize the active form of vitamin D, and control the production of erythropoiesis. In subacute studies, changes in kidney weight may reflect renal toxicity (particularly if accompanied by increases in other markers of kidney toxicity, e.g., increased Kim-1) and/or tubular hypertrophy. Decreased kidney weights in subacute studies are typically of unknown toxicological significance.

Heart: The heart drives the circulatory system, supplying oxygen and essential macro- and micronutrients to the tissues. Increased heart weight in subacute studies would indicate severe cardiotoxicity, compensatory myocardial hypertrophy, and/or pulmonary injury. Decreased heart weight in subacute studies is often of unknown toxicological significance; however, it may be caused by decreased load on the heart from dehydration or modulation of contractility.

Appendix F. Supplemental Data

The following supplemental files are available at https://doi.org/10.22427/NIEHS-DATA-NIEHS-09.[26]

F.1. Apical Benchmark Dose Analysis

Mean Body Weight Summary
C20042-01_Mean_Body_Weight_Summary.docx

Organ Weights Summary
C20042-01_Organ_Weights_Summary.docx

Clinical Chemistry Summary
C20042-01_Clinical_Chemistry_Summary.docx

Hematology Summary
C20042-01_Hematology_Data_Summary.docx

Hormone and Enzymes Summary
C20042-01_Hormone_Summary.docx

BMD, NOEL and LOEL Summary for Apical Endpoints
C20042-01_BMD_BMDL_LOEL_and_NOEL_Summary_for_Apical_Endpoints_Sorted_by_BMD_LOEL_from_Low_to_High.docx

Male BMD Apical Endpoints Model Fits
C20042-01_Appendix_Male_07282021.docx

Female BMD Apical Endpoints Model Fits
C20042-01_Appendix_Female_07282021.docx

BMD Model Recommendation Selection Rules
C20042-01_Benchmark_Dose_Model_Recommendation_Selection_Rules_for_Apical_Endpoints.docx

Read Me
C20042-01_ReadME.docx

Male Model Parameters
C20042-01_Parameter_Male_07282021.xlsx

Female Model Parameters
C20042-01_Parameter_Female_07282021.xlsx

BMDs code package
C20042-01_bmds.zip

F.2. Genomic Benchmark Dose Analysis

BMDExpress Project File (bm2 format)
C20042-01_BMDExpress_Project_File_bm2_format.bm2

Top 10 Genes Ranked by Potency of Perturbation_Kidney
C20042-01_Kidney_Top_10_Genes_Ranked_by_Potency_of_Perturbation_Sorted_by_BMD_Median.docx

Top 10 GO Biological Process Gene Sets_Kidney
C20042-01_Kidney_Top_10_GO_Biological_Process_Gene_Sets_Ranked_by_Potency_of_Perturbation_Sorted_by_BMD_Median.docx

Top 10 Genes Ranked by Potency of Perturbation_Liver
C20042-01_Liver_Top_10_Genes_Ranked_by_Potency_of_Perturbation_Sorted_by_BMD_Median.docx

Top 10 GO Biological Process Gene Sets_Liver
C20042-01_Liver_Top_10_GO_Biological_Process_Gene_Sets_Ranked_by_Potency_of_Perturbation_Sorted_by_BMD_Median.docx

BMDExpress Expression Data_Kidney_Female
~~C~~C20042-01_Kidney_2,3-Benzofluorene_Female.txt

BMDExpress Expression Data_Kidney_Male
C20042-01_Kidney_2,3-Benzofluorene_Male.txt

BMDExpress Expression Data_Liver_Female
C20042-01_Liver_2,3-Benzofluorene_Female.txt

BMDExpress Expression Data_Liver_Male
C20042-01_Liver_2,3-Benzofluorene_Male.txt

BMDExpress Individual Gene BMD Results_Kidney_Male
C20042-01_Kidney_2,3-Benzofluorene_Male_williams_0.05_NOMTC_foldfilter1.5_BMD_S1500_Plus_Rat_GENE_true_true_pval0.1_ratio40_foldchange2_conf0.5.txt

BMDExpress GO Biological Process Deduplicated BMD Results_Kidney_Male
C20042-01_Kidney_2,3-Benzofluorene_Male_williams_0.05_NOMTC_foldfilter1.5_BMD_S1500_Plus_Rat_GO_BP_true_true_pval0.1_ratio40_conf0.5_deduplicate.txt

BMDExpress Individual Gene BMD Results_Kidney_Female
C20042-01_Kidney_2,3-Benzofluorene_Female_williams_0.05_NOMTC_foldfilter1.5_BMD_S1500_Plus_Rat_GENE_true_true_pval0.1_ratio40_foldchange2_conf0.5.txt

BMDExpress GO Biological Process Deduplicated BMD Results_Kidney_Female
C20042-01_Kidney_2,3-Benzofluorene_Female_williams_0.05_NOMTC_foldfilter1.5_BMD_S1500_Plus_Rat_GO_BP_true_true_pval0.1_ratio40_conf0.5_deduplicate.txt

BMDExpress Individual Gene BMD Results_Liver_Male
C20042-01_Liver_2,3-Benzofluorene_Male_williams_0.05_NOMTC_foldfilter1.5_BMD_S1500_Plus_Rat_GENE_true_true_pval0.1_ratio40_foldchange2_conf0.5.txt

BMDExpress GO Biological Process Deduplicated BMD Results_Liver_Male
C20042-01_Liver_2,3-Benzofluorene_Male_williams_0.05_NOMTC_foldfilter1.5_BMD_S1500_Plus_Rat_GO_BP_true_true_pval0.1_ratio40_conf0.5_deduplicate.txt

BMDExpress Individual Gene BMD Results_Liver_Female
C20042-01_Liver_2,3-Benzofluorene_Female_williams_0.05_NOMTC_foldfilter1.5_BMD_S1500_Plus_Rat_GENE_true_true_pval0.1_ratio40_foldchange2_conf0.5.txt

BMDExpress GO Biological Process Deduplicated BMD Results_Liver_Female
C20042-01_Liver_2,3-Benzofluorene_Female_williams_0.05_NOMTC_foldfilter1.5_BMD_S1500_Plus_Rat_GO_BP_true_true_pval0.1_ratio40_conf0.5_deduplicate.txt

BMDExpress Prefilter Results_ Kidney _Female
C20042-01_BMDExpress_Prefilter_Results_Kidney_Female.txt

BMDExpress Prefilter Results_ Kidney _Male
C20042-01_BMDExpress_Prefilter_Results_Kidney_Male.txt

BMDExpress Prefilter Results_ Liver _Female
C20042-01_BMDExpress_Prefilter_Results_Liver_Female.txt

BMDExpress Prefilter Results_ Liver _Male
C20042-01_BMDExpress_Prefilter_Results_Liver_Male.txt

Animal and Fastaq Metadata
C20042-01_Animal_and_FASTQ_Metadata.zip

Kidney Principal Components Analysis Files
C20042-01_Kidney_PCA.zip

Liver Principal Components Analysis Files
C20042-01_Liver_PCA.zip

Individual Gene BMD Analysis Results File
C20042-01_Individual_Gene_Defined_Category_Files_for_Gene_Level_BMD_Analysis_of_Array_Platform_GPL1355.zip

BMDExpress Software
C20042-01_Software.zip

BMDExpress Project File (JSON format)
C20042-01_BMDExpress_Project_File_JSON_format

GO Biological Process BMD Analysis Results
C20042-01_Functional_Classification_Annotation_Files_for_GO_Biological_Process_Analysis_of_Array_Platform_GPL1355.zip

F.3. Study Tables

I04 – Mean_Body_Weight_Summary
C20042-01_I04_–_Mean_Body_Weight_Summary.pdf

I05 – Clinical_Observations_Summary
C20042-01_I05_–_Clinical_Observations_Summary.pdf

PA06 – Organ_Weights_Summary
C20042-01_PA06_–_Organ_Weights_Summary.pdf

PA41 – Clinical_Chemistry_Summary
C20042-01_PA41_–_Clinical_Chemistry_Summary.pdf

PA43 – Hematology Summary
C20042-01_PA43_–_Hematology_Summary.pdf

PF48 – Summary of Tissue Concentration
C20042-01_PA48_-_Summary_of_Tissue_Concentration.pdf

R07 – Hormone_Summary
C20042-01_R07_–_Hormone_Summary.pdf

F.4. Individual Animal Data

Individual Animal Body Weight Data
C20042-01_Individual_Animal_Body_Weight_Data.xlsx

Individual Animal Clinical Chemistry Data
C20042-01_Individual_Animal_Clinical_Chemistry_Data.xlsx

Individual Animal Clinical Observations Data
C20042-01_Individual_Animal_Clinical_Observations_Data.xlsx

Individual Animal Hormone Data
C20042-01_Individual_Animal_Hormone_Data.xlsx

Individual Animal Organ Weight Data
C20042-01_Individual_Animal_Organ_Weight_Data.xlsx

Individual Animal Hematology Data
C20042-01_Individual_Animal_Hematology_Data.xlsx

Individual Animal Tissue Concentration Data
C20042-01_Individual_Animal_Tissue_Concentration_Data.xlsx

National Institute of
Environmental Health Sciences
Division of Translational Toxicology
Office of Policy, Review, and Outreach
P.O. Box 12233
Durham, NC 27709

www.niehs.nih.gov/reports

ISSN 2768-5632